Zoological Journal of the Linnean Society, 2021, **XX**, 1–44. With 22 figures.

Integrative systematics of the tooth-tailed scorpions, *Odontobuthus* (Buthidae), with descriptions of three new species from the Iranian Plateau

HOSSEIN BARAHOEI[1], LORENZO PRENDINI[2], SHAHROKH NAVIDPOUR[3], H. MUHAMMAD TAHIR[2,4], MANSOUR ALIABADIAN[1,5], ROOHOLLAH SIAHSARVIE[1,6] and OMID MIRSHAMSI[1,5,*]

[1]*Department of Biology, Faculty of Science, Ferdowsi University of Mashhad, Mashhad, Iran*
[2]*Scorpion Systematics Research Group, Division of Invertebrate Zoology, American Museum of Natural History, New York, USA*
[3]*Razi Reference Laboratory of Scorpion Research, Razi Vaccine and Serum Research Institute, Agricultural Research Education and Extension Organization, Karaj, Iran*
[4]*Department of Zoology, GC University, Lahore, Pakistan*
[5]*Research Department of Zoological Innovations (RDZI), Institute of Applied Zoology, Faculty of Science, Ferdowsi University of Mashhad, Mashhad, Iran*
[6]*Rodentology Research Department (RRD), Institute of Applied Zoology, Faculty of Science, Ferdowsi University of Mashhad, Mashhad, Iran*

accepted for publication 16 April 2021

The 'tooth-tailed' scorpions of the buthid genus *Odontobuthus* comprises six species with an allopatric or parapatric pattern of distribution in the Middle East, but the diversity of *Odontobuthus* in Iran appears to be underestimated, with the limits of several species remaining unclear. In the present contribution, an integrative approach to the systematics of *Odontobuthus* was applied, to determine the taxonomic validity and phylogenetic relationships among its species. Statistical analyses of five meristic characters, 38 morphometric characters and 21 morphometric ratios, combined with molecular phylogenetic analyses of DNA sequences from the mitochondrial cytochrome *c* oxidase subunit I (*COI*) gene, were conducted. All previously described species of *Odontobuthus* were found to be well supported, and new morphological diagnoses are here presented. Additionally, three new species: ***Odontobuthus baluchicus* sp. nov.** from the Makkoran Mountains, ***Odontobuthus chabaharensis* sp. nov.** from the coast of the Gulf of Oman (Sistan and Baluchistan Provinces) and ***Odontobuthus kermanus* sp. nov.** from Kerman Province, are described, raising the total number of *Odontobuthus* species to nine, six of which are endemic or subendemic to the Iranian Plateau. A distribution map and identification key to the species of *Odontobuthus* are also provided.

ADDITIONAL KEYWORDS: *COI* – molecular phylogenetics – morphology – morphometrics – taxonomy.

INTRODUCTION

The 'tooth-tailed' scorpions of the Asian buthid genus *Odontobuthus* Vachon, 1950 are characterized by the presence of prominent tooth-like processes (enlarged spiniform granules) on the ventrosubmedian carinae of metasomal segments II and III, and the ventrolateral carinae of metasomal segment V (Farzanpay, 1987; Lowe, 2010; Mirshamsi *et al.*, 2013). These fossorial, pelophilous scorpions, which construct burrows in consolidated sandy to silty substrates on alluvial plains (Farzanpay, 1987; Lowe, 2010), use the tooth-like projections to loosen the substrate by raking with the ventral surface of the metasoma, a behaviour referred to as 'tail-scraping' (Newlands, 1972; Prendini,

*Corresponding author. E-mail: mirshams@um.ac.ir
[Version of record, published online 25 June 2021; http://zoobank.org/ urn:lsid:zoobank.org:pub:F67DA6EF-32D6-43C4-909E-0A762246AAAC]

2001). Members of this genus are distributed from central-eastern Iraq, throughout Iran and Pakistan, to north-western India, with one species occurring on the Arabian Peninsula in Oman and the United Arab Emirates (Lourenço & Pézier, 2002; Lowe, 2010; Mirshamsi *et al.*, 2013).

The first species of the genus, *Buthus doriae* Thorell, 1876, was described from Tehran, Persia, now central Iran (Thorell, 1876). Twenty years later, the second species, *Buthus odonturus* Pocock, 1897, was described from the Khelat Frontier, British India, now Pakistan (Pocock, 1897). Pocock (1900) subsequently treated *B. odonturus* as a subspecies of *B. doriae*. Half a century later, as part of a revision of the traditional buthid genus *Buthus* Leach, 1815, Vachon (1950) reinstated *B. odonturus* as a distinct species, and created the genus *Odontobuthus*, based on carapacial and metasomal carination, to accommodate the two species.

After the work of Vachon (1950), another 50 years passed before interest in the systematics of *Odontobuthus* renewed. In the past two decades, the work of several authors (Lourenço & Pézier, 2002; Lowe, 2010; Mirshamsi *et al.*, 2013; Navidpour *et al.*, 2013; Azghadi *et al.*, 2014) added four species, namely *Odontobuthus bidentatus* Lourenço & Pézier, 2002, *O. brevidigitus* Lowe, 2010, *O. tavighiae* Navidpour *et al.*, 2013 and *O. tirgari* Mirshamsi *et al.*, 2013.

Lourenço & Pézier (2002) described *Odontobuthus bidentatus* from Iraq and western Iran, confirmed the validity of *O. doriae* (Thorell, 1876) and *O. odonturus* (Pocock, 1897), and concluded that a previous report of *O. odonturus* from Iran was a misidentification. *Odontobuthus bidentatus* was characterized by the presence of two pairs of tooth-like processes on the ventrosubmedian carinae of metasomal segments II and III, two or three prominent lobate granules on the ventrolateral carinae and three lobes laterally on the anal arch of metasomal segment V. *Odontobuthus brevidigitus*, from northern Oman, was the first *Odontobuthus* to be reported from the Arabian Peninsula (Lowe, 2010). *Odontobuthus brevidigitus* was characterized by short pedipalp chela fingers and the presence of two or three pairs of tooth-like processes on the ventrosubmedian carinae of metasomal segments II and III, ten granules along the anteroventral margin of segment IV, three lobes laterally and enlarged spiniform granules ventrally on the anal arch of segment V. *Odontobuthus tavighiae*, the first species to be described from Hormozgan Province in southern Iran, was characterized by the presence of two pairs of tooth-like processes on the ventrosubmedian carinae of metasomal segments II and III and three long, conical lobes laterally on the anal arch of segment V (Navidpour *et al.*, 2013). In the first contribution to apply an integrative approach to the systematics of *Odontobuthus*, Mirshamsi *et al.* (2013) described *O. tirgari* from north-eastern and eastern Iran using qualitative morphological characters, morphometrics and mitochrondrial DNA (hereafter, mtDNA) sequences from the cytochrome *c* oxidase subunit I gene (hereafter, *COI*) and confirmed the validity of *O. bidentatus* and *O. doriae*. *Odontobuthus tirgari* was characterized by the presence of three to five pairs of tooth-like processes on the ventrosubmedian carinae of metasomal segments II and III and one small and two large lobes laterally on the anal arch of segment V.

In the most recent contribution to the systematics of *Odontobuthus*, Azghadi *et al.* (2014) confirmed the validity of all species recorded in Iran based on phylogenetic analysis of mtDNA sequences from the *COI* and 16S rDNA (hereafter, 16S) genes. The topology obtained from simultaneous phylogenetic analysis of the *COI* and 16S sequences recovered two major clades: the first comprising *O. bidentatus*, *O. doriae* and *O. tavighiae*, the second comprising *O. tirgari* and an undescribed species from Kerman Province in south-eastern Iran. According to Azghadi *et al.* (2014), this undescribed species was characterized by the presence of three pairs of rounded processes on the ventrosubmedian carinae of metasomal segments II and III, four to six rounded processes along the anteroventral margin of metasomal segment IV, one large and two lobes laterally, and six to eight small, equal spiniform granules ventrally on the anal arch of segment V. However, Azghadi *et al.* (2014) concluded that a detailed morphological study was required to describe this clade as a distinct species.

Few comprehensive systematic studies of Iranian scorpion species have been presented to date, and few were described based on an integrative approach. Despite several studies, the species diversity of *Odontobuthus* in Iran appears to be underestimated, and the limits of several species inhabiting the country remain unclear. In the present contribution, an integrative approach to the systematics of *Odontobuthus* was applied, to determine the taxonomic validity and phylogenetic relationships among its species. Statistical analyses of five meristic characters, 38 morphometric characters and 21 ratios calculated from the morphometric characters, as well as molecular phylogenetic analyses of mtDNA sequences from the *COI* gene, were conducted. All previously described species of *Odontobuthus* were found to be well supported and new morphological diagnoses are presented to separate them. Additionally, three new Iranian species, one from the Makkoran Mountains, one from the coast of the Gulf of Oman (both in Sistan and Baluchistan Province) and another from Kerman Province, are described here, increasing the

number of *Odontobuthus* species to nine, six of which are endemic or subendemic to the Iranian Plateau. A distribution map and identification key to the species of *Odontobuthus* are also provided.

MATERIAL AND METHODS

Material, mapping, microscopy and imaging

Specimens were collected by excavation of burrows during the day and, rarely, by ultraviolet (UV) light detection at night. Newly collected material, transferred to 75–96% alcohol, is mostly deposited in the Zoological Museum of Ferdowsi University of Mashhad (ZMFUM), Iran, or the American Museum of Natural History (AMNH), New York, USA. Some tissue samples are stored in liquid nitrogen at –150 °C in the Ambrose Monell Cryocollection (AMCC) at the AMNH. Holotypes of the three new species are deposited at the Senckenberg Museum, Frankfurt (SMF), Germany.

Other material referred to in the taxonomic treatment is deposited in the following collections: Natural History Museum (BMNH), London, UK; František Kovařík Private Collection (FKCP), Prague, Czech Republic; Museo Civico de Storia Naturale 'Giacomo Doria' (MCSN), Genoa, Italy; Museum d'Histoire Naturelle (MHNG), Geneva, Switzerland; Naturhistorisches Museum Basel (NHMB), Basel, Switzerland; Razi Reference Laboratory of Scorpion Research (RRLS), Razi Vaccine and Serum Research Institute, Ahvaz, Iran; Iziko South African Museum (SAM), Cape Town, South Africa; Museum für Naturkunde (ZMB), Berlin, Germany; Zoologisches Museum, Universität Hamburg (ZMH), Hamburg, Germany.

Maps of species distributions were prepared using DIVA-GIS 7.5 by superimposing point locality records of collection localities on spatial datasets depicting political boundaries and topography (elevation) at 2.5 arc-minutes altitude (Hijmans *et al.*, 2004) (Fig. 1).

Morphological characters of adult *Odontobuthus* specimens, adopted from Lamoral (1979) and Stahnke (1970), were recorded with a > 0.02 mm Olympus micrometer ocular lens (OSM-4) attached to an optical Olympus SZ40 stereomicroscope. Cuticular macrosculpture was studied and documented with UV fluorescence imaging using a LED excitation source (Lowe *et al.*, 2003; Prendini, 2004; Volschenk, 2005) and digital images taken by long exposure using a Canon EOS 550D digital camera (Lowe *et al.*, 2003). Morphological terminology is adopted from Sissom (1990). However, the terms 'internal' and 'external' are replaced with 'prolateral' and 'retrolateral', respectively, for referring to the surfaces of the pedipalps and legs, following Acosta *et al.* (2008). Character systems assessed to be uninformative at the species level in *Odontobuthus*, e.g. trichobothrial patterns and morphology of hemispermatophores, were not illustrated.

Statistical analysis of meristic and morphometric data

Five meristic (counts) and 38 morphometric characters (measurements, in mm) were recorded in 149 adults of the nine species, deposited in ZMFUM (Table 1): *O. baluchicus* (N = 10); *O. bidentatus* (N = 16); *O. brevidigitus* (N = 1); *O. chabaharensis* (N = 5); *O. doriae* (N = 28); *O. kermanus* (N = 13); *O. odonturus* (N = 1); *O. tavighiae* (N = 23); *O. tirgari* (N = 52).

The five meristic characters, 38 morphometric characters and 21 ratios calculated from the morphometric characters (Table 2), used for statistical analysis, are abbreviated as follows. **Counts:** MFDR: number of median denticle subrows on pedipalp chela movable finger; PDR: pectinal tooth count of male and female; MtIIIVC: number of pairs of tooth-like processes on ventrosubmedian carinae of metasomal segment III; NLLAA: number of lateral lobes of anal arch on metasomal segment V; NVDAA: number of spiniform granules ventrally on anal arch of metasomal segment V. **Measurements:** PeL: pedipalp length; FL: pedipalp femur length; FW: pedipalp femur width; PaL: pedipalp patella length; PaW: pedipalp patella width; ChL: pedipalp chela length; ML: pedipalp chela manus length; MW: pedipalp chela manus width; MD: pedipalp chela manus depth; MFL: pedipalp chela movable finger length; CAW: carapace anterior width; CPW: carapace posterior width; CL: carapace length; CX: distance between anterior margin of carapace and anterior edge of median ocelli; CY: distance between anterior edge of median ocelli and posterior margin of carapace; MsL: mesosoma length; TIIIL: mesosomal tergite III length; TIIIW: mesosomal tergite III width; MtIL, MtIIL, MtIIIL, MtIVL, MtVL: length of metasomal segments I–V; MtIW, MtIIW, MtIIIW, MtIVW, MtVW: width of metasomal segments I–V; MtID, MtIID, MtIIID, MtIVD, MtVD: depth of metasomal segments I–V; TL: telson length; TW: telson width; TD: telson depth; MtTL: metasoma and telson length; BL: total length. **Ratios:** FL/W: pedipalp femur length to width; PaL/W: pedipalp patella length to width; ChL/ML: pedipalp chela length to chela manus length; CAW/PW: carapace anterior width to posterior width; CL/AW: carapace length to anterior width; CL/PW: carapace length to posterior width; CX/CY: distance between anterior margin of carapace and anterior edge of median eyes to distance between anterior edge of median ocelli and posterior margin of carapace; TIIIL/W: mesosomal tergite III length to width;

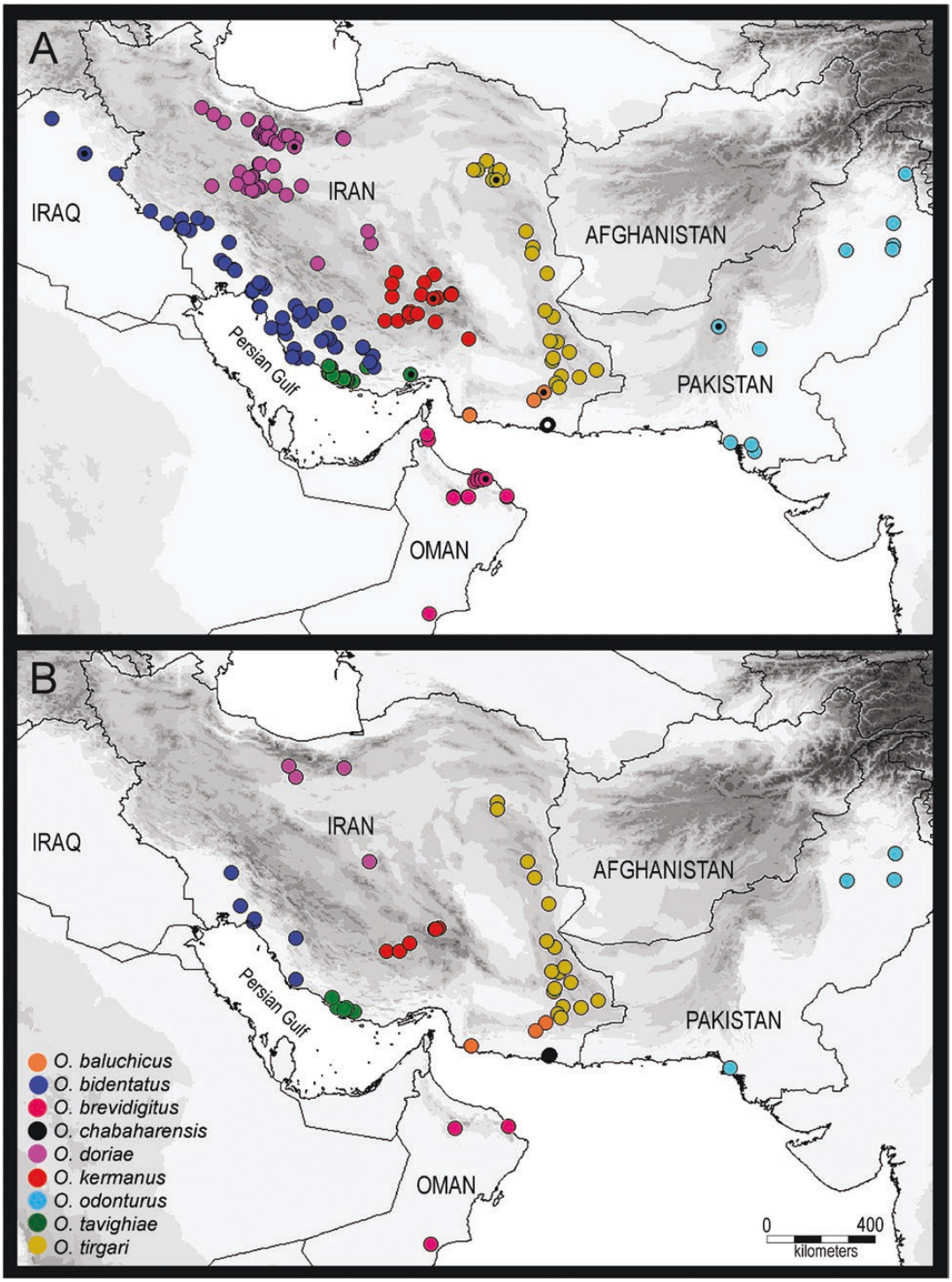

Figure 1. Geographical distribution of the buthid scorpion genus *Odontobuthus* plotted on topography of the Middle East. A, known locality records obtained from fieldwork and the literature. Circles with black or white dots indicate type localites of each species. B, localities of material used in molecular phylogenetic analysis (see Table 1 for details).

MtIL/W, MtIIL/W, MtIIIL/W, MtIVL/W, MtVL/W: metasomal segments I–V length to width; MtIL/D, MtIIL/D, MtIIIL/D, MtIVL/D, MtVL/D: metasomal segments I–V length to depth; TL/W: telson length to width; TL/D: telson length to depth: TW/D: telson width to depth.

Table 1. Specimens, populations and provenance data (country, province or governate and abbreviated locality) of the buthid scorpion genus *Odontobuthus* deposited in the collections of the Zoological Museum of Ferdowsi University of Mashhad (ZMFUM), Iran, used for morphometric analysis

Species	Population	Locality	Sex	ZMFUM
O. baluchicus	Nikshahr	IRAN: *Sistan and Baluchistan*: Nikshahr, Chanf	3♂♂, 2♀♀	1301–1305
		IRAN: *Sistan and Baluchistan*: Nikshahr, Konari	2♀♀	1306, 1308
	Jask	IRAN: *Hormozgan*: Jask	3♀♀	1309–1311
O. bidentatus	Daylam	IRAN: *Bushehr*: Abdan	1♀	1314
		IRAN: *Bushehr*: Daylam	1♂, 1♀	1315–1316
		IRAN: *Bushehr*: Sardasht	1♂, 1♀	1317–1318
	Khuzestan	IRAN: *Khuzestan*: Omidiyeh	2♂♂, 9♀♀	2061–2064, 2066, 2067, 2069–2073
O. brevidigitus	Oman	OMAN: *Al Wusta*: Wadi Rawnab	1♂	1348
O. chabaharensis	Chabahar	IRAN: *Sistan and Baluchistan*: Chabahar, Parak Sheykhan	1♂, 4♀♀	1321, 1323–1326
O. doriae	Semnan	IRAN: *Semnan*: Semnan	2♂♂, 7♀♀	1328–1329, 2031–2037
	Tehran	IRAN: *Tehran*, Tehran	3♂♂, 16♀♀	2001–2010, 2012–2019, 2038
O. kermanus	Neyriz	IRAN: *Fars*: Ghatrooieh, Neyriz	1♂♂, 3♀♀	1330–1333
	Bardsir	IRAN: *Kerman*: Sirjan	2♂♂, 2♀♀	1334–1337
		IRAN: *Kerman*: Bardsir–Negar–Baft road	2♂♂, 4♀♀	1338–1342, 2039
O. odonturus	Karachi	PAKISTAN: *Karachi*: Karachi	1♀	1349
O. tavighiae	Parsian	IRAN: *Hormozgan*: Hameyran, Maragh	1♂, 3♀♀	1345–1348
		IRAN: *Hormozgan*: Parsian, Chahvaz	6♂♂, 2♀♀	1349–1350, 1354–1359
		IRAN: *Hormozgan*: Parsian, Pishab	1♂, 2♀♀	1351–1353
	Mohr	IRAN: *Hormozgan*: Lavar-e Khasht	2♀♀	1362–1363
		IRAN: *Fars*: Mohr	1♂, 3♀♀	1364–1367
		IRAN: *Hormozgan*: Parsian, Behdeh	1♂, 1♀	2074–2075
O. tirgari	Zahedan	IRAN: *Sistan and Baluchistan*: Zahedan, Manzel Aab	2♂♂, 1♀	1369, 1371–1372
		IRAN: *Sistan and Baluchistan*: Zahedan, Cheshmeh Ziarat	1♂, 3♀♀	1375–1378
	Birjand	IRAN: *South Khorasan*: Shosf	1♂, 2♀♀	1387–1389
		IRAN: *South Khorasan*: Sahl Abad	1♂, 1♀	1390, 1392
	Gonabad	IRAN: *Razavi Khorasan*: Gonabad, Kakhk	6♂♂, 11♀♀	1393–1398, 2091, 2093, 2131–2133, 2135–2140
		IRAN: *Razavi Khorasan*: Ghouzhd	2♂♂	1385–1386
	Iranshahr	IRAN: *Sistan and Baluchistan*: 30 km E of Iranshahr	2♂♂	1416–1417
		IRAN: *Sistan and Baluchistan*: 40 km Iranshahr to Rask	2♀	1418, 1421
		IRAN: *Sistan and Baluchistan*: Iranshahr, Zimdan	1♂, 1♀	1423–1424
	Khash	IRAN: *Sistan and Baluchistan*: Khash, Karvandar	4♂♂	1374, 1427–1429
		IRAN: *Sistan and Baluchistan*: Khash, Dasht robat	1♂, 3♀♀	1399–1402
		IRAN: *Sistan and Baluchistan*: Saravan	1♂, 1♀	1405–1406
		IRAN: *Sistan and Baluchistan*: Mehrestan	4♀♀	1407, 1410, 1412–1413
		IRAN: *Sistan and Baluchistan*: Khash, Dehpabid	1♀	1432

Univariate and multivariate statistical analyses were applied to the meristic and morphometric data to evaluate inter- and intraspecific variation in morphology. The morphometric measurement data were considered in two aspects of body form, i.e. size and shape. For this purpose, the overall size of each specimen was calculated

as the square root of the sum of all squared variables (Navarro *et al.*, 2004). Shape variables were calculated as the log shape ratio of the morphometric variables (Eldredge, 1972; Navarro *et al.*, 2004). A type-II two-way analysis of variance (ANOVA) was performed on the overall size, using the factors of sex and species, to investigate interspecific size differences. The same analysis was conducted on all morphometric and ratio variables to reveal characters, which differed among the species. When a difference was found to be significant with the ANOVA, it was followed by a Tukey's Post-Hoc Honestly Significant Difference (HSD) Test. Because sexually dimorphic differences were statistically significant for most morphometric characters, and the sex ratio varied among the populations studied, the effect of sex was removed by regressing the variables on the sex discriminant factor and performing subsequent analyses on the residuals. A box plot was performed on the sex-corrected total length to illustrate the size difference among species. Two species for which only a single specimen was available at ZMFUM, i.e. *O. brevidigitus* and *O. odonturus*, were excluded from this analysis.

In the multivariate analyses, pairwise correlation among the characters was calculated and, in cases of high correlation (R > 0.95), one character removed. Interspecific variation in shape was tested via multivariate analysis of variance (MANOVA) on the sex-corrected shape variables and followed by a pairwise MANOVA among species (Table 3). A linear discriminant analysis (LDA) was conducted on the sex-corrected shape variables using population factor, in order to explore the morphological similarity among populations and species. Populations represented by fewer than five specimens (Jask, Karachi, Neyriz and Oman) were excluded from the discriminant factors and projected onto them a posteriori. A neighbour-joining (NJ) tree of Mahalanobis distances among populations was estimated using the sex-corrected shape data to reveal the magnitude of shape differences among populations.

All the morphometric analyses were performed using R (R Development Core Team, 2019). The *MASS* package (Venables & Ripley, 2002) was used for LDA, the *ape* package (Paradis *et al.*, 2004) for NJ, the *ggplot2* package (Wickham, 2016) for plots, the *Picante* package (Kembel *et al.*, 2010) for pairwise correlation among characters, and the *RVAideMemoire* package (Hervé, 2020) for pairwise MANOVA.

Molecular laboratory methods and phylogenetic analysis

DNA was extracted from muscle tissue using the GenNetBio DNA Extraction kit (Seoul, South Korea) or the Qiagen DNeasy Blood and Tissue Kit (Hilden, Germany). The polymerase chain reaction (PCR) employed a variety of optimization protocols (Azghadi *et al.*, 2014) for amplifying an approximately 700 nucleotide base-pair (bp) fragment of the *COI* gene, using LCO1490 and HCO (Folmer *et al.*, 1994) or Nancy (Simon *et al.*, 1994) as forward and reverse primers, respectively. Each PCR reaction contained 12.5 µL Ampliqon ready master mix (Odense, Denmark), 7.5 µL deionized H_2O, 1 µL (= 1 pmol) of each primer and 3 µL of DNA template. Sequencing was conducted using ABI Big Dye terminator chemistry on an ABI Prism 3700 (Applied Biosystems, Foster City, CA, USA). Sequences were edited and assembled using SEQUENCHER v.4.5.6 (GeneCodes Corporation, Ann Arbor, Michigan, USA). Sequence quality was visually examined, and any unreliable base-calls excluded from the multiple sequence alignment, created using MUSCLE (Edgar, 2004).

The 37 newly generated *COI* sequences were deposited in GenBank [http://www.ncbi.nlm.nih.gov] with the accession numbers MW655751 to MW655784 and MW655793 to MW655795 (Table 4). In addition, 19 *Odontobuthus* sequences were retrieved from GenBank, for an ingroup comprising 51 individuals, representing the nine species (Table 4): *O. baluchicus* (*N* = 4); *O. bidentatus* (*N* = 7); *O. brevidigitus* (*N* = 3); *O. chabaharensis* (*N* = 2); *O. doriae* (*N* = 5); *O. kermanus* (*N* = 6); *O. odonturus* (*N* = 4); *O. tavighiae* (*N* = 6); *O. tirgari* (*N* = 14). Two species of *Buthus*, a genus considered closely related to *Odontobuthus*, were used as outgroups: *Buthus occitanus* (Amoreux, 1789) and *Buthus paris* (C.L. Koch, 1837).

DNASP 5 (Rozas *et al.*, 2003) and MEGA7 (Kumar *et al.*, 2016) were used to assess the phylogenetic information content of the sequences. Intra- and interspecific genetic divergence among *Odontobuthus* populations and the two outgroups (*B. paris* and *B. occitanus*) were calculated using ExCaliBAR (Aliabadian *et al.*, 2014).

Bayesian Inference (BI) was conducted using MrBayes v.3.2 (Ronquist & Huelsenbeck 2003). The number of generations was set to $5vx10^7$, and a tree sampled every 1000^{th} generation. The average standard deviation of split frequencies of the two simultaneous and independent runs performed was applied to resolve the stationary point of likelihoods (Ronquist & Huelsenbeck, 2003). Bayesian tree and posterior probabilities were calculated by majority rule consensus after burning off all pre-asymptotic topologies.

Maximum likelihood (ML) analysis was conducted using RAxML v.1.3 (Silvestro & Michalak, 2012) using the GTR+G substitution model, determined to be the best-fitting model of sequence evolution for *COI* by jMODELTEST v.2.1.10 (Posada, 2008) under the

Akaike Information Criterion (AIC) (–*ln*L = 3370.6533; AIC 6967.3065). The rapid bootstrap analysis was run for 10 000 replicates.

RESULTS

MORPHOMETRIC ANALYSIS

A statistically significant difference among the species is obtained for all variables assessed in the type-II two-way ANOVA of sex and species factors, except four ratios, i.e. CL/PW, CX/CY, TL/D and TW/D. Results of the Tukey's Post-Hoc HSD Test on metric and meristic variables, which differ significantly among the species in the ANOVA, indicate significant differences between *O. bidentatus* and *O. kermanus* and between *O. doriae* and *O. tirgari* in all metric characters (Table 2). Differences in metric variables are not significant between *O. bidentatus* and *O. doriae*, or between *O. chabaharensis* and *O. kermanus*, *O. tavighiae* or *O. tirgari*. Statistically significant differences between most species are observed in the characters of the carapace (CX and CY) and pedipalp (MFL, ChL, MW, MD and FW). The box-plot of sex-corrected total length (Fig. 2) reveals that *O. bidentatus* and *O. doriae* are generally larger than the other species; *O. baluchicus* is medium-sized and the other species are smaller.

Two-way MANOVA of shape variables using sex and species factors obtain a significant difference among the species studied ($F = 4.7727$; $P < 10^{-15}$). The pairwise MANOVA reveals that *O. baluchicus* and *O. tavighiae* are significantly different from other species whereas *O. chabaharensis* and *O. doriae* are the most similar (Table 3).

The linear discriminant analysis (LDA) on population factor using sex-corrected shape variables (Fig. 3) indicates that all described species of *Odontobuthus*, as well as the three new species, form well-defined phenetic groups. The greatest morphological divergence is observed between *O. baluchicus* and *O. tavighiae.* A similar pattern is recovered by NJ analysis of the same data (Fig. 4).

DNA SEQUENCE DATA AND GENETIC DISTANCES

The aligned *COI* sequences are 627 bp in length, with 451 (71.92%) positions conserved, 176 (28.07%) variable and 148 (23.60%) parsimony-informative. Nucleotide (π) and haplotype diversity among the *Odontobuthus* sequences are 0.090 and 0.93, respectively.

The Kimura 2-parameter (K2P) genetic distances between each *Odontobuthus* species and the two outgroup species range from 11.6%, between *O. bidentatus* and *B. occitanus*, to 15.9%, between *O. baluchicus* and *B. occitanus* (Table 5). The K2P genetic distances among *Odontobuthus* species range from 6.0%, between *O. kermanus* and *O. tirgari*, to 13.5%, between *O. bidentatus* and *O. doriae* (Table 5). The K2P genetic distances between the three new species, *O. baluchicus*, *O. chabaharensis* and *O. kermanus*, and other *Odontobuthus* species range from 9% to 12.4%, 8.4% to 13.5% and 6% to 13.4%, respectively. The average intraspecific genetic distance within the genus *Odontobuthus* is 1.9% ± 0.4.

PHYLOGENETIC ANALYSIS

Tree topologies produced by BI and ML are almost entirely congruent. Both recover the monophyly of *Odontobuthus* and the nine species with high support values. The species are grouped into two major clades (Fig. 5), clade A comprising seven species and clade B comprising *O. kermanus* and *O. tirgari*. Clade A is further divided into two clades, clade A1 comprising *O. doriae*, placed sister to a clade comprising *O. baluchicus* and *O. odonturus*, and clade A2, comprising *O. bidentatus*, placed sister to a clade comprising *O. brevidigitus*, *O. chabaharensis*, and *O. tavighiae*, with *O. chabaharensis* in turn placed sister to a clade comprising the other two species. The average genetic distance between the species of clade A and the species of clade B ranges from 9.5% to 13.4%. The average genetic distance among the species of clade A1 is 11.3% and among the species of clade A2, 9.3%.

SYSTEMATICS

FAMILY BUTHIDAE C.L.KOCH, 1837

GENUS *ODONTOBUTHUS* VACHON, 1950

(FIGS 1–22, TABLES 1–5)

Odontobuthus Vachon, 1950: 153, 154.
Type species: Buthus doriae Thorell, 1876 [= *Odontobuthus doriae* (Thorell, 1876)]; Vachon, 1952: 325, 326; Pringle, 1960: 83, fig. 8; Khalaf, 1963: 59; Vachon, 1966: 213; Habibi, 1971: 44; Stahnke, 1972: 132; Vachon, 1974: 906; Tikader & Bastawade, 1983: 247–253, figs 714–726; Francke, 1985: 10, 16; Kinzelbach, 1985: map I; Farzanpay, 1987: 154–156; Vachon & Kinzelbach, 1987: 92; Farzanpay, 1988: 39; Farzanpay, 1990: 7; Sissom, 1990: 92, 98, 101, 102, fig. 3.17J; Nenilin & Fet, 1992: 17; El-Hennawy, 1992: 102, 105, 128; Akbari *et al.*, 1997: 112; Kovarik, 1997: 47, 49, figs 11–13; Dehghani *et al.*, 1998: 126; Kovarik, 1998: 115; Pooladgar, 1999: 176; Fet & Lowe, 2000: 187; Kovařík, 2002: 9; Lourenço & Pézier, 2002: 115–124, figs 1–27; Soleglad & Fet, 2003: 26; Fet *et al.* 2005: 3, 12, 22; Prendini & Wheeler, 2005: 481; Vignoli & Crucitti, 2005: 6–7, fig. 2d; Dehghani *et al.*, 2008: 176; Navidpour

Table 2. Statistically significant *P* values from pairwise comparisons among species of the buthid scorpion genus *Odontobuthus* occurring in Iran, for each metric and ratio character using Tukey's Post-Hoc HSD Test (*N* = 149 specimens). Asterisks indicate significant *P* values: * (0.05–0.01); ** (0.01–0.001); *** (< 0.001). *bal* = *O. baluchicus*; *bid* = *O. bidentatus*; *cha* = *O. chabaharensis*; *dor* = *O. doriae*; *ker* = *O. kermanus*; *tav* = *O. tavighiae*; *tir* = *O. tirgari*. See text for abbreviations of metrics and ratios

Species / **Character**	***bal—bid***	***bal—cha***	***bal—dor***	***bal—ker***	***bal—tav***	***bal—tir***	***bid—cha***	***bid—dor***	***bid—ker***	***bid—tav***
Metric characters										
MFL	0.98	**	0.99	***	***	*	*	1.00	***	***
ChL	0.98	**	0.99	***	***	*	*	1.00	***	***
ML	1.00	0.06	0.99	**	*	0.05	*	0.99	**	**
MW	***	0.99	***	0.99	0.23	0.76	***	1.00	***	*
MD	***	1.00	***	1.00	0.14	0.92	**	1.00	***	*
PaL	0.96	*	1.00	**	***	0.06	0.07	0.97	*	**
PaW	0.11	0.59	0.50	0.15	0.76	0.13	**	0.88	***	***
FL	0.96	*	1.00	**	***	0.07	0.14	0.94	*	**
FW	*	0.82	*	0.56	0.87	0.73	**	0.99	***	***
PeL	0.99	*	1.00	**	**	0.05	0.05	0.98	**	**
CAW	0.45	0.82	0.06	0.54	0.95	0.54	0.05	0.97	***	**
CPW	0.64	0.82	0.23	0.28	0.87	0.39	0.09	0.99	***	**
CL	0.71	0.64	0.28	0.13	0.85	0.16	*	0.99	***	*
CX	0.93	*	1.00	***	*	***	0.11	0.75	***	0.11
CY	***	0.99	***	0.99	0.52	0.99	0.05	0.99	***	*
MsL	0.99	**	0.99	**	0.24	***	*	1.00	*	0.46
TIIIL	0.99	*	0.71	*	0.81	***	***	0.12	***	0.22
TIIIW	0.46	0.88	0.19	0.48	0.93	0.36	0.08	0.99	***	**
MtIL	0.99	0.10	1.00	**	*	*	0.19	0.99	**	0.08
MtIW	0.99	0.10	0.95	*	0.44	0.24	*	0.99	**	*
MtID	0.99	0.19	0.67	*	0.72	0.16	*	0.94	***	0.13
MtIIL	0.99	0.15	1.00	**	*	*	0.17	0.99	**	*
MtIIW	0.85	0.29	0.36	0.08	0.73	0.19	*	0.98	***	*
MtIID	0.97	0.19	0.64	*	0.66	0.10	*	0.98	***	0.05
MtIIIL	1.00	0.26	0.99	*	*	0.05	0.13	0.99	**	**
MtIIIW	0.57	0.47	0.09	0.30	0.99	0.34	*	0.96	***	0.06
MtIIID	0.95	0.17	0.55	0.06	0.75	0.16	*	0.98	***	*
MtIVL	0.99	0.30	0.92	*	0.25	*	0.06	0.99	***	**
MtIVW	0.47	0.58	0.19	0.37	1.00	0.25	*	0.99	***	0.10
MtIVD	0.70	0.38	0.22	0.15	0.99	0.23	*	0.99	***	0.07
MtVL	0.99	0.37	0.99	*	0.12	0.05	0.12	1.00	***	**
MtVW	0.31	0.90	0.08	0.40	0.99	0.22	*	0.99	***	*
MtVD	0.82	0.37	0.73	0.21	0.87	0.60	*	1.00	**	*
TL	0.98	0.49	0.92	*	0.06	0.07	0.13	0.99	***	***
TW	*	0.84	0.23	0.21	0.99	0.26	**	0.87	***	***
TD	*	0.94	0.28	0.16	1.00	0.36	*	0.85	***	**
MtTL	0.99	0.26	0.99	*	0.07	*	0.11	0.99	***	**
BL	1.00	0.12	0.99	**	0.12	**	*	0.99	***	*
Morphometric ratios										
PaL/W	***	**	***	*	***	0.99	0.74	**	***	0.94
PeL/ChL	*	0.37	0.09	0.71	**	1.00	0.99	0.90	0.41	0.99
FL/W	***	***	***	***	***	**	0.53	*	*	0.78
CAW/PW	0.95	0.99	0.42	0.17	0.71	0.71	0.99	0.94	0.63	0.99
CL/AW	0.81	0.56	0.22	**	0.84	*	0.98	0.95	0.15	1.00
CL/PW	0.99	0.83	0.98	0.75	1.00	0.34	0.96	1.00	0.94	0.98

bid—tir	***cha—dor***	***cha—ker***	***cha—tav***	***cha—tir***	***dor—ker***	***dor—tav***	***dor—tir***	***ker—tav***	***ker—tir***	***tav—tir***
0.08	**	1.00	1.00	0.45	***	***	*	1.00	0.06	*
0.08	**	1.00	1.00	0.45	***	***	*	1.00	0.06	*
**	**	1.00	0.99	0.89	***	***	***	0.99	0.69	0.88
***	***	1.00	0.18	0.99	***	**	***	*	0.96	***
***	***	1.00	0.38	0.99	***	**	***	0.05	0.90	***
0.29	**	0.99	0.99	0.55	***	***	**	1.00	0.44	0.16
***	*	1.00	0.98	1.00	***	***	***	0.77	0.99	0.81
0.36	*	1.00	1.00	0.71	***	***	**	1.00	0.38	0.09
***	**	1.00	0.99	0.99	***	***	***	0.99	0.99	1.00
0.06	**	1.00	0.99	0.76	***	***	***	1.00	0.54	0.45
***	**	1.00	0.99	1.00	***	***	***	0.93	0.99	0.96
***	*	0.99	0.99	1.00	***	***	***	0.83	0.99	0.96
***	**	0.99	0.98	1.00	***	***	***	0.57	0.99	0.74
**	**	0.99	0.95	0.99	***	***	***	0.37	0.76	0.94
***	**	1.00	0.98	1.00	***	***	***	0.84	1.00	0.55
***	**	0.98	0.33	0.99	**	0.17	***	0.54	0.99	0.05
***	0.09	0.96	0.07	0.95	0.13	1.00	**	0.12	1.00	**
***	*	1.00	0.99	1.00	***	***	***	0.92	1.00	0.87
*	0.06	0.99	0.99	0.98	***	**	***	0.72	0.55	1.00
**	**	0.99	0.75	0.77	***	**	***	0.73	0.72	1.00
**	**	1.00	0.74	0.96	***	**	***	0.38	0.80	0.92
*	*	1.00	0.99	0.99	***	***	***	0.94	0.79	1.00
***	**	1.00	0.85	0.98	***	***	***	0.59	0.94	0.93
***	**	1.00	0.75	0.98	***	***	***	0.42	0.89	0.85
**	*	0.99	1.00	0.99	***	***	***	0.98	0.83	0.99
***	***	1.00	0.65	0.99	***	***	***	0.43	0.99	0.42
***	**	0.99	0.67	0.94	***	***	***	0.48	0.92	0.88
***	*	0.99	0.99	0.99	***	***	***	0.74	0.92	0.99
***	**	1.00	0.60	0.99	***	**	***	0.29	1.00	0.09
***	**	1.00	0.62	0.99	***	**	***	0.27	0.98	0.38
***	0.09	0.99	1.00	1.00	***	***	***	0.95	0.94	1.00
***	*	0.99	0.96	0.99	***	***	***	0.46	1.00	0.16
**	*	0.99	0.82	0.90	***	**	***	0.73	0.84	0.99
***	0.05	0.99	1.00	1.00	***	***	***	0.99	0.93	0.99
***	*	0.99	0.91	1.00	***	**	***	0.18	0.99	0.15
***	0.06	0.97	0.93	0.99	***	*	***	0.05	0.93	0.09
**	*	0.99	0.99	0.99	***	***	***	0.93	0.86	1.00
***	*	1.00	0.97	0.99	***	***	***	0.79	0.98	0.95
***	0.95	0.75	0.97	***	0.98	*	***	**	**	***
***	1.00	0.96	0.99	0.14	0.91	0.64	***	0.17	0.24	***
***	1.00	0.99	0.96	*	0.99	0.50	***	0.25	**	***
0.99	0.95	0.74	0.99	0.99	0.97	0.99	0.98	0.85	0.65	1.00
0.36	1.00	0.96	0.96	0.99	0.49	0.84	0.88	0.06	0.92	0.13
0.58	0.97	1.00	0.72	1.00	0.95	0.92	0.47	0.48	0.99	*

Table 2. Continued

Species Character	*bal—bid*	*bal—cha*	*bal—dor*	*bal—ker*	*bal—tav*	*bal—tir*	*bid—cha*	*bid—dor*	*bid—ker*	*bid—tav*
CX/CY	***	***	***	***	***	***	1.00	0.82	0.92	0.89
TIIIL/W	0.52	*	***	0.67	0.99	0.19	0.30	*	1.00	0.48
MtIL/W	***	0.99	***	***	***	**	**	0.98	1.00	0.99
MtIL/D	**	0.91	***	**	***	0.11	0.65	0.91	1.00	0.88
MtIIL/W	***	0.92	***	**	***	0.13	*	0.99	0.18	1.00
MtIIL/D	*	0.99	**	0.22	***	0.46	0.40	1.00	0.90	0.56
MtIIIL/W	***	0.96	***	***	***	0.09	0.10	0.98	1.00	**
MtIIIL/D	0.48	0.99	0.23	0.38	***	0.70	0.34	0.99	1.00	*
MtIVL/W	**	0.69	**	***	***	0.19	0.90	0.99	0.92	*
MtIVL/D	0.41	0.99	0.11	0.13	***	0.31	0.91	0.99	0.99	0.21
MtVL/W	**	0.32	***	*	***	0.73	0.99	0.96	0.99	0.58
MtVL/D	0.36	1.00	0.19	0.48	*	0.05	0.49	1.00	1.00	0.83
TL/W	***	0.85	*	0.81	***	0.99	*	**	***	0.99
TL/D	***	0.38	0.14	0.93	***	0.88	0.47	**	***	0.76
TW/D	1.00	0.58	0.99	0.99	0.53	0.91	0.40	0.99	1.00	0.22
Meristic characters										
MFDR	0.99	***	0.90	0.15	0.45	0.16	***	0.99	0.36	0.82
PDN	***	***	0.99	0.39	***	0.35	***	***	***	0.83
NLLAA	***	**	***	***	***	**	1.00	***	***	1.00
MtIIIVC	***	***	**	0.05	***	0.99	0.99	**	**	*
NVDAA	**	***	0.16	0.74	*	1.00	***	0.43	0.15	0.99

et al., 2008a: 3, 5, 13–14, 28, figs 18, 22, 52–55; 2008b: 1, 3, 15, 21, figs 33–36; 2008c: 3, 11–12, 17, figs 21–24; 2008d: 3, 7–8, 14, figs 27–30; Shahi *et al.*, 2008: 207, 210–212; Kovařík, 2009: 24; Lourenço & Duhem, 2009: 38, 44, 45, 48; Navidpour & Lowe, 2009: 49, 58; Pirali-Kheirabadi *et al.*, 2009: 1, 3, 9–10, 13, figs 10, 24–24; Vatani & Khoobdel, 2009: 7–8, 10; Lowe, 2010: 1–22, figs 1–65; Ramezani *et al.*, 2010: 55–56, 58–59, figs 2, 3, 5; Navidpour *et al.*, 2011: 3, 13, 22, figs 5, 8, 16, 21–24; Fekri *et al.*, 2012: 137, 138, 140; Karataş *et al.*, 2012: 116; Navidpour *et al.*, 2012: 3, 14, 23, figs 2, 4, 5, 11, 25, 26; Mirshamsi *et al.*, 2013: 153–170, figs 4–41; Mozaffari *et al.*, 2013: 5414, fig. 7; Navidpour *et al.*, 2013: 3, 11–14, 21, figs 3, 7, 10, 13–23, 38, 39; Pirali-Kheirabadi *et al.*, 2013: 48; Azghadi *et al.*, 2014: 169–179, figs 2, 6; Moradi *et al.*, 2014: 8; Navidpour & Mirshamsi, 2014: 112; Nejati *et al.*, 2014: 219–220; Ghassemi *et al.*, 2015: 264, 265, fig. 3; Kassiri *et al.*, 2015: 101–103, fig. 1; Moradi *et al.*, 2015: 13; Nazari *et al.*, 2015: 257, 259; Ahmadi *et al.*, 2016:1568; Ahmadimarzale *et al.*, 2017: 337–339; Dehghani & Kassiri, 2017: 433–438, figs 2, 3; Dehghani *et al.*, 2017:113–116, figs 1, 3; Sharifinia *et al.*, 2017: 243, 245, 246; Nejati *et al.*, 2018: 7141, 7142; Navidpour *et al.*, 2019: 2, 5, figs 45, 46, 49, 57; Barahoei *et al.*, 2020: 399–402, figs 18–20; Motevalli Haghi *et al.*, 2020: 69–72.

Odonbuthus: Pérez Minnocci, 1974: 28.

Diagnosis: The triangular sternum and absence of trichobothria on the ventral part of the pedipalp patella place *Odontobuthus* in the family Buthidae. The presence of prominent tooth-like processes (spiniform granules) on the ventrosubmedian carinae of metasomal segments II and III separate *Odontobuthus* from most other Iranian Buthidae, except *Buthacus tadmorensis* (Simon, 1892) and *Kraepelinia palpator* Vachon, 1974. Species of *Odontobuthus* are easily distinguished from *B. tadmorensis* by the lyriform configuration of the carapacial carinae, and from *Kraepelinia* by their larger size (> 35 mm) and relatively longer fingers of the pedipalp chela. *Kraepelinia* is also easily distinguished from *Odontobuthus* by the extremely thickened base of the aculeus, the height of which is about half the height of the telson vesicle in lateral aspect, much greater than in *Odontobuthus*.

Odontobuthus may be separated from other genera of Buthidae by the following combination of characters (Stahnke, 1972; Farzanpay, 1987; Lourenço & Pézier, 2002; Lowe, 2010; Mirshamsi *et al.*, 2013; Navidpour *et al.*, 2013): cheliceral movable finger with two ventral denticles; carapace dorsal surface entirely horizontal in lateral aspect; carapacial carinae distinct, with lyriform configuration; pedipalp trichobothriotaxy type A-β; trichobothrium *eb* situated at distal end of chela manus or on fixed finger; patella trichobothrium d_3 situated prolateral to dorsomedian carina; proximal

bid—tir	*cha—dor*	*cha—ker*	*cha—tav*	*cha—tir*	*dor—ker*	*dor—tav*	*dor—tir*	*ker—tav*	*ker—tir*	*tav—tir*
0.21	0.97	0.98	0.98	0.74	0.15	1.00	0.92	0.22	**	0.90
0.99	1.00	0.25	**	0.29	*	***	***	0.68	0.99	0.07
0.58	**	**	**	*	0.98	1.00	0.94	0.99	0.65	0.84
0.48	0.17	0.63	0.16	0.99	0.95	1.00	**	0.93	0.47	**
***	**	0.63	**	0.99	*	1.00	***	0.06	0.43	***
0.14	0.34	0.90	*	0.99	0.85	0.38	*	0.05	0.94	***
*	*	0.12	***	0.97	0.98	**	***	**	*	***
0.99	0.18	0.27	***	0.51	1.00	*	0.81	0.08	0.95	***
0.30	0.95	0.45	*	1.00	0.67	**	0.31	0.56	*	***
1.00	0.71	0.67	0.09	0.92	1.00	0.32	0.96	0.73	0.94	*
*	0.91	1.00	0.62	0.79	0.84	0.96	***	0.38	0.12	***
0.99	0.36	0.58	0.07	0.19	0.99	0.82	0.99	0.78	0.99	0.95
***	0.97	1.00	*	0.96	0.59	***	**	***	0.94	***
***	0.99	0.85	0.05	0.74	0.72	***	0.28	***	1.00	***
0.65	0.18	0.33	0.99	0.89	1.00	*	0.11	0.17	0.53	0.90
0.40	***	***	***	***	0.47	0.93	0.49	0.96	0.99	0.99
***	***	*	***	***	0.39	***	**	***	***	***
0.13	***	***	1.00	0.69	1.00	***	***	***	***	0.05
***	0.37	0.36	0.13	***	1.00	***	***	***	***	***
***	***	***	***	***	0.96	0.85	**	0.42	0.43	***

dentate margins of chela fixed and movable fingers not sexually dimorphic in adult male, i.e. without notch and lobe, respectively, in lateral aspect; median denticle row of chela fixed and movable fingers each comprising 10–14 oblique, non-imbricate subrows of denticles, each flanked by single prolateral and retrolateral accessory denticles; tibial spurs present on legs III and IV; pectines with fulcra; ventrosubmedian carinae of metasomal segments II and III comprising prominent tooth-like processes (spiniform granules); anteroventral carina of metasomal segment IV comprising prominent granules; ventrolateral carinae of metasomal segment V with prominent lobate processes; anal arch with prominent lobes laterally and reduced lobes posteroventrally; telson globose, without subaculear tubercle; hemispermatophore capsule with hook-like basal lobe and sperm hemiduct of three lobes.

ODONTOBUTHUS BALUCHICUS SP. NOV.

(FIGS 1–8, TABLES 1–5)

Zoobank registration: urn:lsid:zoobank.org:act:BA97ECB6-A884-4088-922A-FFAD47EA0C84

Odontobuthus doriae: Shahi *et al.*, 2008: 211 (misidentification); Fekri *et al.*, 2012: 137 (misidentification); Navidpour *et al.*, 2013: 12 (misidentification).

Type material: Holotype ♀ (SMF), three ♂♂, two ♀♀ paratypes (ZMFUM), IRAN: Sistan and Baluchistan Province: Nikshahr, Chanf, Goank village, 26°38′N 60°27′E, 1199 m, 3.viii.2017, H. Barahoei, daytime excavation, sandy soil.

Etymology: The specific epithet is an adjective, derived from Baluchistan, the Iranian province where the type locality is located.

Diagnosis: Odontobuthus baluchicus may be separated from other species of the genus by the following combination of characters. Scorpions of medium to large size, adults 66–68 mm (♂) and 56–82 mm (♀) (Fig. 6A–D). Colour yellow to brownish-green. Median ocular tubercle situated in anterior half of carapace, distance from anterior carapace margin, 0.35–0.39. Pedipalp chela movable finger long relative to manus (MFL/ML, 2.44–2.57). Median denticle rows of pedipalp chela fixed and movable fingers each comprising 13 or 14 oblique subrows of denticles. Pectinal tooth count, 29–31 (♂) and 20–24 (♀). Ventrosubmedian carinae of metasomal segments II and III each with two to four pairs of prominent tooth-like processes (Fig. 7C, D, G, H). Metasomal segment length to width (L/W), 1.83–2.11. Ventrolateral carinae of metasomal segment V with three or four

KEY TO IDENTIFICATION OF THE SPECIES OF *ODONTOBUTHUS*

1. Metasomal segment V, anal arch with two lobes laterally 2
- Metasomal segment V, anal arch with three lobes laterally 4
2. Metasomal segment II, ventrosubmedian carinae with three pairs of tooth-like processes ..... *O. doriae*
- Metasomal segment II, ventrosubmedian carinae with four or five pairs of tooth-like processes 3
3. Adult length, 66–68 mm (♂), 56–82 mm (♀); metasomal segment I longer than wide ..... *O. baluchicus*
- Adult length, 43–55 mm (♂), 48–68 mm (♀); metasomal segment I equal to or wider than long .. *O. kermanus*
4. Colour greenish brown; metasomal segment III, ventrosubmedian carinae with four or five pairs of tooth-like processes; segment V, anal arch with two large and one small lobes laterally ..... O. *tirgari*
- Colour light brown to yellow; metasomal segment III, ventrosubmedian carinae with two or three pairs of tooth-like processes; segment V, anal arch with three large lobes laterally 5
5. Colour light brown; pedipalp chela movable finger, median denticle row comprising 13 or 14 subrows; metasomal segment I equal to or wider than long; segments II and III, ventrosubmedian carinae with two pairs of tooth-like processes 6
- Colour yellow; pedipalp chela movable finger, median denticle row comprising 10–12 subrows; metasomal segment I longer than wide; segments II and III, ventrosubmedian carinae with three or more pairs of tooth-like processes 7
6. Metasomal segment V, anal arch with four reduced lobes posteroventrally ..... *O. bidentatus*
- Metasomal segment V, anal arch with six reduced lobes posteroventrally ..... *O. tavighiae*
7. Metasomal segment V, anal arch with six lobes posteroventrally; adult length < 50 mm; occurs in India and Pakistan ..... *O. odonturus*
- Metasomal segment V, anal arch with two distinct lobes posteroventrally; adult length > 50 mm; does not occur in India or Pakistan 8
8. Pedipalp chela movable finger short relative to chela manus (MFL/ML = 1.40–1.75); pectinal tooth count (♀), 20–25; occurs in the Arabian Peninsula (Oman and United Arab Emirates ..... *O. brevidigitus*
- Pedipalp chela movable finger long relative to chela manus (MFL/ML = 2.00–2.30); pectinal tooth count (♀), 18–20; occurs in Iran ..... *O. chabaharensis*

prominent lobate processes; anal arch with two prominent lobes laterally; posteroventral margin of metasomal segment V with six reduced lobes. Telson small, narrow, length to width (TL/W), 2.22–2.63 and length to height (TL/H), 2.42–2.63 (Fig. 7A, B, E, F).

Affinities: *Odontobuthus baluchicus* is closely related to *O. doriae*, with which it shares the presence of two prominent lateral lobes on the anal arch of metasomal segment V, and differs from all other species of the genus, which possess three lateral lobes. It differs from *O. doriae* in its coloration, longer than wide metasomal segment I and three pairs of prominent tooth-like processes on the ventrosubmedian carinae of metasomal segment II, and from *O. kermanus* in its larger body size and longer than wide metasomal segment I.

Description: Based on holotype ♀ (SMF) (Figs 6A, B, 7A–D, 8A, C, E) and paratype ♂ (ZMFUM 1302) (Figs 6C, D, 7E–H, 8B, D, F). **Measurements:** ♀: BL: 71.0; CL: 8.0; CWP: 9.3; CWA: 5.6; CX: 3.2; CY: 8.1; CHL: 15.4; ML: 4.3; MFL: 11.1; MtIL: 5.5; MtIH: 4.1; MtIW: 5.4; MtIIL: 6.0; MtIIH: 3.9; MtIIW: 4.7; MtIIIL: 6.2; MtIIIH: 3.8; MtIIIW: 4.2; MtIVL: 7.2; MtIVH: 3.6; MtIVW: 4.1; MtVL: 8.5; MtVH: 3.3; MtVW: 3.4; TL: 8.1; TW: 3.5; TH: 3.2. ♂: BL: 67.8; CL: 7.2; CWP: 7.6; CWA: 4.7; CX: 2.7; CY: 7.0; CHL: 14.7; ML: 4.2; MFL: 10.5; MtIL: 5.8; MtIH: 5.2; MtIW: 4.3; MtIIL: 6.5; MtIIH: 3.8; MtIIW: 4.6; MtIIIL: 6.7; MtIIIH: 3.5; MtIIIW: 4.0; MtIVL: 7.8; MtIVH: 3.2; MtIVW: 3.8; MtVL: 9.0; MtVH: 3.0; MtVW: 3.0; TL: 7.3; TW: 3.0; TH: 3.0. **Colour:** Carapace and mesosoma brownish-green, slightly paler ventrally; dark pigmentation around median and lateral ocelli. Pedipalps and legs lighter, distal part of femur and proximal part of patella darker especially on legs III and IV. Pectines light yellow to cream. Metasoma brown to yellow, segments darker dorsally, segment V darker than preceding segments. Telson vesicle yellowish-brown; aculeus brown anteriorly, becoming dark brown to black posteriorly. **Chelicerae:** Fixed finger ventral

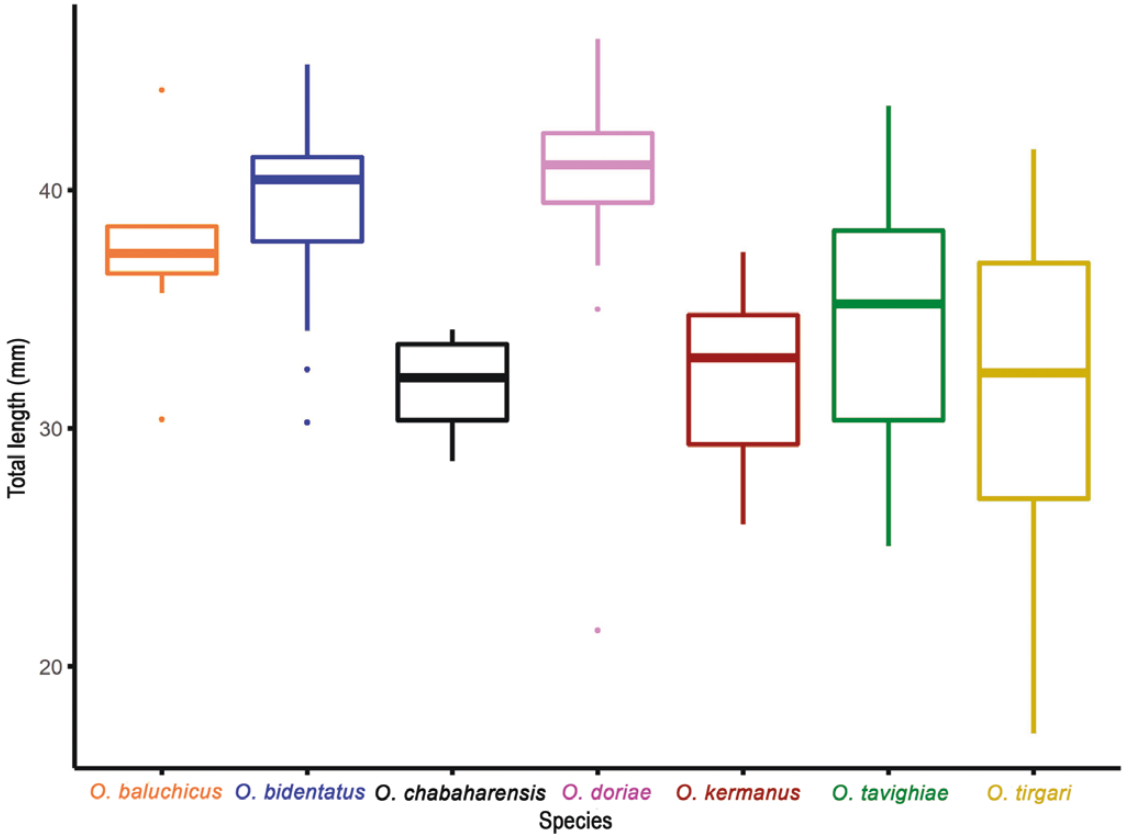

Figure 2. Boxplots of sex-corrected total length for species of *Odontobuthus* occurring in Iran.

Table 3. Pairwise MANOVA test among species of the buthid scorpion genus *Odontobuthus* occurring in Iran, using 38 sex-corrected shape variables (N = 149 specimens). Significant P values indicated in boldface

	O. baluchicus	***O. bidentatus***	***O. chabaharensis***	***O. doriae***	***O. kermanus***	***O. tavighiae***
O. bidentatus	**0.0003**	–	–	–	–	–
O. chabaharensis	**0.0034**	0.1276	–	–	–	–
O. doriae	**0.0035**	0.1901	0.1716	–	–	–
O. kermanus	**0.0035**	**0.0050**	0.0680	**0.0081**	–	–
O. tavighiae	**0.0035**	**0.0029**	**0.0038**	**0.0010**	**0.0038**	–
O. tirgari	**0.0090**	**0.0016**	0.1276	**0.0003**	**0.0048**	**0.0003**

surface with two basal denticles. Movable finger prolateral and retrolateral distal denticles equal in size. **Carapace:** Trapezoid, wider than long, CWA/CL, 0.70 (♀) or 0.65 (♂), CWP/CL, 1.16 (♀) or 1.05 (♂); anterior margin moderately emarginate; median ocular tubercle situated in anterior half of carapace, CX/CL, 0.40 (♀) or 0.37 (♂), CX/CY, 0.39 (♀) or 0.38 (♂), distance between median ocelli twice ocular diameter; five pairs of lateral ocelli (Fig. 6A, C); anteromedian and posteromedian sulci deep (♂) or shallow (♀); posterolateral sulci wide, curved; carinae distinct, central lateral and posteromedian carinae completely aligned; anteromedian carinae granular; central median, posteromedian and central lateral carinae granular (♀) or serratocrenulate (♂); intercarinal surfaces of prosoma finely granular. **Pedipalps:** Pedipalp segments relatively long. Femur 3.8 (♀) or 3.9 (♂) times longer than wide; four complete, granular carinae; retrodorsal, prodorsal and proventral carinae granular (♀) or serratocrenulate (♂); prolateral carinae comprising isolated spiniform

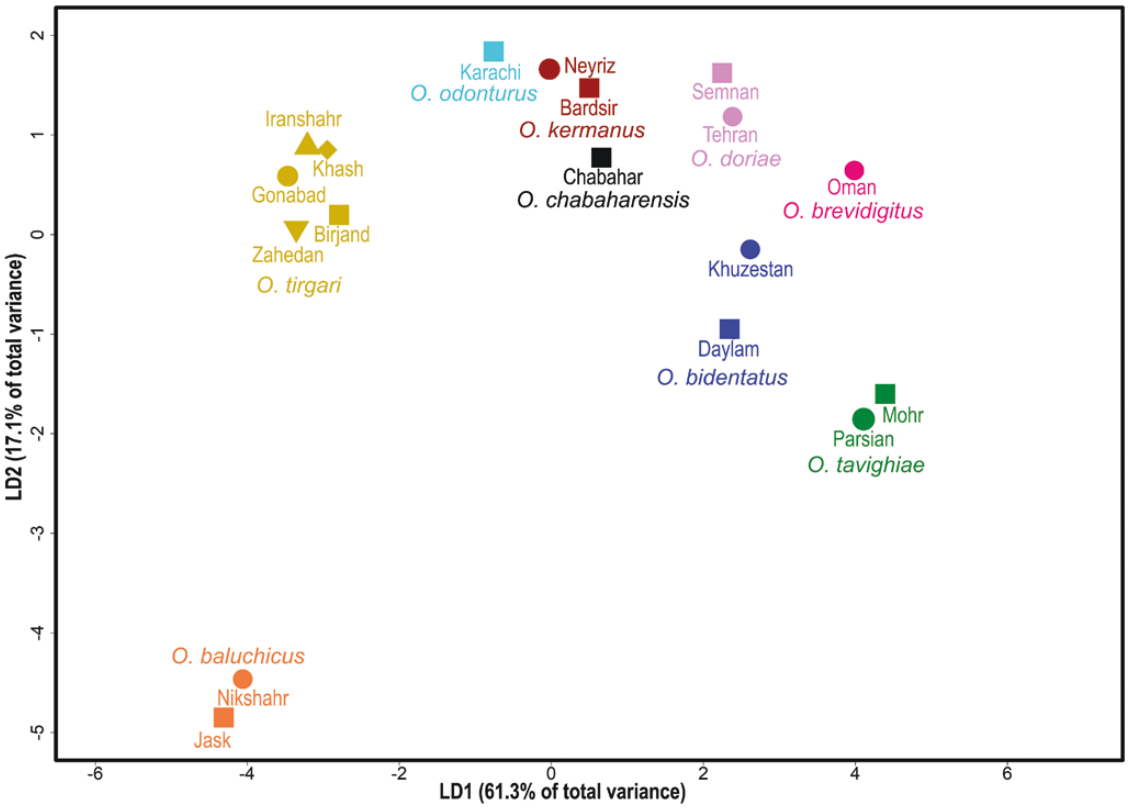

Figure 3. Linear discriminant analysis (LDA) of 38 metric and five meristic variables among 18 populations of *Odontobuthus*. Conspecific populations in same colour.

granules; intercarinal surfaces smooth (Fig. 8A, B). Patella 2.96 (♀) or 3.5 (♂) times longer than wide; eight complete carinae; prodorsal carinae distinct, granular; dorsomedian, retrodorsal, retrolateral, retroventral and ventromedian carinae obsolete to moderate, smooth (Fig. 8C); proventral and prolateral carinae comprising several spiniform granules (♂) (Fig. 8D). Chela 3.6 (♀) or 3.5 (♂) times longer than manus; manus narrower (♀) or wider (♂) than patella; fingers 2.6 (♀) or 2.5 (♂) times longer than manus; median denticle subrows, including proximal subrow (left/right) of fixed finger, 13/13 and movable finger, 14/14; all subrows except proximal flanked by prolateral and retrolateral accessory denticles; movable finger with five (♂) or six (♀) subdistal denticles, two prolateral and three (♂) or four (♀) retrolateral. Orthobothriotaxic type A-β, with following segment totals: femur, 11 (five dorsal, four internal, two external) (Fig. 8A, B), patella, 13 (five dorsal, one internal, seven external) (Fig. 8C, D) and chela, 15 (eight manus, seven fixed finger) (Fig. 8E, F), totalling 39 trichobothria per pedipalp; trichobothria *esb* (fixed finger), *Esb*, Eb_3 (manus), d_2 (patella) and d_2 (femur) petite; trichobothrium *et* adjacent to proximal (♀) or distal (♂) end of median denticle subrow 7; *est* adjacent to midpoint (♀) or distal end (♂) of subrow 9 (Fig. 8E, F). **Legs:** Legs III and IV each with tibial spurs; I–IV each with bifurcate prolateral pedal spurs; telotarsi, ventral surfaces with two rows of fine setae. **Sternum:** Type I, triangular; slightly wider than long (♀) or longer than wide (♂); with deep median depression. **Genital operculum:** Completely divided longitudinally with fine, short bristles (Fig. 6B, D). **Pectines:** Distal margin extending to (♀) or beyond (♂) coxa-trochanter joint of leg IV; three marginal and eight (♀) or nine (♂) median lamellae; fulcra present; teeth present along entire posterior margin of pecten, count (left/right), 29/30 (♂) and 21/21 (♀). **Mesosoma:** Tergites I–VI tricarinate; VII pentacarinate, lateral carinae granular (♀) or serratocrenulate (♂), median carinae incomplete, restricted to anterior half of segment and weakly granular; intercarinal surfaces finely (♀) or coarsely (♂) granular. Sternites III–VI acarinate; VII with four moderate, granular carinae, lateral carinae restricted to anterior half of segment. **Metasoma:** Metasomal segment I decacarinate; II–IV octocarinate; V pentacarinate; all complete carinae moderately to markedly granular on segments

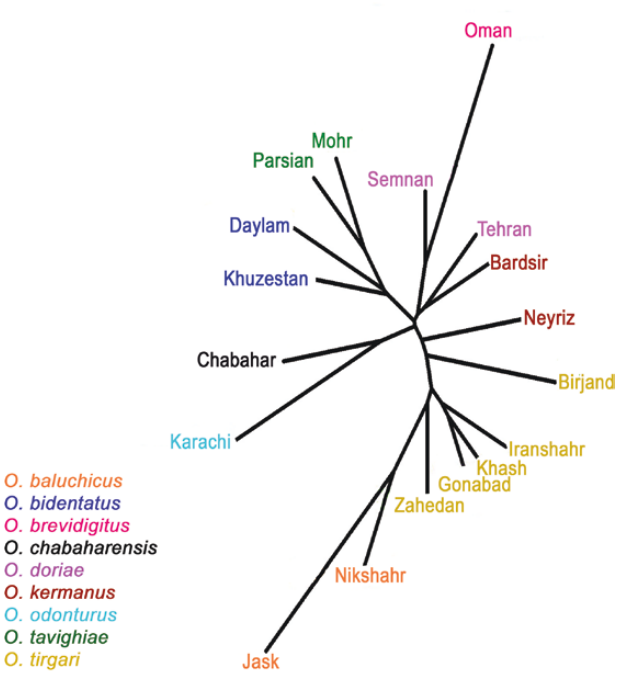

Figure 4. Neighbour-joining phenogram generated from morphometric Mahalanobis distance matrix of 18 populations of *Odontobuthus*. Conspecific populations in same colour.

I–III and weakly to moderately granular on IV (♀) or weakly to moderately granular on I–IV (♂). Lateral inframedian carinae incomplete, restricted to posterior half of segment II; vestigial, reduced to few granules posteriorly, on III. Ventrosubmedian carinae on segments II and III each with four pairs of rounded (♀) or subtriangular (♂) tooth-like processes. Anteroventral margins of segment III with six large, rounded granules, IV with four (♂) to six (♀) large, rounded granules. Ventrolateral carinae on segment V markedly dentate with large, rounded (♀) or subtriangular (♂) lobate processes posteriorly; anal arch with two large (♀) or one small and two large (♂) lobes laterally and six distinct lobes posteroventrally (Fig. 7A–H). **Telson:** Oblong-ovoid, TH/TL, 0.39 (♀) or 0.41 (♂), TW/TL, 0.43 (♀) or 0.41 (♂); slightly wider than (TW/MtVW, 1.02) (♀) (Fig. 7A, B) or similar to (TW/MtVW, 1.00) (♂) (Fig. 7E, F) width of metasomal segment V; dorsal surface flat, ventral surface curved, smooth (♀) or sparsely granular (♂).

Distribution: Odontobuthus baluchicus is endemic to Iran and recorded in only two provinces: Hormozgan; Sistan and Baluchistan. The distributions of *O. baluchicus*, in south-eastern Iran, and *O. kermanus*, in central Iran, are allopatric.

Additional material: IRAN: Hormozgan Province: Jask–Beshagard road, 25°50′N 57°50′E, 149 m, 6.iv.2018, H. Barahoei, daytime excavation, four ♀♀ (ZMFUM). Sistan and Baluchistan Province: Nikshahr, Konari village, 26°20′N 60°06′E, 660 m, 3.iv.2018, H. Barahoei, daytime excavation, sandy soil, two ♀♀, one subad. ♀ (ZMFUM).

Odontobuthus bidentatus Lourenço & Pézier, 2002

(Figs 1–5, 15A–D, 20A, 21A, 22A, Tables 1–5)

Odontobuthus doriae: Habibi, 1971: 44; Farzanpay, 1987: 154–156; Farzanpay, 1990: 7; Akbari *et al.*, 1997:112; Kovařík, 1997:47, 49, figs 11–13; Pooladgar, 1999: 176.

Odontobuthus bidentatus Lourenço & Pézier, 2002: 118–122, figs 1–27; Navidpour *et al.*, 2008a: 3, 5, 13–14, 28, figs 18, 22, 52–55; 2008b: 1, 3, 15, 21, figs 33–36; 2008c: 3, 11–12, 17, figs 21–24; 2008d: 3, 7–8, 14, figs 27–30; Pirali-Kheirabadi *et al.*, 2009: 1, 3, 9–10, 13, fig. 10; Lowe, 2010: 1, 5, 15, 16, 17, figs 31, 32, 43, 44, 45–48, 51–55, 58, 59, 60–63; Navidpour *et al.*, 2011: 3, 13, 22, figs 5, 8, 16, 21–24; Karataş *et al.*, 2012: 116; Navidpour *et al.*, 2012: 3, 14, 23, figs 2, 4, 5, 11, 25, 26; Mirshamsi *et al.*, 2013: 153–160, 168, figs 1–3; Azghadi *et al.*, 2014: 169–170, 172–173, 176–178, figs 1, 2g–i; Kassiri *et al.*, 2015: 101; Ahmadi *et al.*, 2016: 1568; Sharifinia *et al.*, 2017: 243, 245, 246; Nejati *et al.*, 2018: 7141, 7142; Barahoei *et al.*, 2020: 399, 400, figs 18, 20.

Type material: Holotype ♂ (MHNG), IRAQ: Khanagin-Dyala, 180 km N of Baghdad, ii.1964, G. Pringle.

Diagnosis: Odontobuthus bidentatus may be separated from other species of the genus by the following combination of characters. Scorpions of medium to large size, adults 51–76 mm (♂) and 56–83 mm (♀) (Fig. 15). Colour yellow. Median ocular tubercle situated in anterior half of carapace, distance from anterior carapace margin, 0.32–0.37. Pedipalp chela movable finger long relative to manus (MFL/ML, 1.93–2.51). Median denticle rows of pedipalp chela fixed and movable fingers each comprising 13 or 14 oblique subrows of denticles. Pectinal tooth count, 33–35 (♂) and 24–29 (♀). Ventrosubmedian carinae of metasomal segments II and III each with two to three pairs of prominent tooth-like processes (Fig. 22A). Metasomal segment IV length to width (L/W), 1.67–2.09. Ventrolateral carinae

Table 4. Provenance data (country, province or governate and abbreviated locality) for tissue samples from which DNA was extracted, deposited in the collections of the Zoological Museum of Ferdowsi University of Mashhad (ZMFUM), Iran, and the Ambrose Monell Cryocollection (AMCC) at the American Museum of Natural History, New York, USA, and Genbank accession codes of DNA sequences from the *COI* gene among species of *Odontobuthus* and two outgroup species of *Buthus* used for molecular phylogenetic analysis.

Species	Collection	Locality	Genbank
B. occitanus	–	SPAIN	GQ168524.1
B. paris	–	MOROCCO	KF548111.1
O. baluchicus	ZMFUM 1303	IRAN: *Sistan and Baluchistan*: Nikshahr	MW655753
	ZMFUM 1306	IRAN: *Sistan and Baluchistan*: Nikshahr	MW655754
	ZMFUM 1307	IRAN: *Sistan and Baluchistan*: Nikshahr	MW655755
	ZMFUM 1309	IRAN: *Hormozgan*: Jask	MW655756
O. bidentatus	ZMFUM 1314	IRAN: *Bushehr*: Daylam	MW655752
	ZMFUM 1316	IRAN: *Bushehr*: Daylam	MW655751
	AMCC [LP 9702]	IRAN: *Khuzestan*: Baghmalek	MW655776
	ZMFUM 2061	IRAN: *Khuzestan*: Omidiyeh	KF701314
	ZMFUM 2062	IRAN: *Khuzestan*: Omidiyeh	KF701315
	ZMFUM 2063	IRAN: *Khuzestan*: Omidiyeh	KF701316
	ZMFUM 2076	IRAN: *Fars*: Kazerun	KF701317
O. brevidigitus	ZMFUM 1438	OMAN: *Al Wusta*: Wadi Rawnab	MW655773
	AMCC [LP 14256]	OMAN: *Al Dakhiliyah*: Bahla	MW655777
	AMCC [LP 15780]	OMAN: *Muscat*: Bimma	MW655778
O. chabaharensis	ZMFUM 1323	IRAN: *Sistan and Baluchistan*: Chabahar	MW655757
	ZMFUM 1326	IRAN: *Sistan and Baluchistan*: Chabahar	MW655758
O. doriae	ZMFUM 1328	IRAN: *Semnan*: Semnan	MW655795
	AMCC [LP 2908]	IRAN: *Yazd*: Ardakan	MW655779
	AMCC [LP 4350]	IRAN: *Tehran*: Tehran	MW655780
	ZMFUM 2001	IRAN: *Tehran*: Tehran	KF701309
	ZMFUM 2004	IRAN: *Tehran*: Tehran	KF701311
O. kermanus	ZMFUM 1330	IRAN: *Fars*: Neyriz	MW655793
	ZMFUM 1338	IRAN: *Kerman*: Bardsir	MW655760
	ZMFUM 1339	IRAN: *Kerman*: Bardsir	MW655759
	AMCC [LP 11067]	IRAN: *Kerman*: Bardsir	MW655775
	ZMFUM 2151	IRAN: *Kerman*: Bardsir	KF701325
	ZMFUM 2152	IRAN: *Kerman*: Bardsir	KF701326
O. odonturus	AMCC [LP 7008]	PAKISTAN	MW655784
	AMCC [LP 11333]	PAKISTAN: *Punjab*: Bhakar	MW655781
	AMCC [LP 11421]	PAKISTAN: *Punjab*: Kalar Kahar	MW655782
	AMCC [LP 11487]	PAKISTAN: *Punjab*: Aliabad	MW655783
O. tavighiae	ZMFUM 1346	IRAN: *Hormozgan*: Parsian	MW655761
	ZMFUM 1351	IRAN: *Hormozgan*: Parsian	MW655762
	ZMFUM 1365	IRAN: *Fars*: Mohr	MW655763
	ZMFUM 1366	IRAN: *Fars*: Mohr	MW655764
	ZMFUM 2074	IRAN: *Hormozgan*: Behdeh	KF701323
	ZMFUM 2075	IRAN: *Hormozgan*: Behdeh	KF701324

Table 4. Continued

Species	Collection	Locality	Genbank
O. tirgari	ZMFUM 1369	IRAN: *Sistan and Baluchistan*: Zahedan	MW655771
	ZMFUM 1372	IRAN: *Sistan and Baluchistan*: Zahedan	MW655794
	ZMFUM 1374	IRAN: *Sistan and Baluchistan*: Khash	MW655772
	ZMFUM 1379	IRAN: *Sistan and Baluchistan*: Zahedan	MW655765
	ZMFUM 1387	IRAN: *South Khorasan*: Birjand	MW655766
	ZMFUM 1401	IRAN: *Sistan and Baluchistan*: Khash	MW655767
	ZMFUM 1406	IRAN: *Sistan and Baluchistan*: Khash	MW655768
	ZMFUM 1425	IRAN: *Sistan and Baluchistan*: Iranshahr	MW655769
	ZMFUM 1433	IRAN: *Sistan and Baluchistan*: Khash	MW655770
	AMCC [LP 15795]	IRAN: *Sistan and Baluchistan*: Khash	MW655774
	ZMFUM 2099	IRAN: *Razavi Khorasan*: Gonabad	KF701318
	ZMFUM 2100	IRAN: *Razavi Khorasan*: Gonabad	KF701319
	ZMFUM 2133	IRAN: *Razavi Khorasan*: Gonabad	KF701320
	ZMFUM 2136	IRAN: *Razavi Khorasan*: Gonabad	KF701322

of metasomal segment V with three or four prominent lobate processes; anal arch with three prominent lobes laterally; posteroventral margin of metasomal segment V with four reduced lobes. Telson small, narrow, length to width (TL/W), 1.94–2.27 and length to height (TL/H), 2.00–2.43 (Figs 20A, 21A).

Distribution: Odontobuthus bidentatus has been recorded in Iraq (Lourenço & Pézier, 2002) and five provinces of Iran: Bushehr; Fars; Ilam; Khuzestan; Kohgilouyeh and Boyer Ahmad (Habibi, 1971; Farzanpay, 1987, 1990; Akbari *et al.*, 1997; Kovařík, 1997; Pooladgar, 1999; Lourenço & Pézier, 2002; Navidpour *et al.*, 2008a, 2008b, 2008c, 2008d, 2012; Lowe, 2010; Karataş *et al.*, 2012; Azghadi *et al.*, 2014; Kassiri *et al.*, 2015; Ahmadi *et al.*, 2016; Sharifinia *et al.*, 2017; Nejati *et al.*, 2018).

Material examined: IRAN: *Bushehr Province:* Abdan, 28°09′N 51°39′E, 108 m, 14.iv.2018, H. Barahoei, daytime excavation, loam, one ♀ (ZMFUM); Bushehr to Dayer road, Jeirani village, 27°51′N 51°46′E, xi.2007, B. Masihipour, H. Bahrani & A. Habibzadeh, Bu-22, one ♀ (AMCC [LP 11083]); Park Jangali-e Ameri, 20 km N of Deylam Port, 30°12′N 50°10′E, 44 m, 15.iv.2018, H. Barahoei, daytime excavation, silty soil, one ♂, one ♀ (ZMFUM); Tangestan, Farshanbeh, 28°53′N 51°19′E, 95 m, xi.2007, B. Masihipour, H. Bahrani & A. Habibzadeh, Bu-35.1, 1 ♀ [AMCC (LP 11084)]. *Khuzestan Province:* Baghmalek, 31°55′N 49°22′E, 185 m, i.2007, M. Kazemi, BA839/1, one ♀ [AMCC (LP 9702)]; Omidiyeh, 30°57′N 49°31′E, 23.iii.2007, H. Barahoei, two ♂♂, ten ♀♀ (ZMFUM); Sardasht, Tal-e Chega Oliya, 30°17′N 50°11′E, 44 m, 15.iv.2018, H. Barahoei, daytime excavation, two ♂♂, one ♀, one subad. ♀ (ZMFUM).

ODONTOBUTHUS BREVIDIGITUS LOWE, 2010

(FIGS 1, 3–5,16A, B, 20B, 21B, 22B, TABLES 1, 4, 5)

Odontobuthus brevidigitus Lowe, 2010: 2–15, figs 1–30, 37–38, 49–57, 60–65; Mirshamsi *et al.*, 2013: 153, 169; Azghadi *et al.*, 2014: 169, 175, 178.

Type material: Holotype ♂ (NHMB), OMAN: Batinah Plain, *c.* 4 km E of Seeb, 23°41.39′N 58°06.93′E, 0 m, 22.x.1993, G. Lowe & A. S. Gardner.

Diagnosis: Odontobuthus brevidigitus may be separated from other species of the genus by the following combination of characters. Scorpions of medium size, adults 50–65 mm (Fig. 16A, B). Colour golden yellow. Median ocular tubercle situated in anterior half of carapace, distance from anterior carapace margin, 0.34. Pedipalp chela movable finger short relative to manus (MFL/ML, 1.40–1.75). Median denticle rows of pedipalp chela fixed and movable fingers each comprising 10–12 oblique subrows of denticles. Pectinal tooth count, 29–36 (♂) and 20–25 (♀). Ventrosubmedian carinae of metasomal segments II and III each with two or three pairs of prominent tooth-like processes (Fig. 22B). Metasomal segment IV length to width (L/W), 1.67–1.96. Ventrolateral carinae of metasomal segment V with several prominent spiniform processes; anal arch with three lateral lobes;

Table 5. Average Kimura 2-parameter (K2P) genetic distances for 53 DNA sequences of the *COI* gene among and within (boldface) species of *Odontobuthus* and two outgroup species of *Buthus*. Standard error estimate(s) shown above the boldface diagonal

	O. bidentatus	***O. baluchicus***	***O. brevidigitus***	***O. chabaharensis***	***O. doriae***	***O. kermanus***	***O. odonturus***	***O. tirgari***	***O. tavighiae***	***B. paris***	***B. occitanus***
O. bidentatus	**0.021**	0.013	0.013	0.013	0.016	0.014	0.015	0.015	0.013	0.017	0.015
O. baluchicus	0.1	**0.030**	0.014	0.014	0.015	0.014	0.013	0.013	0.014	0.016	0.019
O. brevidigitus	0.109	0.113	**0.043**	0.012	0.016	0.014	0.015	0.014	0.012	0.016	0.018
O. chabaharensis	0.101	0.108	0.092	**0.018**	0.015	0.016	0.016	0.015	0.012	0.016	0.017
O. doriae	0.135	0.124	0.139	0.125	**0.013**	0.017	0.016	0.016	0.014	0.017	0.017
O. kermanus	0.109	0.103	0.116	0.118	0.134	**0.025**	0.015	0.01	0.015	0.016	0.016
O. odonturus	0.112	0.09	0.119	0.113	0.125	0.111	**0.008**	0.015	0.017	0.017	0.017
O. tirgari	0.108	0.095	0.117	0.114	0.126	0.059	0.112	**0.014**	0.015	0.016	0.018
O. tavighiae	0.089	0.103	0.084	0.084	0.114	0.1	0.126	0.103	**0.005**	0.017	0.017
B. paris	0.132	0.13	0.137	0.125	0.143	0.127	0.134	0.123	0.133	–	0.018
B. occitanus	0.116	0.159	0.145	0.139	0.138	0.124	0.134	0.137	0.13	0.139	–

posteroventral margin of metasomal segment V with two large lobes. Telson small, narrow, length to width (TL/W), 1.86–2.40 and length to height (TL/H), 2.09–2.40) (Figs 20B, 21B).

Distribution: Odontobuthus brevidigitus is endemic to the Arabian Peninsula and has only been recorded from Oman and the United Arab Emirates (Lowe, 2010).

Material examined: OMAN: *Al Dakhiliyah Governate:* Bahla Public Picnic Site, *c.* 3.5 km SW Bahla, 22°56′N 57°16′E, 533 m, 19–20.v.2017, L. Prendini & M. Roppo, arid savanna on alluvial floodplain near rocky hills, many large and smaller *Acacia* trees and spiny bushes on compact greyish alluvial silt, powdery with crust, somewhat degraded, specimens very common, mostly excavated during daytime from burrows, *c.* 30–50 cm deep in open ground and near bushes, others collected with UV light detection on warm, still, moonless night, many doorkeeping at burrow entrances, few collected sitting on ground surface, eight ♂♂, seven ♀♀ (AMNH), one juv. ♀ [AMCC (LP 14256)]. *Al Wusta Governate:* Wadi Rawnab, 18°49′N 56°24′E, 111 m, 15.v.2019, M. Stockmann, daytime excavation, one ♂ (ZMFUM). *Muscat Governate:* Bimma, 22°58′N 59°10′E, 7 m, iii.2017, M. Seiter & A. Ullrich, one juv. ♀ [AMCC (LP 15780)].

ODONTOBUTHUS CHABAHARENSIS SP. NOV.

(FIGS 1–5, 9–11, TABLES 1–5)

Zoobank registration: urn:lsid:zoobank.org:act:9D7EDE35-D7A4-4212-98C1-62875DE1B881

Type material: Holotype ♀ (SMF), one ♂, two ♀♀ paratypes (ZMFUM), IRAN: *Sistan and Baluchistan Province:* Chabahar, Parak-e Sheykhan village, 25°30′N 60°35′E, 19 m, 13.vi.2019, H. Barahoei, daytime excavation, silty clay.

Etymology: The specific epithet is an adjective derived from Chabahar, the type locality.

Diagnosis: Odontobuthus chabaharensis may be separated from other species of the genus by the following combination of characters. Scorpions of small to medium size, adults 36 mm (♂) and 53–63 mm (♀) (Fig. 9A–D). Colour golden yellow. Median ocular tubercle situated in anterior half of carapace, distance from anterior carapace margin, 0.33–0.36. Pedipalp chela movable finger long relative to manus (MFL/ML, 2.00–2.30). Median denticle rows of pedipalp chela fixed and movable fingers each comprising 12 oblique subrows of denticles. Pectinal tooth count,

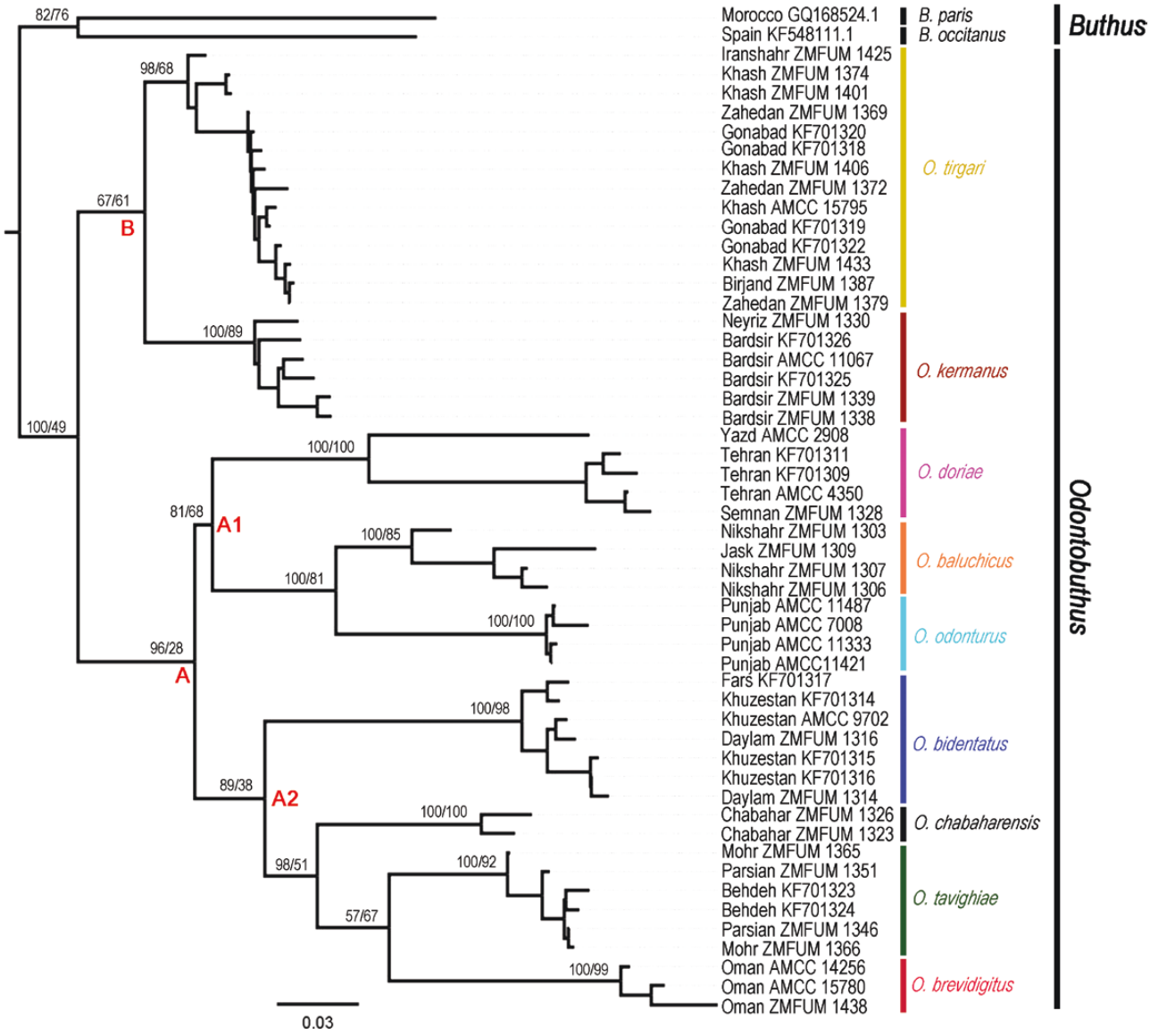

Figure 5. Fifty per cent majority rule consensus obtained by analysis of partial DNA sequences of mitochondrial *COI* gene from *Odontobuthus* with Bayesian inference (BI). Nodal support values above branches represent posterior probability values from BI and bootstrap values from maximum likelihood analyses, respectively. Letters A and B refer to clades also recovered by Azghadi *et al.* (2014).

31 (♂) and 18–20 (♀). Ventrosubmedian carinae of metasomal segments II and III each with two or three pairs of large spiniform processes (Fig. 10C, D, G, H). Metasomal segment IV length to width (L/W), 1.82–1.93. Ventrolateral carinae of metasomal segment V with two or three prominent lobate processes; anal arch with three prominent spiniform lobes laterally; posteroventral margin of segment V with two prominent lobes. Telson small, wide, length to width (TL/W), 2.26–2.50 and length to height (TL/H), 2.26–2.57 (Fig. 10A, B, E, F).

Affinities: Odontobuthus chabaharensis is closely related to *O. odonturus*, with which it shares the presence of three prominent lateral lobes on the anal arch of metasomal segment V. It differs from

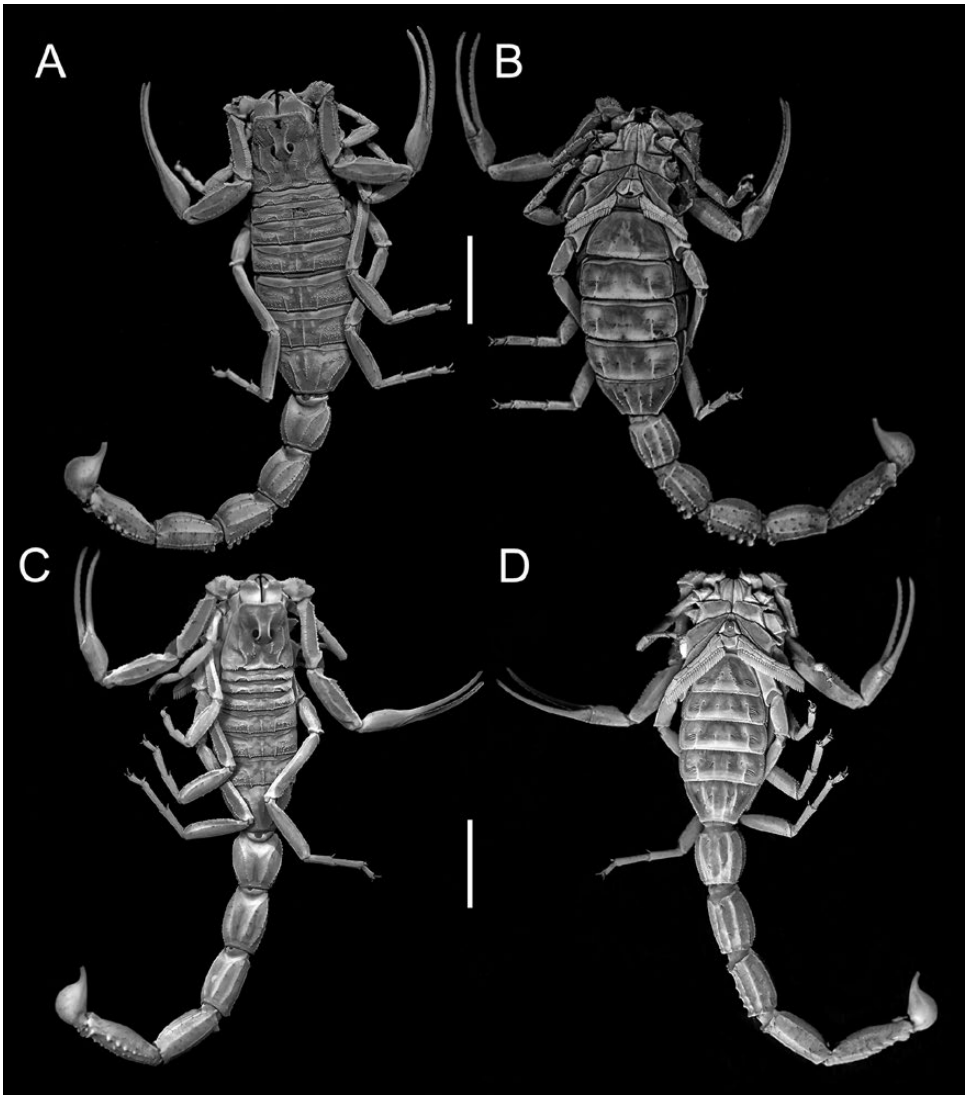

Figure 6. *Odontobuthus baluchicus*. Habitus, dorsal aspect (A, C), ventral aspect (B, D). A, B, holotype ♀ (SMF). C, D, paratype ♂ (ZMFUM 1302). Scale bars = 10 mm.

all other species of the genus, except *O. brevidigitus*, in the presence of two large conical lobes on the posteroventral margin of metasomal segment V, and from *O. brevidigitus* in possessing longer pedipalp chela fingers, e.g. the movable finger length to manus length (MFL/ML) is 2.00–2.30 in *O. chabaharensis* compared with 1.40–1.75 in *O. brevidigitus*, and a lower pectinal tooth count in the female, 18–20 in *O. chabaharensis* compared with 20–25 in *O. brevidigitus*.

Description: Based on holotype ♀ (SMF) (Figs 9A, B, 10A–D, 11A, C, E) and paratype ♂ (ZMFUM 1324) (Figs 9C, D, 10E–H, 11B, D, F). As for *O. baluchicus* except where noted. **Measurements:** ♀: BL: 62.1; CL: 7.6; CWP: 8.8; CWA: 5.2; CX: 2.5; CY: 7.2; CHL: 13.5; ML: 4.5; MFL: 9.0; MtIL: 4.6; MtIH: 3.7; MtIW: 4.2; MtIIL: 5.2; MtIIH: 3.5; MtIIW: 3.9; MtIIIL: 5.6; MtIIIH: 3.3; MtIIIW: 3.6; MtIVL: 6.6; MtIVH: 3.2; MtIVW: 3.5; MtVL: 8; MtVH: 2.8; MtVW: 3.3; TL: 8.5; TW: 3.4; TH: 3.3. ♂: BL: 35.8; CL: 4.5; CWP: 5.0; CWA: 3.4; CX: 1.6; CY: 4.4; CHL: 8.6; ML: 2.6; MFL: 6.0; MtIL: 2.7; MtIH: 2.2; MtIW: 2.5; MtIIL: 3.0; MtIIH: 2.0; MtIIW: 2.3; MtIIIL: 3.2; MtIIIH: 1.9; MtIIIW: 2.1; MtIVL: 4.0; MtIVH: 1.8; MtIVW: 2.1; MtVL: 4.9; MtVH: 1.5; MtVW: 1.8; TL: 4.5; TW: 1.9; TH: 1.9. **Colour:** Carapace and mesosoma light brown, slightly paler ventrally; dark pigmentation around median and lateral ocelli. Legs lighter. Pectines light yellow to cream. Metasoma yellowish-brown. Telson vesicle yellow to yellowish-brown; aculeus light brown anteriorly, becoming dark brown to black posteriorly. **Carapace:** Trapezoid, wider

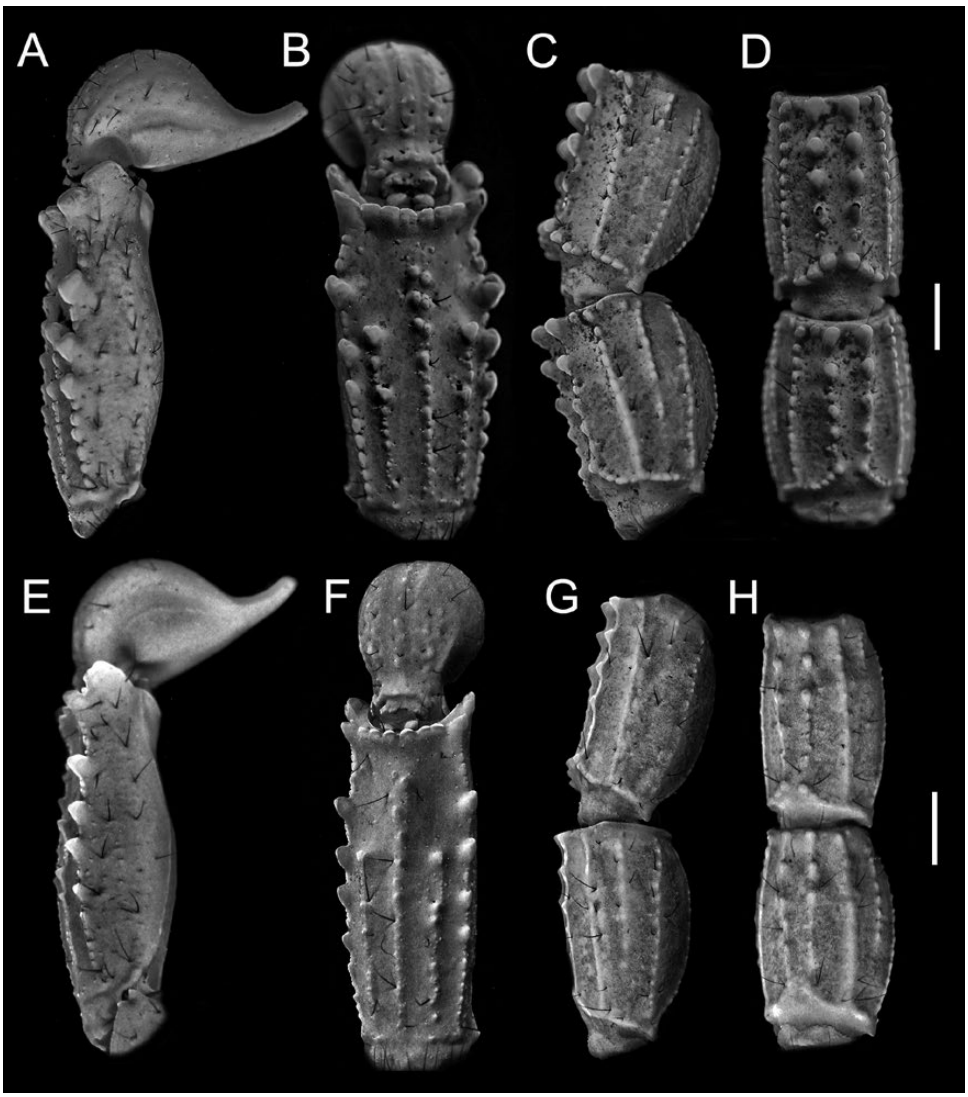

Figure 7. *Odontobuthus baluchicus*. Metasomal segment V and telson, lateral aspect (A, E), ventral aspect (B, F), metasomal segments II and III, lateral aspect (C, G), ventral aspect (D, H). A–D, holotype ♀ (SMF). E–H, paratype ♂ (ZMFUM 1302). Scale bars = 3 mm (A–D), 2.5 mm (E–H).

than long, CWA/CL, 0.68 (♀) or 0.75 (♂), CWP/CL, 1.15 (♀) or 1.11 (♂); anterior margin moderately emarginate; median ocular tubercle situated in anterior half of carapace, CX/CL, 0.32 (♀) or 0.35 (♂), CX/CY, 0.34 (♀) or 0.36 (♂), distance between median ocelli twice ocular diameter; five pairs of lateral ocelli (Fig. 9A, C); anteromedian and posteromedian sulci shallow; posterolateral sulci wide, curved; carinae distinct, central lateral and posteromedian carinae completely aligned; anteromedian carinae granular; central median, posteromedian and central lateral carinae granular (♀) or serratocrenulate (♂); intercarinal surfaces of prosoma finely granular. **Pedipalps:** Pedipalp segments relatively short. Femur 3.1 (♀) or 3.4 (♂) times longer than wide; four complete, granular carinae; retrodorsal, prodorsal and proventral carinae granular (♀) or serratocrenulate (♂); prolateral carinae comprising isolated spiniform granules; intercarinal surfaces smooth (Fig. 11A, B). Patella 2.53 (♀) or 3.06 (♂) times longer than wide; eight complete carinae; prodorsal carinae distinct (♀) or moderate (♂), granular; dorsomedian, retrodorsal, retrolateral, retroventral and ventromedian carinae obsolete to moderate, smooth (Fig. 11C, D); proventral and prolateral carinae comprising several spiniform granules (♂) (Fig. 11C, D). Chela 3.0 (♀) or 3.3 (♂) times longer than manus; manus as wide as (♂) or wider than (♀) patella; fingers 2 (♀) or 3.3 (♂) times longer than manus; median denticle subrows, including proximal subrow (left/right) of fixed finger, 11/11 and movable finger, 12/12;

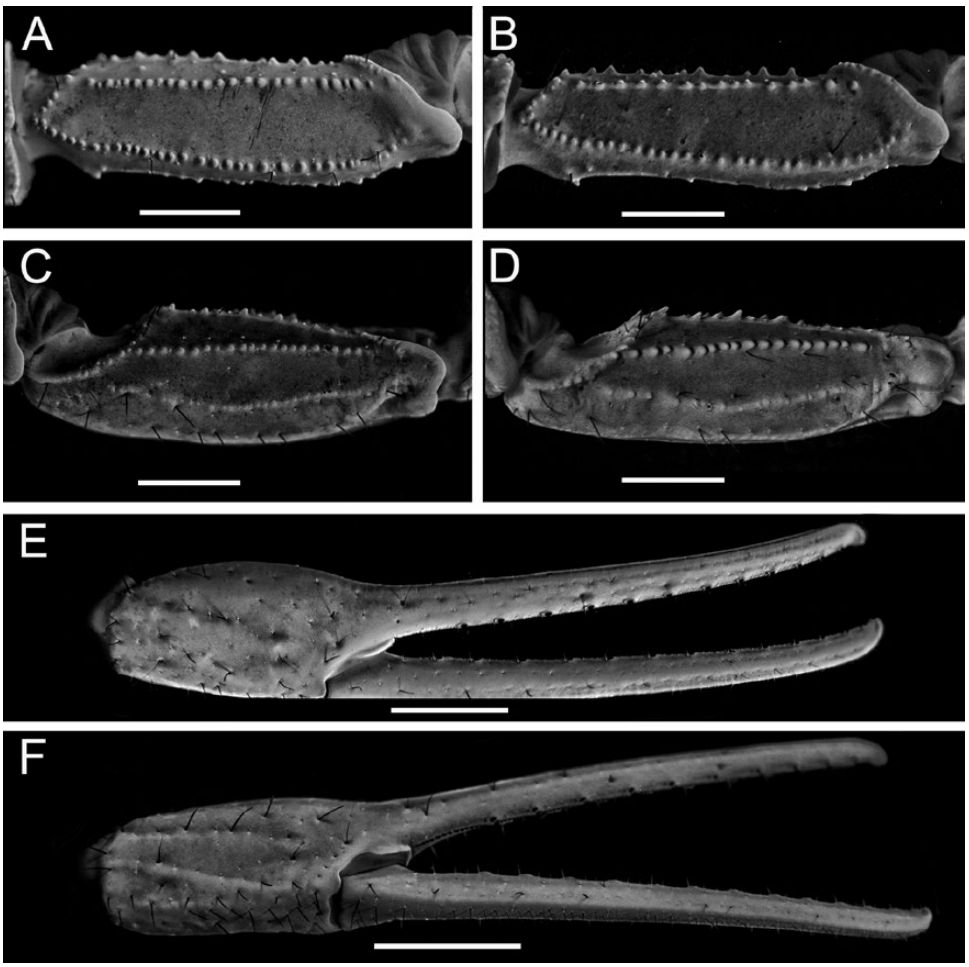

Figure 8. *Odontobuthus baluchicus*. Pedipalp femur, dorsal aspect (A, B), patella, dorsal aspect (C, D) and chela, lateral aspect (E, F). A, C, E, holotype ♀ (SMF). B, D, F, paratype ♂ (ZMFUM 1302). Scale bars = 2.5 mm.

all subrows except proximal flanked by prolateral and retrolateral accessory denticles; movable finger with five (♂) or six (♀) subdistal denticles, one (♀) or two (♂) prolateral and four retrolateral. Trichobothrium *et* adjacent to midpoint of denticle subrow 7; *est* adjacent to midpoint (♂) (Fig. 11F) or proximal end (♀) (Fig. 11E) of denticle subrow 9. **Sternum:** Type I, triangular; longer than wide; with deep median depression. **Genital operculum:** Completely divided longitudinally with fine, short bristles (Fig. 9B, D). **Pectines:** Distal margin extending to (♀) or beyond (♂) coxa-trochanter joint of leg IV; three marginal and seven median lamellae; fulcra present; teeth present along entire posterior margin of pecten, count (left/right), 31/31 (♂) and 19/19 (♀). **Mesosoma**: Tergites I–VI tricarinate; VII pentacarinate, lateral carinae granular (♀) or serratocrenulate (♂), median carinae incomplete, restricted to anterior half of segment and weakly granular; intercarinal surfaces finely granular (♀) or smooth (♂). Sternites III–VI acarinate; VII with four moderate (♀) or obsolete (♂), granular carinae, lateral carinae complete (♂) or restricted to anterior half of segment (♀). **Metasoma:** Metasomal segment I decacarinate; II–IV octocarinate; V pentacarinate; all complete carinae moderately to markedly granular on segments I–III and weakly to moderately granular on IV (♀) or weakly to moderately granular on I–IV (♂). Lateral inframedian carinae almost complete (♀) or incomplete, restricted to posterior two-thirds (♂), on segment II, incomplete, restricted to posterior half (♀) or vestigial, reduced to few granules posteriorly (♂) on III. Ventrosubmedian carinae on segments II and III each with three pairs of prominent conical, tooth-like processes. Anteroventral margins of segments III and IV each with six large, conical granules. Ventrolateral carinae on segment V dentate with (♂) or without (♀) large, subtriangular lobate processes posteriorly; anal arch with three large, conical lobes laterally and two large, conical lobes posteroventrally (Fig. 10A–H). **Telson:** Oblong-ovoid, TH/TL, 0.38 (♀) or 0.42 (♂), TW/

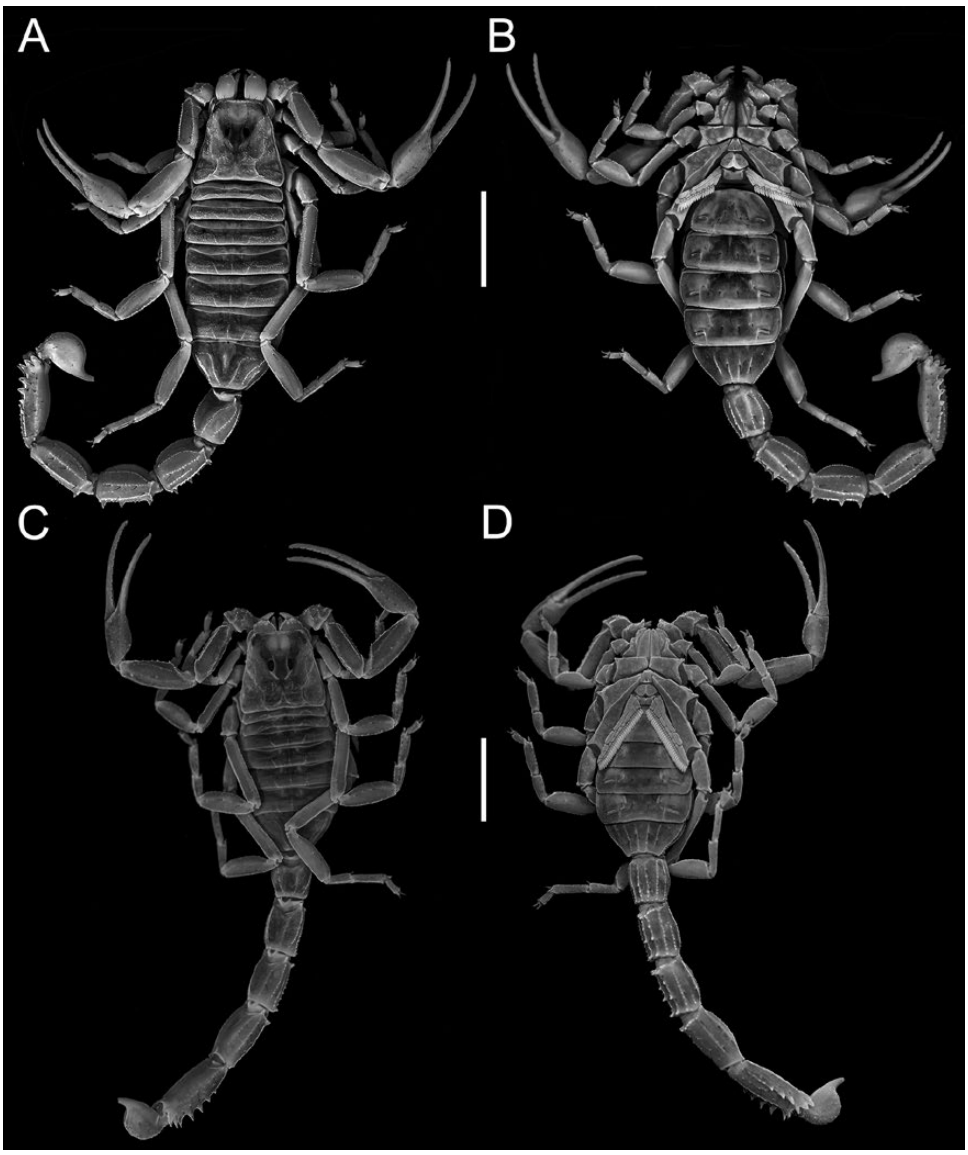

Figure 9. *Odontobuthus chabaharensis*. Habitus, dorsal aspect (A, C), ventral aspect (B, D). A, B, holotype ♀ (SMF). C, D, paratype ♂ (ZMFUM 1325). Scale bars = 10 mm (A, B), 5 mm (C, D).

TL, 0.40 (♀) or 0.42 (♂); wider than metasomal segment V, TW/MtVW, 1.03 (♀) or 1.05 (♂) (Fig. 10A, B, E, F); dorsal surface flat, ventral surface curved, smooth (♀) or sparsely granular (♂).

Distribution: *Odontobuthus chabaharensis* is endemic to Iran and recorded only from Sistan and Baluchistan Province.

Additional material: IRAN: *Sistan and Baluchistan Province:* Parak-e Hootan road, 20 km NW of Chabahar, 25°28′N 60°33′E, 1 m, 3.iv.2018, H. Barahoei, daytime excavation, silty clay, one ♀, one juv. (ZMFUM); Chabahar, N of Parak-e Sheykhan village, 25°30′N 60°35′E, 19 m, 16.xi.2018, H. Barahoei, daytime excavation, silty clay, one ♀ (ZMFUM); Mekran, vii.1913, Kei, one ♂ (ZMH).

ODONTOBUTHUS DORIAE (THORELL, 1876)

(FIGS 1–5, 17A–D, 20C, 21C, 22C, TABLES 1–5)

Buthus doriae Thorell, 1876: 107–110; Simon, 1880: 29; Kraepelin, 1891: 57, 58, pl. I, figs 6, 10; Kraepelin, 1899: 27; Birula, 1900a: 10, 11; Pocock, 1900: 16–18,

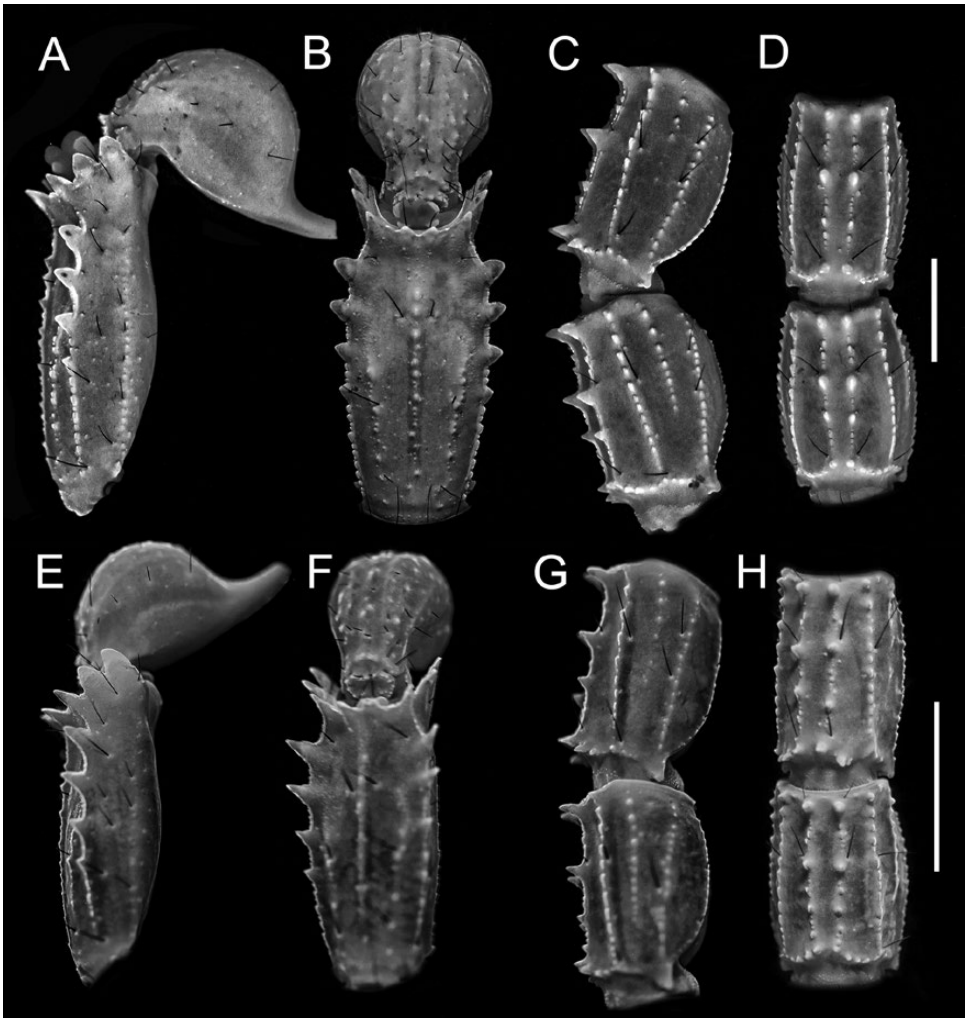

Figure 10. *Odontobuthus chabaharensis*. Metasomal segment V and telson, lateral aspect (A, E), ventral aspect (B, F), metasomal segments II and III, lateral aspect (C, G), ventral aspect (D, H). A, C, E, holotype ♀ (SMF). B, D, F, paratype ♂ (ZMFUM 1325). Scale bars = 2.5 mm.

fig. 8B; Kraepelin, 1901: 267; Birula, 1905: 121, 122; Birula, 1910: 119, 120; Kraepelin, 1913: 124, 125; Werner, 1929: 243, 244; Werner, 1936: 204; Whittick, 1955: (unpaginated).

Buthus (*Buthus*) *doriae:* Birula, 1917: 23, 214; Roewer, 1943: 206.
Buthus (*Buthus*) *doriae doriae:* Birula, 1917: 239.
Odontobuthus doriae: Vachon, 1950: 153, 154; Vachon, 1952: 326; Pringle, 1960: 83, fig. 8; Khalaf, 1963: 59; Vachon, 1966: 213; Habibi, 1971: 44; Kinzelbach, 1985: map I; Farzanpay, 1987: 154, 155; Farzanpay, 1988: 39; Farzanpay, 1990: 7; Sissom, 1990: 92, fig. 3.17J; El-Hennawy, 1992: 102, 128; Kovarik, 1997: 47, 49, fig. 11; Dehghani *et al.*, 1998: 126; Kovarik, 1998: 115; Fet & Lowe, 2000: 187; Kovařík, 2002: 9; Lourenço & Pézier, 2002: 115, 116, 122, figs 1–4; Vignoli & Crucitti, 2005: 6–7; Pirali-Kheirabadi *et al.*, 2009: 1, 3, 9, 13, figs 24–27; Lowe, 2010: 1, 2, 6, 15–17; Karataş *et al.*, 2012: 116; Navidpour *et al.*, 2012: 3, 14, 23, fig. 15; Mirshamsi *et al.*, 2013: 160, 170; Mozaffari *et al.*, 2013: 5414, fig.7; Navidpour *et al.*, 2013: 12, 13, figs 7, 10, 38; Pirali-Kheirabadi *et al.*, 2013: 48; Azghadi *et al.*, 2014: 169–178, fig. 2d–f; Moradi *et al.*, 2014: 8; Moradi *et al.*, 2015: 13; Nazari *et al.*, 2015: 257, 259; Ahmadimarzale *et al.*, 2017: 337–339; Dehghani & Kassiri, 2017: 433–438; Dehghani *et al.*, 2017: 113–116; Navidpour *et al.*, 2019: 2, 5; Barahoei *et al.*, 2020: 400, 401, figs 19, 20.
Odonbuthus doriae: Pérez Minnocci, 1974: 28.

Type material: Two syntypes (MCSN), IRAN: *Tehran Province*: Tehran.

Diagnosis: Odontobuthus doriae may be separated from other species of the genus by the following

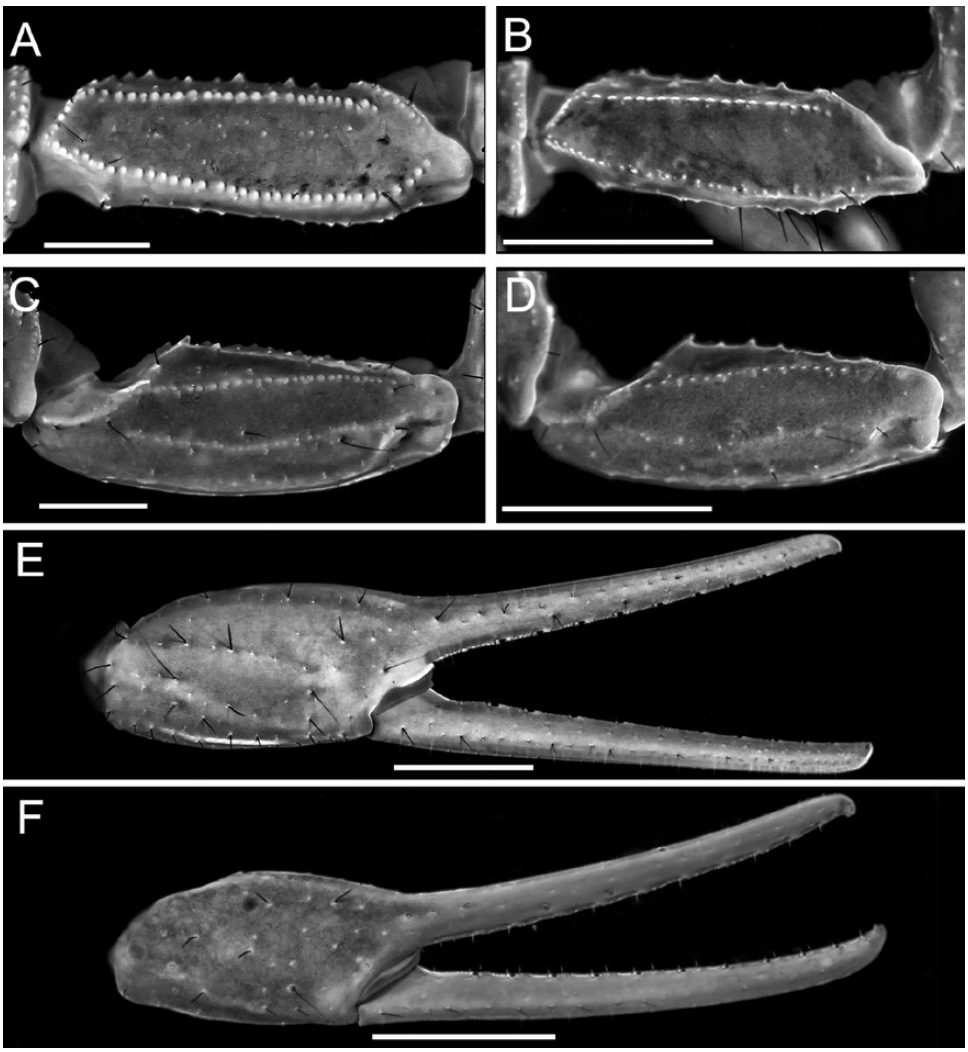

Figure 11. *Odontobuthus chabaharensis*. Pedipalp femur, dorsal aspect (A, B), patella, dorsal aspect (C, D) and chela, lateral aspect (E, F). A, C, E, holotype ♀ (SMF). B, D, F, paratype ♂ (ZMFUM 1325). Scale bars = 2.5 mm (A–D), 2 mm (E, F).

combination of characters. Scorpions of medium to large size, adults 48–72 mm (♂) and 64–84 mm (♀) (Fig. 17A–D). Colour yellow to pale yellow. Median ocular tubercle situated in anterior half of carapace, distance from anterior carapace margin, 0.32–0.37. Pedipalp chela movable finger long relative to manus (MFL/ML, 1.81–2.25). Median denticle rows of pedipalp chela fixed and movable fingers each comprising 13 or 14 oblique subrows of denticles. Pectinal tooth count, 30–32 (♂) and 21–25 (♀). Ventrosubmedian carinae of metasomal segments II and III each with three or four pairs of prominent tooth-like processes (Fig. 22C). Metasomal segment IV length to width (L/W), 1.70–2.00. Ventrolateral carinae of metasomal segment V with four or five prominent lobate processes; anal arch with two large lobes laterally; posteroventral margin of segment V with six reduced lobes. Telson small, narrow, length to width (TL/W), 2.05–2.60 and length to height (TL/H), 2.14–2.71 (Figs 20C, 21C).

Distribution: Odontobuthus doriae is endemic to Iran and recorded in 14 provinces: Alborz; Chahar mahal and Bakhtiyari; East Azerbaijan; Esfahan; Hamadan; Ilam; Kermanshah; Lorestan; Qazvin; Qom; Semnan; Tehran; Yazd; Zanjan (Kraepelin, 1899; Pocock, 1900; Vachon, 1966; Habibi, 1971; Farzanpay, 1987, 1990; Kovařík, 1997, 2002; Dehghani *et al.*, 1998, 2017; Lourenço & Pézier, 2002; Vignoli & Crucitti, 2005;

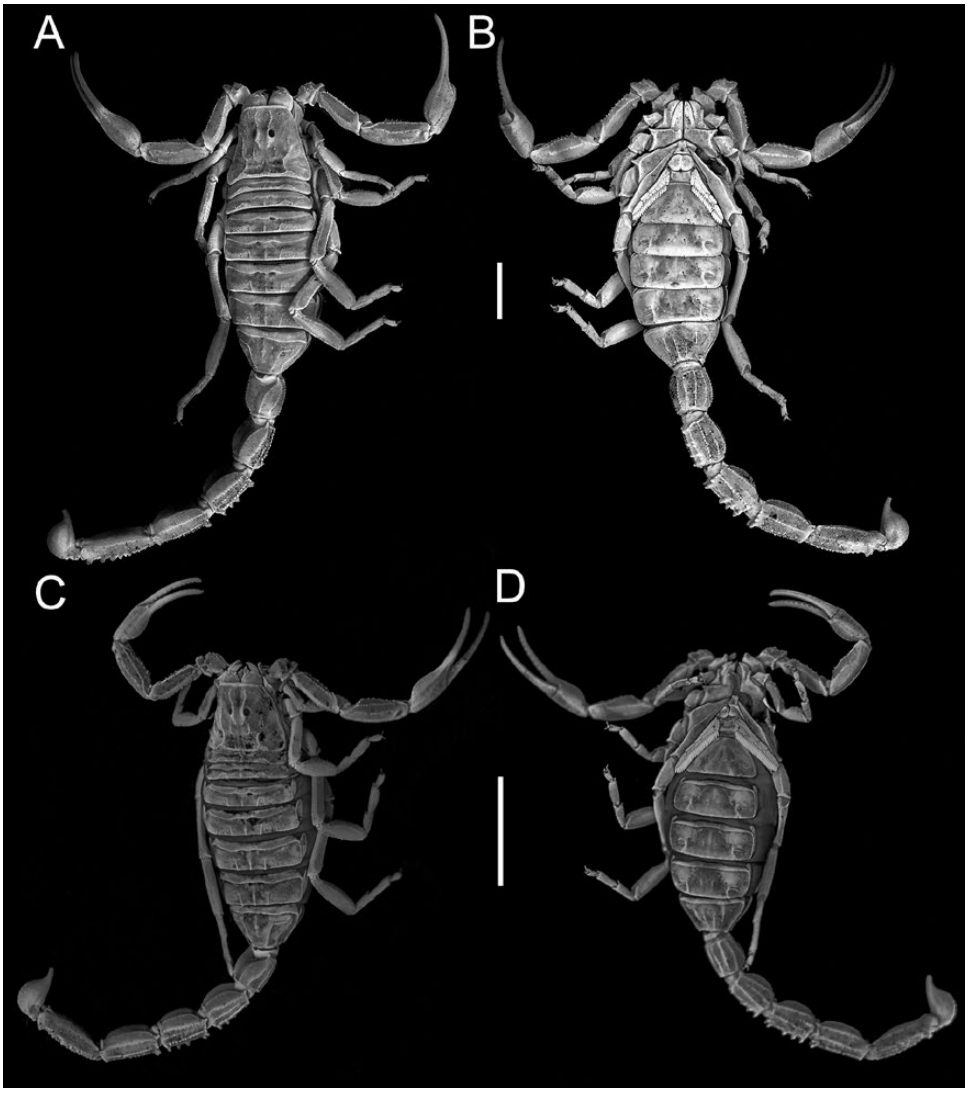

Figure 12. *Odontobuthus kermanus*. Habitus, dorsal aspect (A, C), ventral aspect (B, D). A, B, holotype ♀ (SMF). C, D, paratype ♂ (ZMFUM 1340). Scale bars = 10 mm (A, B), 5 mm (C, D).

Pirali-Kheirabadi *et al.*, 2009, 2013; Lowe, 2010; Karataş *et al.*, 2012; Navidpour *et al.*, 2012, 2019; Mozaffari *et al.*, 2013; Azghadi *et al.*, 2014; Moradi *et al.*, 2014, 2015; Nazari *et al.*, 2015; Ahmadimarzale *et al.*, 2017).

Records of *O. doriae* from Kerman Province (Dehghani *et al.*, 2008: 176; Navidpour *et al.*, 2011: 13) are misidentifications of *O. kermanus*. Records from Hormozgan Province (Shahi *et al.*, 2008: 211; Fekri *et al.*, 2012: 137; Navidpour *et al.*, 2013: 12) are probably misidentifications of *O. baluchicus*. Material originating from Fars, Kermanshah, Ilam, Lorestan and Yazd provinces require further investigation. Material from Kermanshah, Ilam and Lorestan provinces, to the east of the Zagros Mountains, may be referable to *O. bidentatus*; from the north, east, and southwest of Fars, to *O. doriae*, *O. kermanus* and *O. bidentatus*, respectively; and from Yazd, to *O. kermanus*.

Material examined: IRAN: *Semnan Province:* Mehdishahr, Darjazin, 35°37′N 53°21′E, 4388 m, 5.viii.2018, M. Amiri, night with UV light, two ♀♀ (ZMFUM); Semnan, T. Habibi, one ♂, two ♀♀, one subad. ♂, one subad. ♀ (ZMFUM); Semnan, Desert Research Center, 35°35′N 53°26′E; 1182 m, 1.viii.2004, Mohammadi, two ♀♀ (ZMFUM). *Tehran Province:* Teheran, Von Brandis, seven ♀♀, one subad. ♀ (ZMB 7500); Teheran, 1903, one ♂, one ♀ (SAM 6511 ex Museo Torino); Tehran, 15 km SE, 30°41′N 51°25′E, 30.v.2011, O. Mirshamsi, two ♂♂, 28 ♀♀ (ZMFUM); Varamin, v.2005, S. Tehrani, one ♀ [AMCC (LP 4350)];

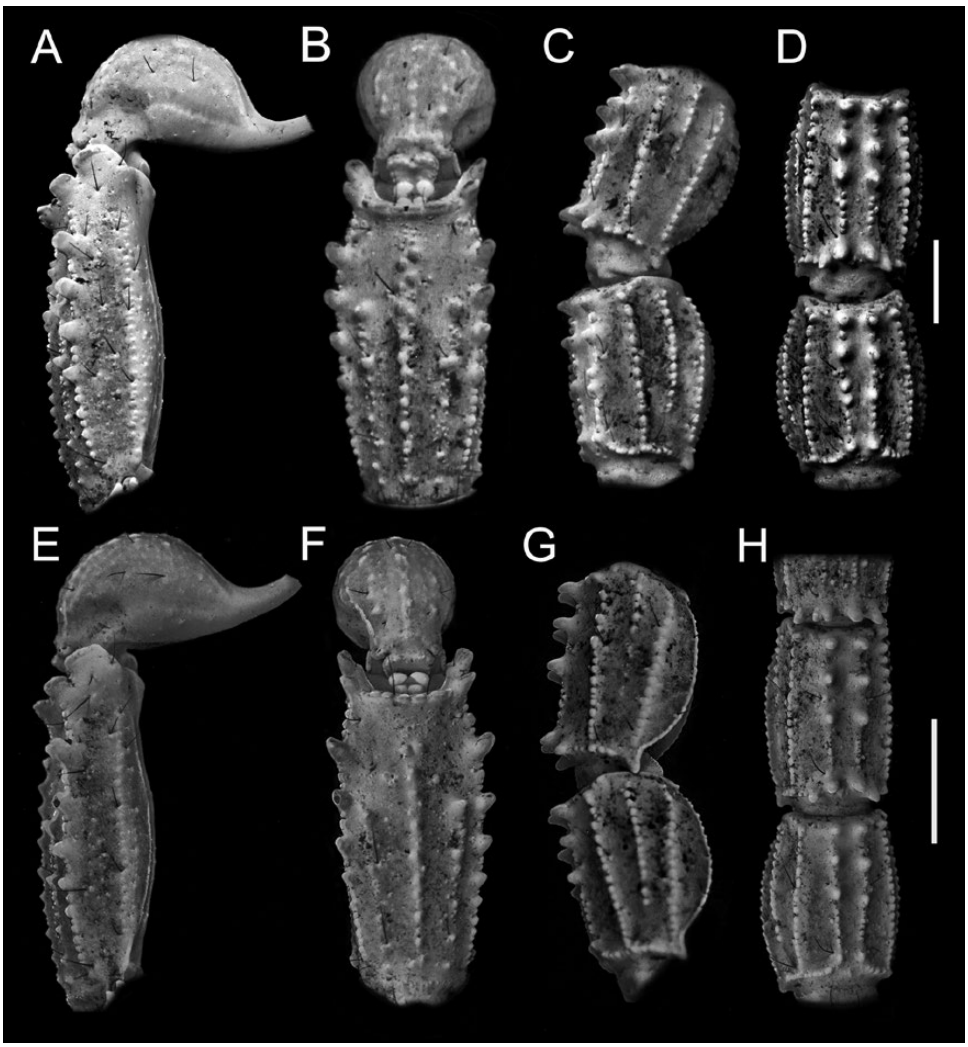

Figure 13. *Odontobuthus kermanus*. Metasomal segment V and telson, lateral aspect (A, E), ventral aspect (B, F), metasomal segments II and III, lateral aspect (C, G), ventral aspect (D, H). A, C, E, holotype ♀ (SMF). B, D, F, paratype ♂ (ZMFUM 1340). Scale bars = 3 mm (A–D), 2.5 mm (E–H).

Varamin, Pishva, Ghale boland village; 39°19′N 51°39′E, 27.x.2008, Mohammadi, one ♂ (ZMFUM). *Yazd Province:* Ardakan, 10 km E, 32°19′N 54°15′E, 1235 m, 11.iv.2004, V. Vignoli & P. Crucitti, VVZC Y165, one ♀ [AMCC (LP 2908)].

ODONTOBUTHUS KERMANUS SP. NOV.

(FIGS 1–5, 12–14, TABLES 1–5)

Zoobank registration: urn:lsid:zoobank.org:act:98D4CF43-580A-43E0-890D-50C5ED84BFD9

Odontobuthus doriae: Dehghani *et al.* 2008: 176 (misidentification); Navidpour *et al.* 2011: 13 (misidentification).

Type material: Holotype ♀ (SMF), two ♂♂, four ♀♀, one subad. ♂ paratypes (ZMFUM), IRAN: *Kerman Province:* Bardsir–Negar–Baft road, 29°58′N 56°42′E, 2238 m, 16.iv.2018, H. Barahoei, daytime excavation, sand.

Etymology: The specific epithet is an adjective, derived from the Iranian province of Kerman, where the type was collected.

Diagnosis: Odontobuthus kermanus may be separated from other species of the genus by the following combination of characters. Scorpions of small to medium size, adults 43–55 mm (♂) and 48–68 mm (♀) (Fig. 12A–D). Colour yellow to yellowish green. Median ocular tubercle situated in anterior half of carapace, distance from anterior carapace margin, 0.31–0.39. Pedipalp chela movable

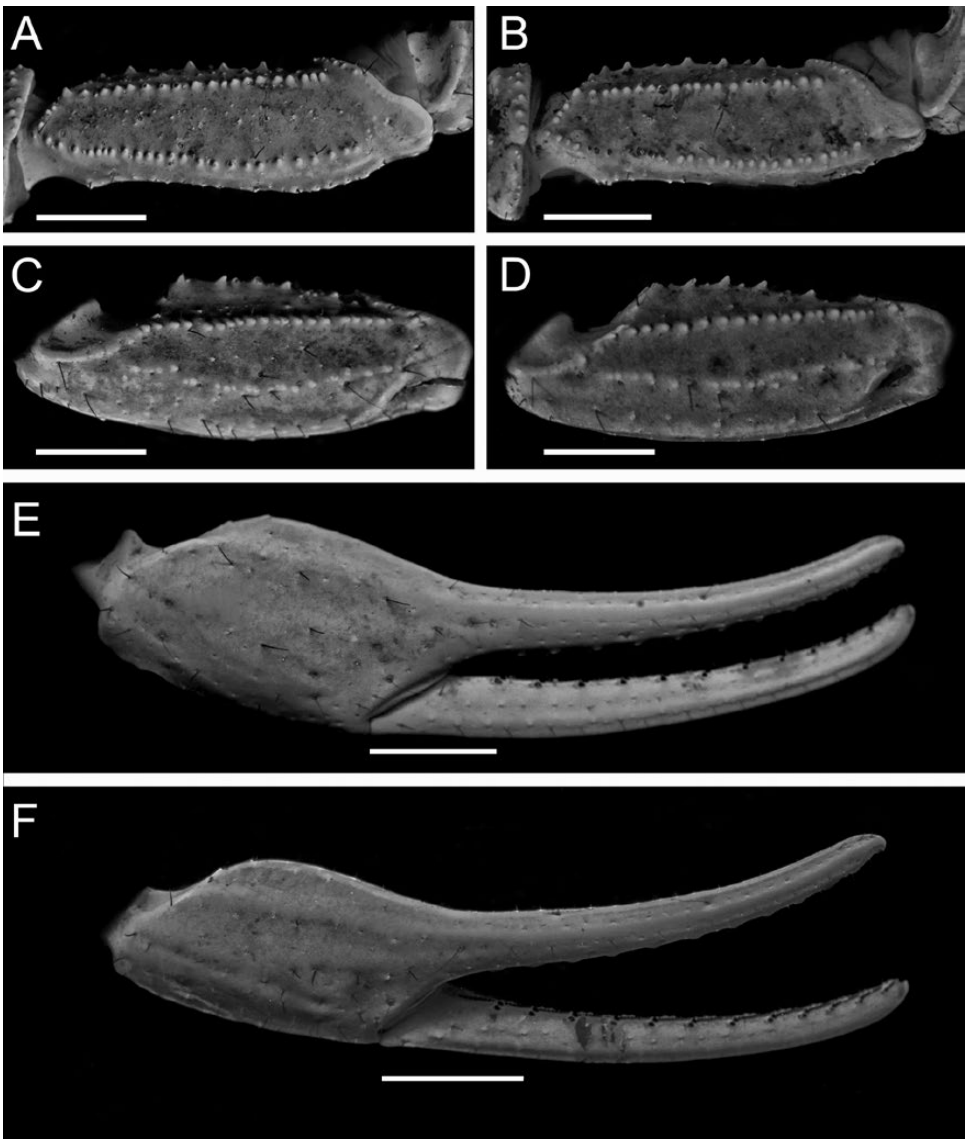

Figure 14. *Odontobuthus kermanus*. Pedipalp femur, dorsal aspect (A, B), patella, dorsal aspect (C, D) and chela, lateral aspect (E, F). A, C, E, holotype ♀ (SMF). B, D, F, paratype ♂ (ZMFUM 1340). Scale bars = 2.5 mm (A, C, E), 1.5 mm (B, D), 2 mm (F).

finger long relative to manus (MFL/ML, 1.91–2.25). Median denticle rows of pedipalp chela fixed and movable fingers each comprising 13 or 14 oblique subrows of denticles. Pectinal tooth count, 28–30 (♂) and 19–21 (♀). Ventrosubmedian carinae of metasomal segments II and III each with three or four pairs of tooth-like processes (Fig. 13C, D, G, H). Metasomal segment IV length to width (L/W), 1.67–1.88. Ventrolateral carinae of metasomal segment V with three or four prominent lobate processes; anal arch with two large lobes laterally; posteroventral margin of segment V with six reduced lobes. Telson small, narrow, length to width (TL/W), 2.22–2.50 and length to height (TL/H), 2.26–2.68 (Fig. 1A, B, E, F).

Affinities: *Odontobuthus kermanus* is closely related to *O. baluchicus* and *O. doriae*, with which it shares the presence of two prominent lateral lobes on the anal arch of metasomal segment V, and differs from all other species of the genus, which possess three lateral lobes. It differs from *O. doriae* in possessing four or five pairs of tooth-like processes on the ventrosubmedian carinae of metasomal segments II and III, and from *O. baluchicus* in metasomal segment I being equal to or wider than long.

Description: Based on holotype ♀ (SMF) (Figs 12A, B, 13A–D, 14A, C, E) and paratype ♂ (ZMFUM 1340) (Figs 12C, D, 13E–H, 14B, D, F). As for *O. baluchicus* except

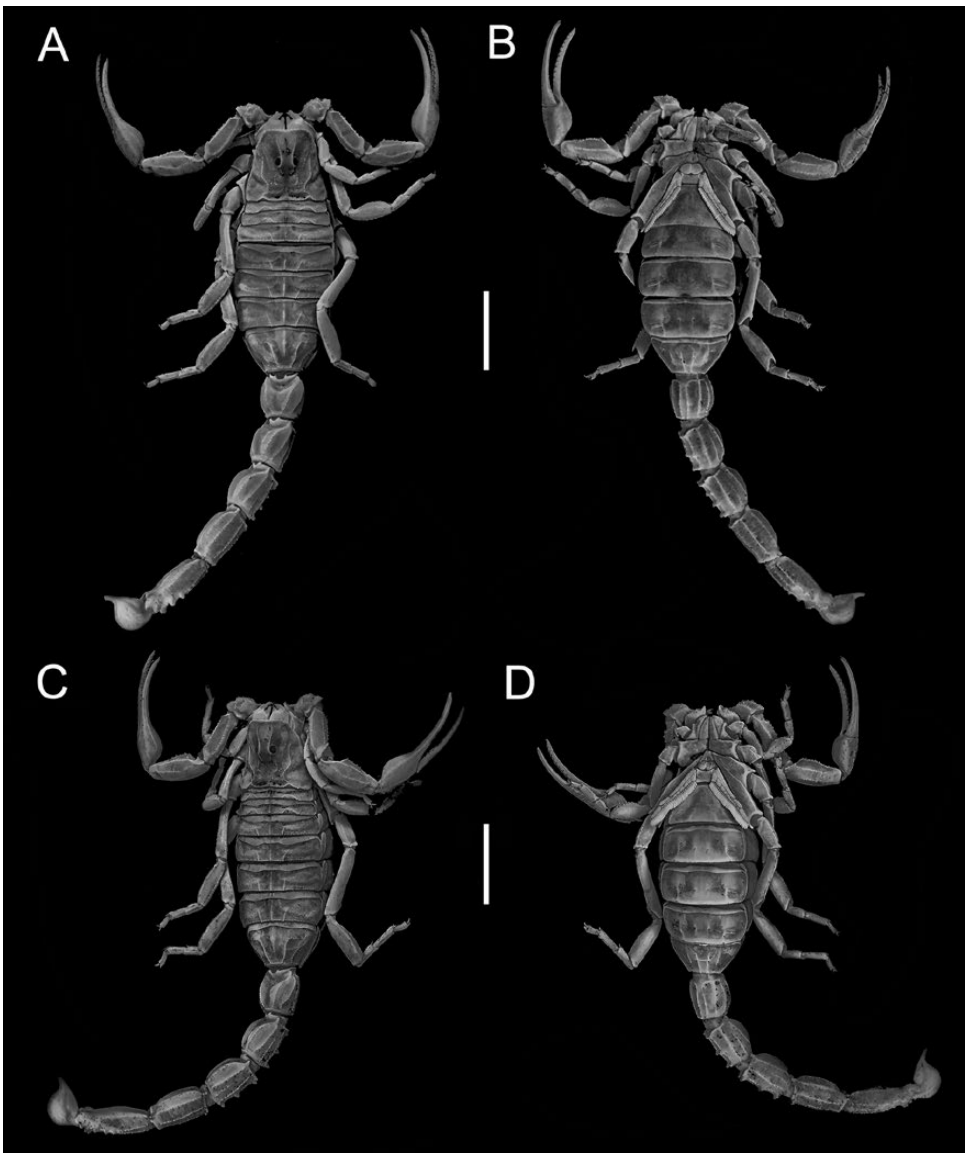

Figure 15. *Odontobuthus bidentatus*. Habitus, dorsal aspect (A, C), ventral aspect (B, D). A, B, ♀ (ZMFUM 2067). C, D, ♂ (ZMFUM 1317). Scale bars = 10 mm.

where noted. **Measurements:** ♀: BL: 68.5; CL: 8.0; CWP: 9.5; CWA: 5.7; CX: 2.8; CY: 8.0; CHL: 14.8; ML: 5.0; MFL: 9.8; MtIL: 5.0; MtIH: 3.9; MtIW: 5.0; MtIIL: 6.0; MtIIH: 3.6; MtIIW: 4.4; MtIIIL: 6.0; MtIIIH: 3.4; MtIIIW: 4.2; MtIVL: 7.0; MtIVH: 3.3; MtIVW: 3.9; MtVL: 8.3; MtVH: 2.8; MtVW: 3.3; TL: 8.0; TW: 3.2; TH: 3.6. ♂: BL: 54.8; CL: 6.3; CWP: 7.2; CWA: 5.4; CX: 2.2; CY: 6.3; CHL: 11.7; ML: 4.0; MFL: 7.7; MtIL: 3.9; MtIH: 3.0; MtIW: 3.7; MtIIL: 4.5; MtIIH: 2.8; MtIIW: 3.5; MtIIIL: 4.7; MtIIIH: 2.8; MtIIIW: 3.1; MtIVL: 5.6; MtIVH: 2.6; MtIVW: 3.1; MtVL: 6.9; MtVH: 2.2; MtVW: 2.7; TL: 6.7; TW: 2.7; TH: 2.50. **Colour:** Carapace brownish-green; dark pigmentation around median and lateral ocelli. Mesosoma dark brown dorsally, paler brown ventrally. Pedipalps and legs lighter brown, distal part of femur and proximal part of patella darker especially on legs III and IV. Pectines light yellow to cream. Metasoma brown, segments darker dorsally, segment V darker than preceding segments. Telson vesicle light brown to yellow; aculeus light brown anteriorly, becoming dark brown to black posteriorly. **Carapace:** Trapezoid, wider than long, CWA/CL, 0.71 (♀) or 0.85 (♂), CWP/CL, 1.18 (♀) or 1.14 (♂); anterior margin moderately emarginate; median ocular tubercle situated in anterior half of carapace, CX/CL, 0.35 (♀) or 0.34 (♂), CX/CY, 0.35 (♀) or 0.34 (♂), distance between median ocelli twice ocular diameter; five pairs of lateral ocelli (Fig. 12A, C); anteromedian and posteromedian sulci deep

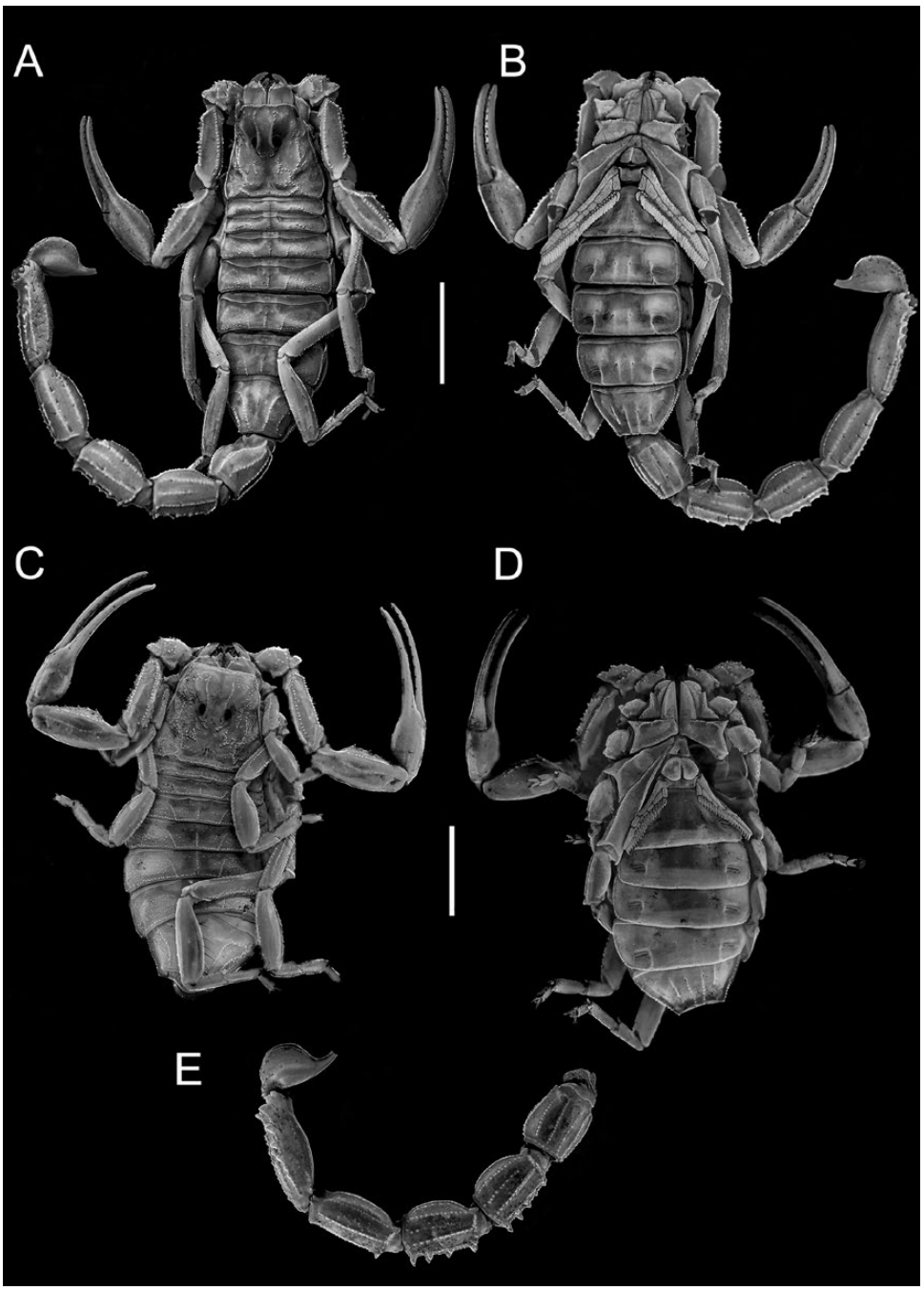

Figure 16. *Odontobuthus*. Habitus, dorsal aspect (A, C, E), ventral aspect (B, D). A, B, *Odontobuthus brevidigitus*, ♂ (ZMFUM 1438). C–E, *Odontobuthus odonturus*, ♀ (ZMFUM 1439). Scale bars = 10 mm (A, B), 5 mm (C–E).

(♂) or shallow (♀); posterolateral sulci wide, curved; carinae distinct, central lateral and posteromedian carinae completely aligned; anteromedian carinae granular; central median, posteromedian and central lateral carinae granular (♀) or serratocrenulate (♂); intercarinal surfaces of prosoma finely granular. **Pedipalps:** Pedipalp segments relatively short. Femur 3.5 (♀) or 3.24 (♂) times longer than wide; four complete, granular carinae; retrodorsal, prodorsal and proventral carinae granular (♀) or serratocrenulate (♂); prolateral carinae comprising isolated spiniform granules; intercarinal surfaces smooth (Fig. 14A, B). Patella 2.89 (♀) or 2.91 (♂) times longer than wide; eight complete carinae; prodorsal carinae distinct (♀)

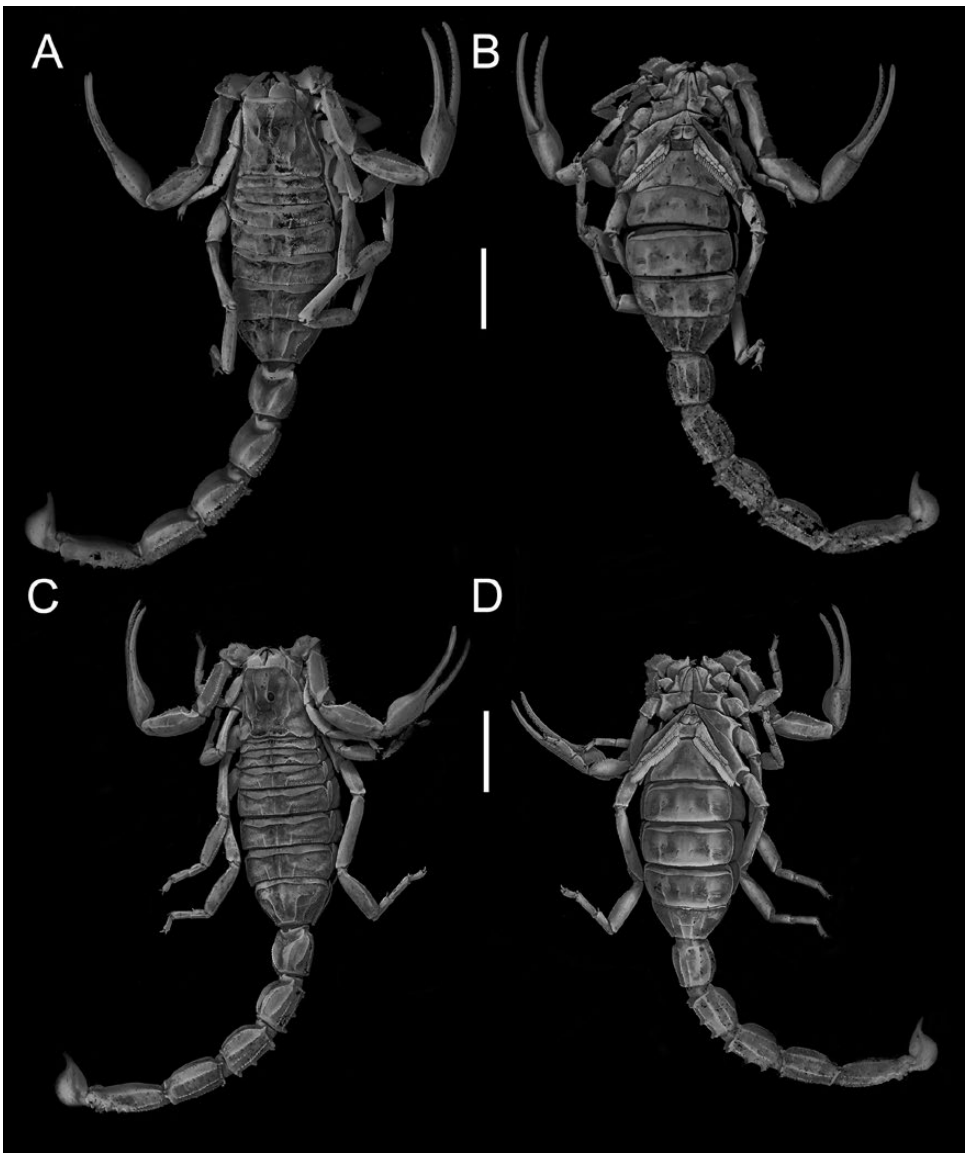

Figure 17. *Odontobuthus doriae*. Habitus, dorsal aspect (A, C), ventral aspect (B, D). A, B, ♀ (ZMFUM 2045). C, D, ♂ (ZMFUM 2016). Scale bars = 10 mm.

or moderate (♂), granular; dorsomedian, retrodorsal, retrolateral, retroventral and ventromedian carinae obsolete to moderate, smooth (Fig. 14C); proventral and prolateral carinae comprising several spiniform granules (♂) (Fig. 14D). Chela 2.96 (♀) or 2.92 (♂) times longer than manus; manus wider than patella; fingers 1.96 (♀) or 1.92 (♂) times longer than manus; median denticle subrows, including proximal subrow (left/right) of fixed finger, 12/12 and movable finger, 13/13; all subrows except proximal flanked by prolateral and retrolateral accessory denticles; movable finger with six (♂, ♀) or seven ♀) subdistal denticles, two prolateral and four (♂, ♀) or five (♀) retrolateral. Trichobothrium *et* adjacent to midpoint of denticle subrow 7; *est* adjacent to distal end of denticle subrow 8 (♂) (Fig. 14F) or midpoint of denticle subrow 9 (♀) (Fig. 14E). **Sternum:** Type I, triangular; slightly wider than long (♀) or longer than wide (♂); with deep median depression. **Genital operculum:** Completely divided longitudinally with fine, short bristles (Figs 12B, 13D). **Pectines:** Distal margin extending to (♀) or beyond (♂) coxa-trochanter joint of leg IV; three marginal and six median lamellae; fulcra present; teeth present along entire posterior margin of pecten,

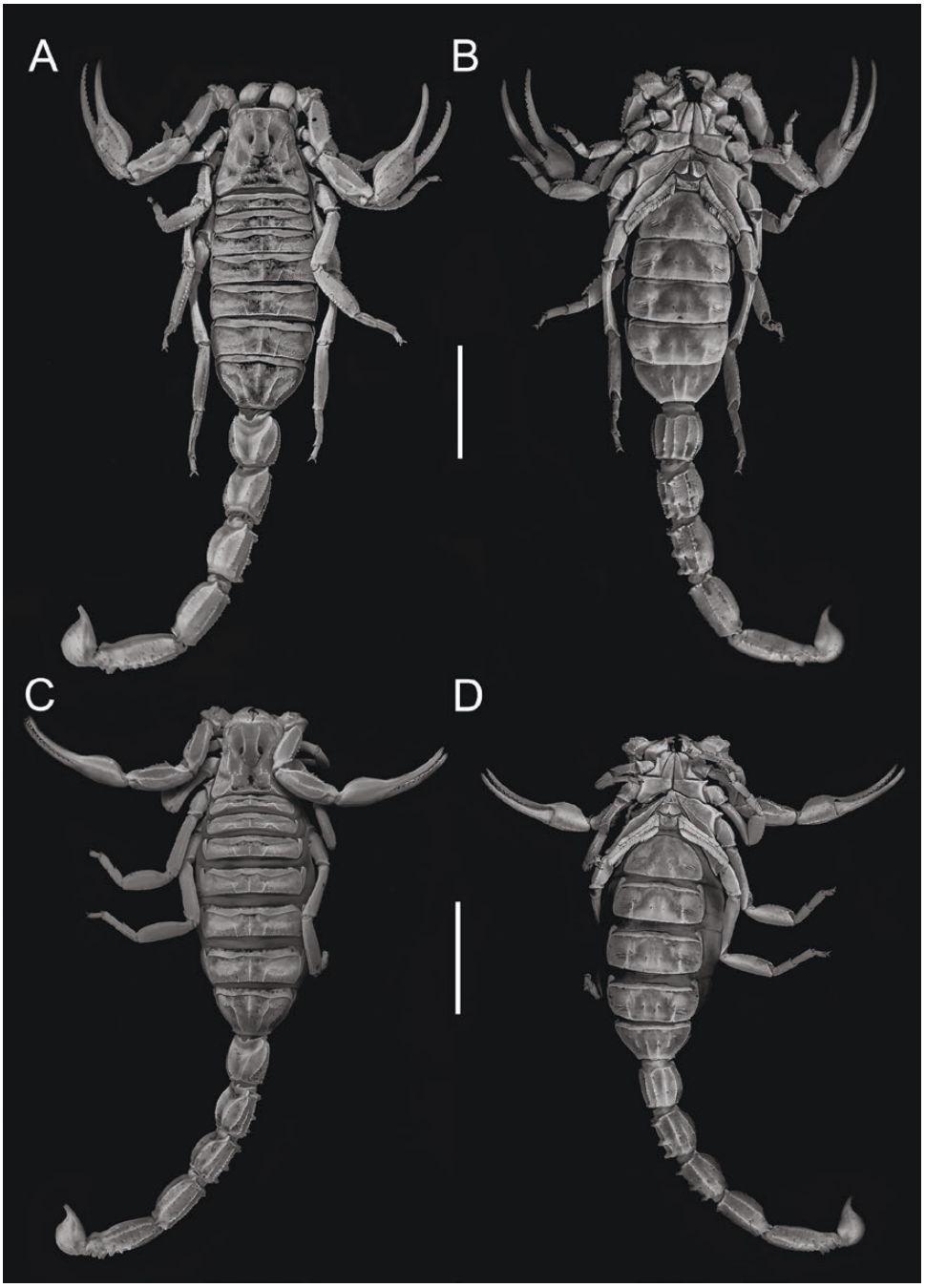

Figure 18. *Odontobuthus tavighiae.* Habitus, dorsal aspect (A, C), ventral aspect (B, D). A, B, ♀ (ZMFUM 1362). C, D, ♂ (ZMFUM 1364). Scale bars = 10 mm.

count (left/right), 28/38 (♂) and 20/20 (♀). **Mesosoma:** Tergites I–VI tricarinate; VII pentacarinate, lateral carinae granular (♀) or serratocrenulate (♂), median carinae incomplete, restricted to anterior half of segment and weakly granular; intercarinal surfaces finely (♀) or coarsely (♂) granular. Sternites III–VI acarinate; VII with four moderate (♀) or obsolete (♂), granular carinae, lateral carinae restricted to anterior half of segment. **Metasoma:** Metasomal segment I decacarinate; II–IV octocarinate; V pentacarinate; all complete carinae moderately to markedly granular on segments I–III and weakly to moderately granular

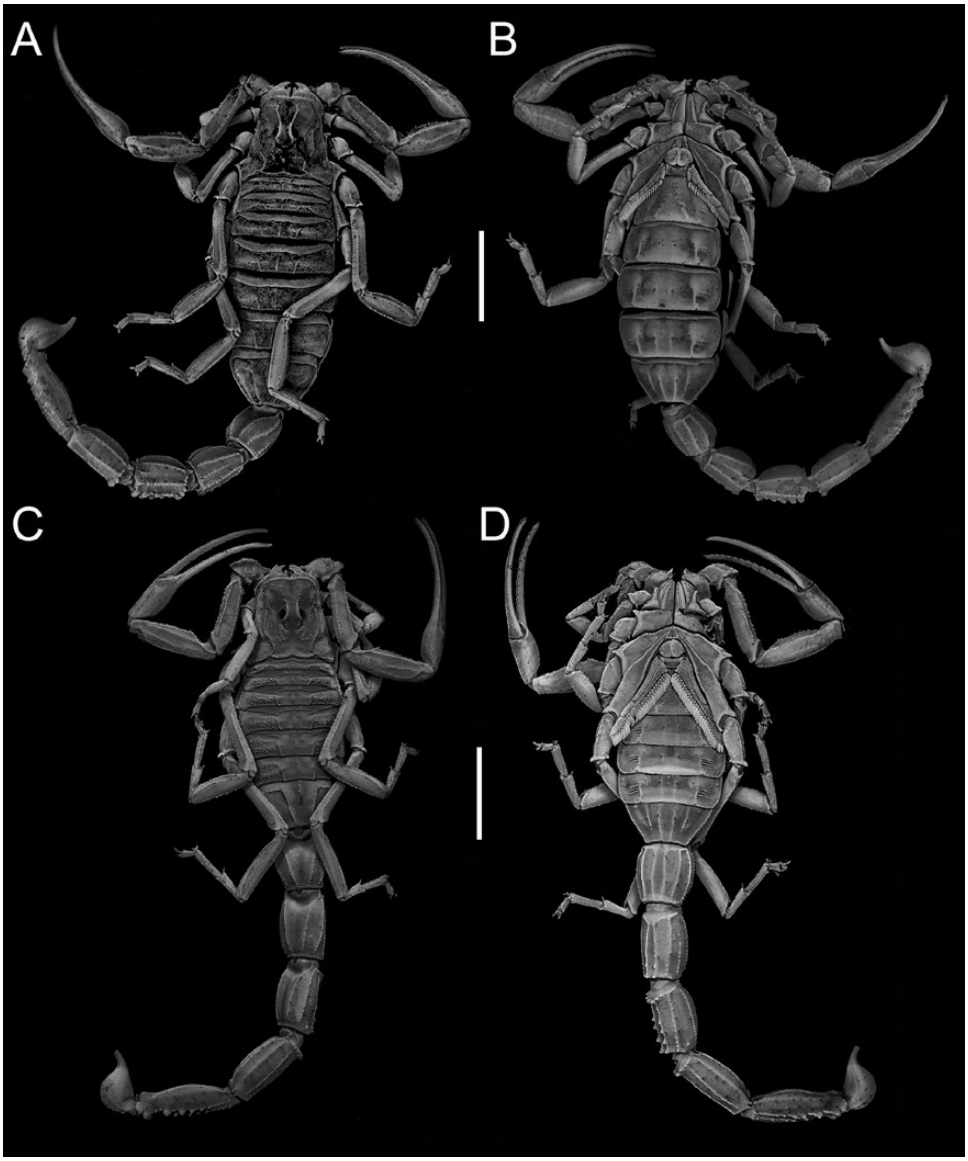

Figure 19. *Odontobuthus tirgari.* Habitus, dorsal aspect (A, C), ventral aspect (B, D). A, B, ♀ (ZMFUM 2091). C, D, ♂ (ZMFUM 2092). Scale bars = 10 mm.

on IV (♀) or weakly to moderately granular on I–IV (♂). Lateral inframedian carinae incomplete, restricted to posterior half of segment II; vestigial, reduced to few granules posteriorly, on III. Ventrosubmedian carinae on segments II and III each with three pairs of rounded (♀) or rounded to subtriangular (♂) tooth-like processes. Anteroventral margins of segments III and IV each with four large, rounded granules. Ventrolateral carinae on segment V markedly dentate with large, rounded lobate processes posteriorly; anal arch with two large lobes laterally and four distinct lobes, sometimes laterally bidentate, posteroventrally (Fig. 13A–H). **Telson:** Oblong-ovoid, TH/TL, 0.40 (♀) or 0.37 (♂), TW/TL, 0.45 (♀) or ♂ (0.40); wider than (TW/MtVW, 1.09) (♀) (Fig. 14A, B) or similar to (TW/MtVW, 1.00) (♂) (Fig. 14E, F) width of metasomal segment V; dorsal surface flat, ventral surface curved, smooth (♀) or sparsely granular (♂).

Distribution: *Odontobuthus kermanus* is endemic to Iran and recorded in only two provinces: Fars and Kerman.

Additional material: IRAN: *Fars Province:* Neyriz, 20 km E of Qatruyeh, 29°10′N 54°51′E, 1657 m, 16.iv.2018, H. Barahoei, daytime excavation, loamy sand, one ♂, three ♀♀ (ZMFUM). *Kerman Province*: Bardsir-Sirjan road, 29°57′N 56°33′E, 2036 m, v.2009, A. Koohpaye, H. Jamalizadeh & A. Ebrahimi, Ke-104,

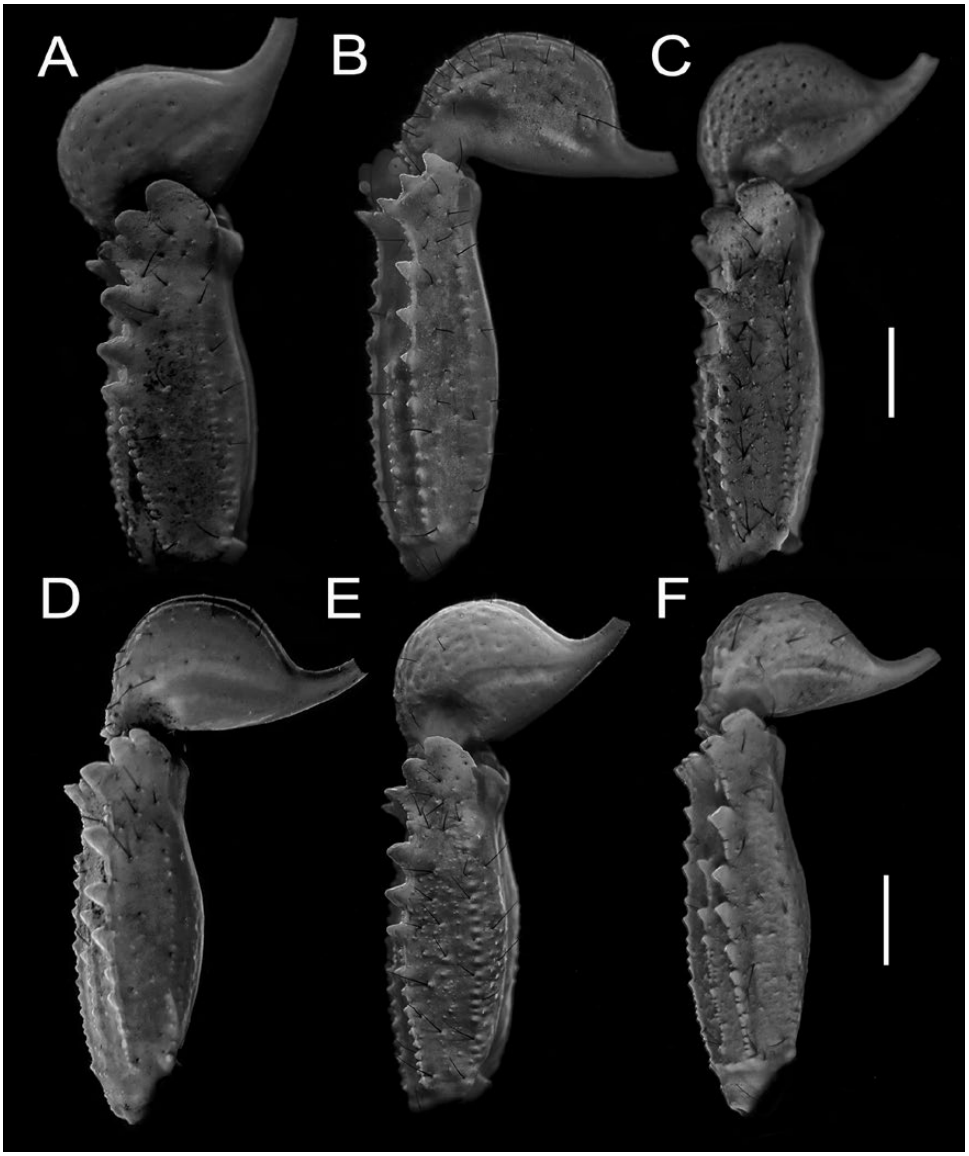

Figure 20. *Odontobuthus*. Metasomal segment V, lateral aspect. A, *Odontobuthus bidentatus* ♀ (ZMFUM 2061) B, *Odontobuthus brevidigitus* ♂ (ZMFUM–1438). C, *Odontobuthus doriae* ♀ (ZMFUM 2014). D, *Odontobuthus odonturus* ♀ (ZMFUM 1439). E, *Odontobuthus tavighiae* ♀ (ZMFUM–2074). F, *Odontobuthus tirgari* ♂ (ZMFUM 1398). Scale bars = 2.5 mm.

one juv. ♀ [AMCC (LP 11067)]. Sirjan, 60 km SW, 29°09′N 55°18′E, 1724 m, 16.iv.2018, H. Barahoei, daytime excavation, loamy sand, two ♀♀, two subad. ♂♂ (ZMFUM).

Odontobuthus odonturus (Pocock, 1897)

(Figs 1, 3–5, 16C–E, 20D, 21D, 22D, Tables 1, 4, 5)

Buthus odonturus Pocock, 1897: 104; Kraepelin, 1899: 27; Birula, 1900b: 357, 358; Birula, 1905: 122; Kraepelin, 1913: 124, 125; Werner, 1936: 204.

Buthus doriae odonturus: Pocock, 1900: 16–18, fig. 8B; Takashima, 1945: 75.

Buthus (Buthus) doriae odonturus: Birula, 1917: 239.

Odontobuthus odonturus: Vachon, 1950: 154; Vachon, 1952: 326; Vachon, 1966: 213; Habibi, 1971: 44; Farzanpay, 1988: 39; Kovarik, 1997: 47, 49, figs 12, 13; Kovarik, 1998: 115; Fet & Lowe, 2000: 187; Lourenço & Pézier, 2002: 118; Lowe, 2010: 1, 2, 7, 15, 16, 17, figs 33, 34, 41, 42, 60–63.

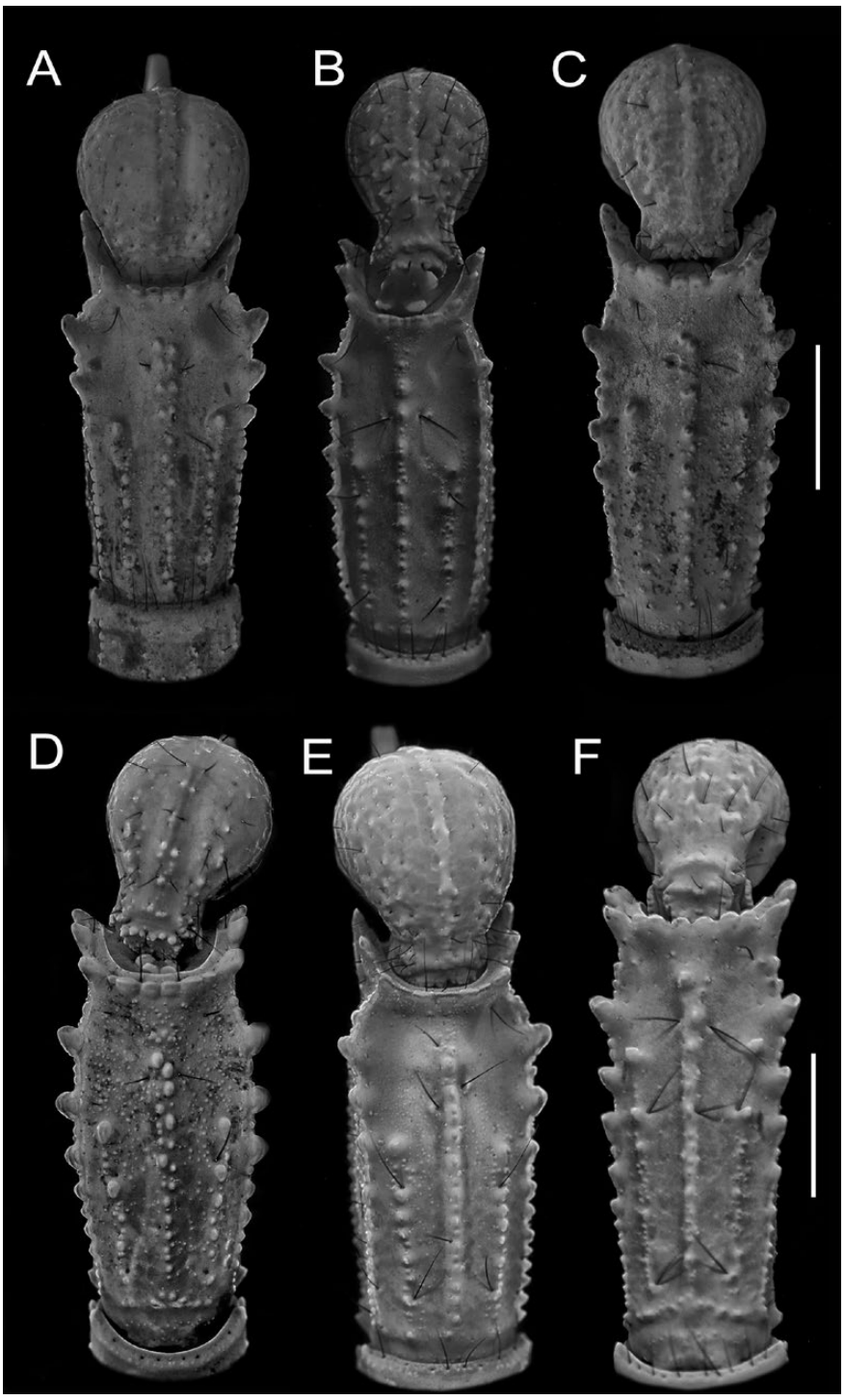

Figure 21. *Odontobuthus*. Metasomal segment V, ventral aspect. A, *Odontobuthus bidentatus* ♀ (ZMFUM 2061) B, *Odontobuthus brevidigitus* ♂ (ZMFUM 1438). C, *Odontobuthus doriae* ♀ (ZMFUM 2014). D, *Odontobuthus odonturus* ♀ (ZMFUM–1439). E, *Odontobuthus tavighiae* ♀ (ZMFUM 2074). F, *Odontobuthus tirgari* ♂ (ZMFUM 1398). Scale bars = 2.5 mm.

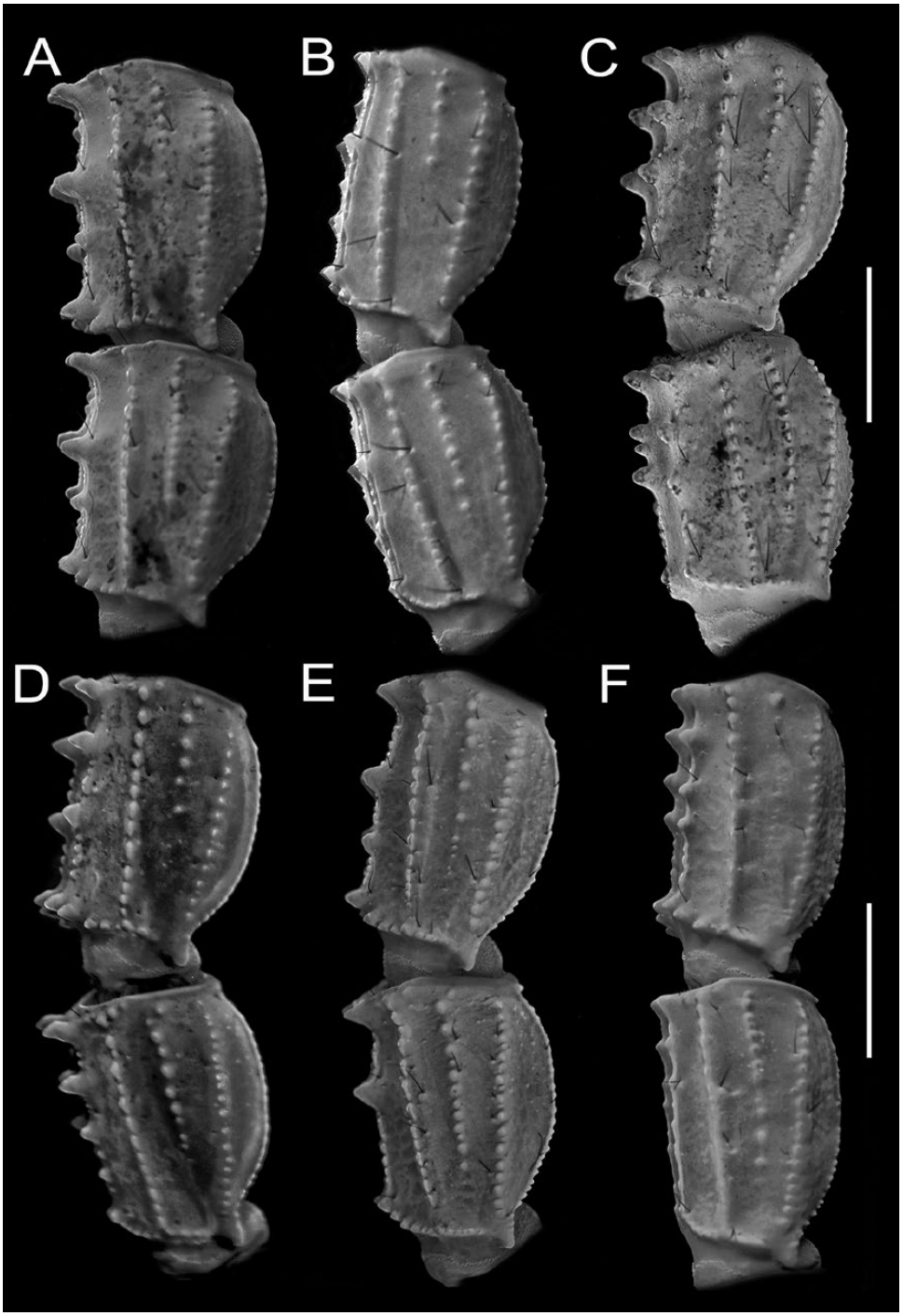

Figure 22. *Odontobuthus.* Metasomal segments II and III, lateral aspect. A, *Odontobuthus bidentatus* ♀ (ZMFUM 2061). B, *Odontobuthus brevidigitus* ♂ (ZMFUM 1438). C, *Odontobuthus doriae* ♀ (ZMFUM 2014). D, *Odontobuthus odonturus* ♀ (ZMFUM 1439). E, *Odontobuthus tavighiae* ♀ (ZMFUM 2074). F, *Odontobuthus tirgari* ♂ (ZMFUM 1398). Scale bars = 2.5 mm.

Odontobuthus doriae odonturus: Tikader & Bastawade, 1983: 248–253, figs 714–726.

Odonbuthus odonturus: Pérez Minnocci, 1974: 28.

Type material: Holotype ♂ (BMNH 1896.10.20.33), PAKISTAN: Kelat Frontier, Upper Sind, A.V. Kemball.

Diagnosis: Odontobuthus odonturus may be separated from other species of the genus by the

following combination of characters. Scorpions of small to medium size, adults 40–51 mm (Fig. 16C–E). Colour yellow. Median ocular tubercle situated in anterior half of carapace, distance from anterior carapace margin, 0.33. Pedipalp chela movable finger long relative to manus (MFL/ML, 2.21). Median denticle rows of pedipalp chela fixed and movable fingers each comprising ten or 11 oblique subrows of denticles. Pectinal tooth count, 26–29 (♂) and 16–21 (♀). Ventrosubmedian carinae of metasomal segments II and III each with three pairs of very prominent tooth-like processes (Fig. 22D). Metasomal segment IV length to width (L/W), 1.86. Ventrolateral carinae of metasomal segment V with three prominent lobate processes; anal arch with three large lobes laterally, first two lobes partially fused; posteroventral margin of segment V with four relatively large lobes. Telson small, narrow, length to width (TL/W), 2.38 and length to height (TL/H), 2.58 (Figs 20D, 21D).

Distribution: *Odontobuthus odonturus* is recorded from Pakistan (Pocock, 1897; Fet & Lowe, 2000; Lourenço & Pézier, 2002) and India (Tikader & Bastawade, 1983: 253). Records of this species from Iran, cited by Birula (1900: 357), Farzanpay (1987: 156, 1990: 7), Akbari *et al.* (1997: 112) and Kovařík (1997: 47) are misidentifications of other species (Lourenço and Pézier, 2002: 122; Navidpour *et al.*, 2008a: 13). Moreover, reports of Nejati *et al.* (2014: 219) and Kassiri *et al.* (2015: 101) are doubtful.

Material examined: x.1912, 1 ♂ (ZMH). PAKISTAN: vii.2007, ex pet trade, one ♀ [AMCC (LP 7008)]. *Karachi Province:* 25°02′N 66°58′E, 30 m, 2007, Z. Ahmed, one ♀ (ZMFUM 1439). *Punjab Province:* Bhakar (Thal) District, Bhakar Tehsil: Bhakar city, 25 km NW, 31°38′N 71°06′E, 537 ft, 19.v.2012, M. Tahir, S. Y. Khan, H. Khan, M. Hussain & T. Ahmed, sand dunes with little grass, night collection with UV light (9–12 pm), one ♂, two juv. ♂♂ (AMNH), one juv. ♂ [AMCC (LP 11333)]. Chakwal District, Kalar Kahar Tehsil: Kalar Kahar, 45 km S on Motorway, 5 km W of Motorway, 32°35′N 72°48′E, 732 ft, 25.vi.2012, M. Tahir, S. Y. Khan, H. Khan, M. Hussain & T. Abbas, semi-sandy area with vegetation, night collection with UV lamps, three ♂♂, two ♀♀, one juv. ♂ (AMNH), three juv. ♂♂ [AMCC (LP 11421)], 26.v.2012, M. Tahir, S. Y. Khan, H. Khan, M. Hussain & T. Khan, semi-sandy with vegetation, UV light collection, 11 pm–1 am, one subad. ♂, four juv. ♂♂, five juv. ♀♀ (AMNH), one juv. ♂, two juv. ♀♀ [AMCC (LP 11346)]. Jhang District, Jhang Tehsil: Aliabad, 1.5 km W on main road near Flood Relief Bank, 31°41′N 72°44′E, 436 ft, 22.vii.2012, M. Jafar & M. Babar, sandy area with short vegetation, night collecting with UV lamp, 9–11 pm, one subad. ♂, two subad. ♀♀ (AMNH), one juv. ♂ [AMCC (LP 11487)]; Aliabad, 2 km E of old bypass, 31°39′N 72°44′E, 432 ft, 23.vii.2012, M. Jafar & M. Babar, sandy area with short vegetation, night collecting with UV lamp, 12 pm, two ♀♀ (AMNH), one ♀ [AMCC (LP 11488)]. Shorkot Tehsil: Cha Fateh wala, 5 km N of Shorkot on S side of road, 1.5 km W of Fateh wala on W side of Multan road, 30°50′N 72°04′E, 431 ft, 23.v.2012, M. Tahir, M. Irfan, S. Y. Khan, N. Ahmed & T. Abbas, sand dunes with grass in patches, UV light detection, 9–11 pm, one ♂, one subad. ♀ (AMNH); Kashmir Sugar Mills, 5 km from Shorkot, Bhudh 2 km from Kashmir Sugar Mills on N side of road, 30°46′N 72°41′E, 438 ft, 23.v.2012, M. Irfan & T. Abbas, natural habitat with sand dunes, long grass and *Calotropis* plants, night collection with UV light, 11 pm–2 am, one ♂ (AMNH). Khushab District, Jhourabad Tesil: Noor Pur Thal, 20 km NW on road to Rooda, E side of road near canal, 32°03′N 72°05′E, 14.v.2012, M. K. Mukhtar, M. Irfan, M. M. Hussain & H. Khan, remnant patch of habitat surrounded by cultivated lands, sand dunes, UV detection at night, one ♂ [AMCC (LP 11315)]; Noor Pur Thal, 21 km NW on road to Rooda, W side of road, 32°06′N 72°06′E, 14.v.2012, M. K. Mukhtar, M. Irfan, M. M. Hussain & H. Khan, remnant patch of habitat surrounded by cultivated lands, sandy soil, UV detection at night, one juv. ♂ [AMCC (LP 11312)]. Sargodha District, Noshara Tehsil: Nory Wala, 6 km NW of Khaliq Abad towards Noshra, near Police Station, 32°26′N 72°32′E, 819 ft, 19.vi.2012, M. Tahir, S. Y. Khan, M. Ahsan & M. Jafer, rocky area with sand, night collecting with UV lamps, 11–12 pm, two ♂♂, one ♀ (AMNH); Sargodha Tehsil: Samavani, 5 km N of motorway towards Sargodha, 1 km S on side road, 32°03′N 73°36′E, 619 ft, 20.v.2012, M. Tahir, S. Y. Khan, H. Khan & T. Ahmed, plain, sandy areas with grass and *Calotropis procera* UV light collection, 9 pm, three ♂♂, two ♀♀, one subad. ♀, four juv. ♂♂, three juv. ♀♀ (AMNH), one juv. ♂ [AMCC (LP 11336)]; Sargodha, 36 km E on Lahore road, 500 m from Doodha stop, on S side of road, 32°03′N 73°36′E, 623 ft, 21.v.2012, M. Tahir, M. Irfan, M. Hussain & M. J. Khan, natural sandy habitat with vegetation, long grass and *Calotropis* plants, pitfall method, 11–12 pm, one ♂, one ♀ (AMNH).

Odontobuthus Tavighiae Navidpour *et al.*, 2013

(Figs 1–5, 18, 20E, 21E, 22E, Tables 1–5)

Odontobuthus odonturus: Nejati *et al.*, 2014: 19–220 (misidentification).

Odontobuthus tavighiae Navidpour *et al.*, 2013: 3, 13, 14, 21, figs 3, 10, 13–23; Azghadi *et al.*, 2014: 169, 170, 172, 173, 175, 176, 177, 178, figs 1, 2j–l; Barahoei *et al.*, 2020: 402, fig. 20.

Type material: Holotype ♂ (FKCP), paratype ♀ (RRLS), IRAN: *Hormozgan Province:* Lengeh Port, 27°08′06”N 55°49′17.5″, 12 m, v.2009, Masihipour, Hayader & Habibzadeh.

Diagnosis: Odontobuthus tavighiae can be separated from other species of the genus by the following combination of characters. Scorpions of medium to large size, adults 52–67 mm (♂) and 45–79 mm (♀) (Fig. 18). Colour yellow. Median ocular tubercle situated in anterior half of carapace, distance from anterior carapace margin, 0.34–0.38. Pedipalp chela movable finger long relative to manus (MFL/ML, 1.69–2.06). Median denticle rows of pedipalp chela fixed and movable fingers each comprising 13 or 14 oblique subrows of denticles. Pectinal tooth count, 30–34 (♂) and 22–27 (♀). Ventrosubmedian carinae of metasomal segments II and III each with two pairs of tooth-like processes (Fig. 22E). Metasomal segment IV length to width (L/W), 1.60–1.95. Ventrolateral carinae of metasomal segment V with three or four prominent lobate processes; anal arch with three large lobes laterally; posteroventral margin of segment V with six reduced lobes. Telson small, narrow, length to width (TL/W), 1.89–2.28 and length to height (TL/H), 1.96–2.35 (Figs 20E, 21E).

Distribution: Odontobuthus tavighiae is endemic to Iran and recorded from only two provinces: Fars; Hormozgan (Navidpour *et al.*, 2013; Azghadi *et al.*, 2014; Navidpour & Mirshamsi, 2014).

Material examined: IRAN: *Fars Province:* Mohr, 27°31′N 52°54′E, 445 m, 13.iv.2018, H. Barahoei, daytime excavation, clay loam, one ♂, three ♀♀ (ZMFUM). *Hormozgan Province:* Hameyran, 27°01′N 53°43′E, 224 m, 12.iv.2018, H. Barahoei, daytime excavation, loam, one ♂, three ♀♀ (ZMFUM); Lavar-e Khasht village, 10 km N, Hameyran–Parsian road, 27°09′N53°26′E,519m,13.iv.2018;H.Barahoei,daytime excavation, two ♀♀ (ZMFUM); Parsian, Behdeh village, 27°04′N 53°29′E, 11.xii.2007, 1 ♂ (ZMFUM); Parsian, SE of Bando village, 27°19′N 52°52′E, 11.xii.2007, one ♀ (ZMFUM); Parsian, Chahvaz, 27°05′N 53°28′E, 231 m, 12.iv.2018, H. Barahoei, daytime excavation, loam, six ♂♂, two ♀♀, two subad. ♂♂ (ZMFUM); Parsian, Pishab village, 27°10′N 53°07′E, 106 m, 13.iv.2018, H. Barahoei, daytime excavation, loam, one ♂, two ♀♀ (ZMFUM).

ODONTOBUTHUS TIRGARI MIRSHAMSI *ET AL.*, 2013 (FIGS 1–5, 19, 20F, 21F, 22F, TABLES 1–5)

Odontobuthus doriae: Vatani & Khoobdel, 2009: 10 (misidentification); Ramezani *et al.*, 2010: 55, 56, 58, 59, 60, figs 2, 3, 5 (misidentification); Karataş *et al.*, 2012: 116 (misidentification); Motevalli Haghi *et al.*, 2020: 69–72 (misidentification).

Odontobuthus tirgari Mirshamsi *et al.*, 2013: 153–168, figs 1–41; Azghadi *et al.*, 2014: 171; Navidpour & Mirshamsi, 2014: 112; Barahoei *et al.*, 2020: 402, fig. 20.

Type material: Holotype ♀ (AMNH), one ♂, one ♀ paratypes (AMNH), IRAN: *Razavi Khorasan Province:* Gonabad, Borjook village, 1.ix.2012, O. Mirshamsi.

Diagnosis: Odontobuthus tirgari may be separated from other species of the genus by the following combination of characters. Scorpions of medium to large size, adults 44–75 mm (♂) and 50–77 mm (♀) (Fig. 19). General coloration yellow to yellowish-green. Median ocular tubercle situated in anterior half of carapace, distance from anterior carapace margin, 0.30–0.40. Pedipalp chela movable finger long relative to manus (MFL/ML, 2.20–2.75). Median denticle rows of pedipalp chela fixed and movable fingers each comprising 13 or 14 oblique subrows of denticles. Pectinal tooth count, 28–33 (♂) and 19–24 (♀). Ventrosubmedian carinae of metasomal segments II and III each with three to five pairs of tooth-like processes (Fig. 20F). Metasomal segment IV length to width (L/W), 1.63–2.33. Ventrolateral carinae of metasomal segment V with three or four prominent lobate processes; anal arch with one small and two large lobes, sometimes presenting as two lobes, laterally; posteroventral margin of segment V with six reduced lobes. Telson small, narrow, length to width (TL/W), 2.22–2.81 and length to height (TL/H), 2.22–2.71 (Figs 20F, 21F).

Distribution: Odontobuthus tirgari is endemic to Iran and recorded in four provinces: North Khorasan; Razavi Khorasan; Sistan and Baluchistan; South Khorasan (Vatani & Khoobdel, 2009; Ramezani *et al.*, 2010; Karataş *et al.*, 2012; Mirshamsi *et al.*, 2013; Azghadi *et al.*, 2014; Mir *et al.*, 2014; Navidpour & Mirshamsi, 2014).

Additional material: IRAN: *Razavi Khorasan Province:* Gonabad, Ghozhd Jungle, 34°25′N 58°44′E, 1035 m, 30.vi.2018, UV light at night, silty soil, H. Barahoei, two ♂♂ (ZMFUM); Gonabad, Kakhk–Ostad road, 34°07′N 58°46′E, 6.viii.2011, O. Mirshamsi, two ♂♂, six subad. ♀♀ (ZMFUM); Gonabad, Kakhk village road, 34°09′N 58°45′E, 1391 m, 15.vii.2018, H. Barahoei, daytime excavation, loamy sand, two ♂♂, two ♀♀, two subad. ♀♀ (ZMFUM); Gonabad, Marghesh village, 3 km NE of Kakhk, 34°08′N 58°38′E, 15.vii.2011, O. Mirshamsi, two ♂♂,

seven ♀♀ (ZMFUM). *Sistan and Baluchistan Province:* Dasht-e Robat village, 30 km S of Khash, 28°04′N 61°19′E, 1382 m, 13.xi.2018, H. Barahoei, daytime excavation, loamy sand, one ♂, two ♀♀, one subad. ♀ (ZMFUM); Iranshahr, 30 km E, 27°13′N 61°03′E, 1605 m, 13. 2018; H. Barahoei, daytime excavation, loam, two ♂♂, one ♀, one subad. ♀ (ZMFUM); 40 km on Iranshahr–Rask road, 26°58′N 60°53′E, 975 m, 14.xi.2018, H. Barahoei, daytime excavation, sand; one ♂, three ♀♀, one subad. ♀ (ZMFUM); Iranshahr, Zimdan village, 26°49′N 60°58′E, 1390 m, 14.xi.2018, H. Barahoei, daytime excavation, loam, one ♂, one ♀, one subad. ♀ (ZMFUM); Khash, Dehpabid village, 28°25′N 60°54′E, 1643 m, 16.xi.2018, H. Barahoei, daytime excavation, loamy sand, one ♀, two subad. ♀♀ (ZMFUM); Khash, Karvandar village, 27°43′N 60°45′E, 1045 m, 2.iv.2018, H. Barahoei, daytime excavation, one ♂ (ZMFUM); Khash, Karvandar village, 27°51′N 60°45′E, 1230 m, 16.xi.2018, H. Barahoei, daytime excavation, sand, three ♂♂, two subad. ♂♂ (ZMFUM); Khash, Nouk Abad, Gowhar Kouh, 28°27′N 60°39′E, 1501 m, 4.iv.2019, H. Barahoei, daytime excavation, clay loam, one ♂, one ♀ (ZMFUM); Mehrestan, 5 km E, 27°10′N 61°41′E, 1285 m, 13.xi.2018, H. Barahoei, daytime excavation, clay loam, one ♂, four ♀♀, two subad. ♀♀ (ZMFUM); Saravan, 5 km N, 27°25′N 62°17′E, 1206 m, 13.xi.2018, H. Barahoei, daytime excavation, loam, two ♂♂, two ♀♀ (ZMFUM); Taftan Mountain, surroundings, iii.2018, A. Zamani, one subad. ♀ [AMCC (LP 15795)]; Zabol, Sefidabeh, Palang Kouh, 30°49′N 60°34′E, 1175 m, 3.iv.2019, H. Barahoei, daytime excavation, clay loam, two ♂♂ (ZMFUM); Zahedan, Cheshmeh Ziarat, Polki village, 29°31′N 60°29′E, 1714 m, 2.iv.2018, H. Barahoei, daytime excavation, sand, one ♂, six ♀♀, three subad. ♀♀ (ZMFUM); Zahedan, Manzel Aab village, 29°18′N 60°47′E, 1605 m, 24.vii.2017, H. Barahoei, UV light at night, clay loam, three ♂♂, one ♀, one subad. ♀ (ZMFUM). *South Khorasan Province:* Nehbandan, Chah-e Zard village, 31°32′N 60°02′E, 28.vii.2008, O. Mirshamsi, one ♂, one ♀ (ZMFUM); Nehbandan, Sahl Abad, 32°19′N 59°49′E, 1618 m, 14.vii.2018, H. Barahoei, daytime excavation, one ♂, two ♀♀ (ZMFUM); Shosf, 31°45′N 60°04′E, 1501 m, 14.vii.2018, H. Barahoei, daytime excavation, one ♂, two ♀♀ (ZMFUM).

DISCUSSION

Previous authors justified or confirmed the taxonomic validity of *O. bidentatus*, *O. brevidigitus*, *O. doriae*, *O. odonturus*, *O. tavighiae* and *O. tirgari* based on morphological and, in a few cases, molecular data (Lourenço & Pézier, 2002; Mirshamsi *et al.*, 2013; Navidpour *et al.*, 2013; Azghadi *et al.*, 2014). In the present contribution, statistical analysis of morphological data confirmed the taxonomic validity of the six previously described species of *Odontobuthus* and demonstrated that characters of the carapace (CX and CY) and pedipalps (MFL, ChL, MW, MD and FW) are diagnostic at the species level (Table 2).

The results of molecular phylogenetic analyses of *COI* sequences from 21 *Odontobuthus* populations (Figs 3, 5) were congruent with the morphological analyses. Maximum likelihood and Bayesian inference supported the monophyly of the six previously described species, and provided additional support for recognizing three new species, from the central and south-eastern parts of the Iranian Plateau: *O. kermanus*, from Kerman Province (Bardsir and Neyriz populations; Fig. 1; Table 1) and two species from Sistan and Baluchistan Province in south-eastern Iran, *O. baluchicus* from the Makkoran Mountains (Nikshahr and Jask populations, Fig. 1, Table 1) and *O. chabaharensis* from the coast of the Gulf of Oman (Chabahar population; Fig. 1; Table 1). Azghadi *et al.* (2014) previously suggested that the population from Kerman Province might be a new species. The new discoveries raise the number of *Odontobuthus* species to nine, six of which are endemic or subendemic to the Iranian Plateau (67% endemism).

Consistent with the tree topology based on *COI* and 16S presented by Azghadi *et al.* (2014), the species of *Odontobuthus* are grouped into two major clades: clade A, comprising *O. baluchicus*, *O. bidentatus*, *O. brevidigitus, O. chabaharensis*, *O. doriae*, *O. odonturus* and *O. tavighiae*, sister to clade B, comprising the remaining two species (Fig. 5). The genetic distance between *O. kermanus* and *O. tirgari* was 6% ± 0.01 (Table 5), consistent with the distance calculated by Azghadi *et al.* (2014). The two species are readily distinguished by the presence of two lateral lobes on the anal arch of metasomal segment V in *O. kermanus*, compared with two large and one smaller lateral lobes in *O. tirgari*.

Clade A was further divided into two subclades: clade A1, comprising *O. baluchicus*, *O. doriae* and *O. odonturus*, and clade A2, comprising *O. bidentatus*, *O. brevidigitus*, *O. chabaharensis* and *O. tavighiae*. The average genetic distance among the species of clade A1 was 11.3%, supporting the recognition of *O. baluchicus* as distinct from *O. doriae* and *O. odonturus*. *Odontobuthus baluchicus* may be distinguished from *O. doriae* by metasomal segment I being longer than wide, and from *O. odonturus* by the presence of two rather than three lateral lobes on the anal arch of metasomal segment V. Similarly, genetic distances between *O. chabaharensis* and the other species of clade A2, *O. bidentatus*, *O. brevidigitus* and *O. tavighiae*, ranged from 8.4% to 10.1% (Table 5).

Odontobuthus chabaharensis may be distinguished from these species by the presence of three prominent spiniform lobes laterally and two prominent lobes posteroventrally on the anal arch of metasomal segment V.

The minimum interspecific genetic distance (6.0%) was observed between *O. kermanus* and *O. tirgari*, distributed in the central and eastern parts of Iran, respectively, their distributional ranges separated by mountains in the eastern part of Iran. The maximum interspecific genetic distance (13.5%), between *O. bidentatus* and *O. doriae*, may be explained by the geographical barrier represented by the Zagros orogeny (Mirshamsi *et al.*, 2013). Whereas Azghadi *et al.* (2014) observed the maximum interspecific divergence (13.2%) between *O. doriae* and *O. tavighiae*, the lower distance between these species observed in the present study (11.4%) may be attributed to the inclusion of more samples of *O. tavighiae* from intervening geographical localities.

Geographical barriers to dispersal, associated with interactions between the Arabian, Eurasian and Indian tectonic plates, e.g. the orogeny of the Zagros and Alborz mountain ranges, which occurred in the late Tertiary approximately (5–10 Mya) and the formation of low basins, e.g. the Lut Desert to the south-east of the Iranian Plateau, probably played an important role in the speciation process within *Odontobuthus* (Lowe, 2010; Mirshamsi *et al.*, 2013; Azghadi *et al.*, 2014). However, the hypothesis of east to west expansion in the evolutionary history of *Odontobuthus* advanced by Lowe (2010) is falsified by the *COI*-based phylogeny, as clade A is distributed in central, south-western, southern and south-eastern parts of Iran, Iraq, Pakistan and India, and clade B is distributed within eastern and north-eastern Iran. Additional markers from the nuclear and mitochondrial genomes may further illuminate the biogeographical history of *Odontobuthus*.

ACKNOWLEDGEMENTS

This study was supported by the Office of Research Affairs, Ferdowsi University of Mashhad, Iran (Project 3/45941), which is gratefully acknowledged. LP and HMT thank the Higher Education Commission (HEC), Pakistan, for a postdoctoral fellowship from the HEC Post-Doctoral Fellowship Program Phase-II, Batch-V-2011, which funded the field collection of scorpions in Pakistan in 2012 and supported HMT in New York for nine months in 2013, and for a grant from the visiting Scholar's Program, which supported LP's visit to Pakistan in 2012; DNA sequencing at the American Museum of Natural History was funded in part by US National Science Foundation grant DEB 1655050, with thanks to D. Casellato and E. Goetz. Aspects of this research conducted at the AMNH were funded by US National Science Foundation grants EAR 0228699, DEB 0413453, a grant from the JRS Biodiversity Foundation, a grant from the Richard Lounsbery Foundation and a Constantine S. Niarchos Expedition grant from the Stavros Niarchos Foundation to LP. The authors thank H. Dastych (ZMH), J. Dunlop (ZMB), P. Jäger (SMF) and M. Cochrane (SAM) for lending material from or permitting access to the collections in their care; the following for donating material and/or assisting the authors with fieldwork or donations of material from Iran: S. Azghadi, H. Bahrani, P. Crucitti, A. Ebrahimi, A. Habibzadeh, H. Jamalizadeh, G. M. Kashani, M. Kazemi, A. Koohpaye, B. Masihipour, S. Tehrani, V. Vignoli, and A. Zamani; Oman: M. Roppo, M. Seiter, M. Stockmann, and A. Ullrich; and Pakistan: T. Abbas, N. Ahmed, T. Ahmed, M. Ahsan, M. Babar, M. M. Hussain, M. Irfan, M. Jafar, H. Khan, M.J. Khan, S. Y. Khan, T. Khan, and M. K. Mukhtar; D. Casellato, D. Chin, P. Rubi and T. Sharma for generating DNA sequence data at the AMNH; P. Colmenares (AMNH) for assistance with import/export logistics from the US; and O. F. Francke, G. Lowe and a third, anonymous reviewer for constructive comments on a previous draft of the manuscript.

REFERENCES

Acosta LE, **Candido DM**, **Buckup EH**, **Brescovit AD. 2008.** Description of *Zabius gaucho* (Scorpiones, Buthidae), a new species from southern Brazil, with an update about the generic diagnosis. *Journal of Arachnology* **36:** 491–501.

Ahmadi K, **Vazirianzadeh B**, **Jalali A**, **Heidari A**, **Joola P. 2016.** A morphometric study of *Odontobuthus bidentatus* (Scorpionida: Buthidae) and its dimorphism in Khuzestan a SW province, Iran. *Journal of Experimental Zoology, India* **19:** 1567–1570.

Ahmadimarzale M, **Sabuhi H**, **Bidgoli MS**, **Dehghani R**, **Hoseindoost G**, **Mesgari L. 2017.** Study of scorpion species abundance in cities Aran and Bidgol and Kashan, Isfahan, Iran. *Journal of Entomological Research* **41:** 337–342.

Akbari A, **Tabatabai M**, **Hedayat A**, **Modiroosta H**, **Alizadeh M**, **Zare MK. 1997.** [Study of the geographical distribution of scorpions in the south of Iran]. *Pajouhesh and Sazandegi* **34:** 112–115 [in Farsi].

Aliabadian M, **Nijman V**, **Mahmoudi A**, **Naderi M**, **Vonk R**, **Vences M. 2014.** ExcaliBAR: a simple and fast software utility to calculate intra- and interspecific distances from DNA barcodes. *Contributions to Zoology* **83:** 79–84.

Azghadi S, **Mirshamsi O**, **Navidpour S**, **Aliabadian M. 2014.** Scorpions of the genus *Odontobuthus* Vachon, 1950 (Scorpiones: Buthidae) from Iran: phylogenetic relationships inferred from mitochondrial DNA sequence data. *Zoology in the Middle East* **60:** 169–179.

Barahoei H, **Navidpour Sh**, **Aliabadian M**, **Siahsarvie R**, **Mirshamsi O. 2020.** Scorpions of Iran (Arachnida: Scorpiones): annotated checklist, DELTA database and identification key. *Journal of Insect Biodiversity and Systematics* **6:** 375–474.

Birula AA. 1900a. [Scorpiones mediterranei Musei Zoologici mosquensis]. *Izvestiya Imperatorskogo Obshchestva Lyubitelei Prirody, Istorii, Antropologii i Etnografii [Societas Caesarea Amicorum Rerum Naturalium, Anthropologiae Ethnographiae Universitatis Moscoviensis]* **3:** 8–20 [in Russian].

Birula AA. 1900b. Beiträge zur Kenntniss der Scorpionenfauna Ost-Persiens. (1. Beitrag). *Bulletin de l'Academie Imperiale des Sciences de St.-Petersbourg* **12:** 355–375.

Birula AA. 1905. Beiträge zur Kenntniss der Scorpionenfauna Persiens. (3. Beitrag). *Bulletin de l'Academie Imperiale des Sciences de St.-Petersbourg* **23:** 119–148.

Birula AA. 1910. Ueber *Scorpio maurus* Linné und seine Unterarten. *Horae Societatis Entomologicae Rossicae* **39:** 115–192.

Birula AA. 1917. Arachnoidea Arthrogastra Caucasica. Pars I. Scorpiones. *Zapiski Kavkazskogo Muzeya [Memoires du Musee du Caucase]*. Tblisi: Imprimerie de la Chancellerie du Comite pour la Transcaucasie, A(5): 1–253 in [Russian; English translation: **Byalynitskii-Birulya AA.** 1964. *Arthrogastric Arachnids of Caucasia. I. Scorpions*. Israel Program for Scientific Translations, Jerusalem].

Dehghani R, **Kassiri H. 2017.** Geographical distribution of scorpion *Odontobuthus doriae* in Esfahan province, central Iran. *Journal of Arthropod-borne Diseases* **11:** 433–440.

Dehghani R, **Tirgari S**, **Doroudgar A**, **Sayyah M. 1998.** [A survey on scorpion fauna in Kashan]. *Pajouhesh va Sazandegi* **38:** 126–127 [in Farsi].

Dehghani R, **Moabed S**, **Kamyabi F**, **Haghdoos AA**, **Mashayekhi M**, **Soltani H. 2008.** [Scorpions Fauna of Kerman Province-IRAN]. *Journal of Medical Sciences University of Kerman* **15:** 172–181 [in Farsi].

Dehghani R, **Kamiabi F**, **Mohammadzadeh N. 2017.** Burrowing habits of two arthropods; *Odonthobutus doriae* and *Hemilepistus schirasi* in desert of Isfahan, Iran. *Journal of Entomological Research* **41:** 113–118.

Edgar RC. 2004. MUSCLE: Multiple sequence alignment with high accuracy and high throughput. *Nucleic Acids Research* **32:** 1792–1797.

Eldredge N. 1972. Systematics and evolution of *Phacops rana* (Green, 1832) and *Phacops iowensis* Delo, 1935 (Trilobita) from the middle Devonian of North America. *Bulletin of the American Museum of Natural History* **147:** 45–114.

El-Hennawy HK. 1992. A catalogue of the scorpions described from the Arab countries (1758–1990) (Arachnida: Scorpionida). *Serket* **2:** 95–153.

Farzanpay R. 1987. [*Knowing scorpions*]. *Central University Publications No. 312, Biology 4*. Tehran: Central University, 231 [in Farsi, with Latin index].

Farzanpay R. 1988. A catalogue of the scorpions occurring in Iran, up to January 1986. *Revue Arachnologique* **8:** 33–44.

Farzanpay R. 1990. A catalogue of the scorpions occurring in Iran up to January 1986. *Archives of the Razi Institute* **41:** 1–12.

Fekri S, **Badzohre A**, **Safari R**, **Azizi K. 2012.** Species identification and geographic distribution of scorpions in Jask town county, Hormozgan province. *Bimonthly Journal of Hormozgan University of Medical Sciences* **16:** 135–142.

Fet V, **Lowe G. 2000.** Family Buthidae C.L. Koch, 1837. In: Fet V, Sissom WD, Lowe G, Braunwalder ME. *Catalog of the scorpions of the world (1758–1998)*. New York: New York Entomological Society, 54–286.

Fet V, **Soleglad ME**, **Lowe G. 2005.** A new trichobothrial character for the high-level systematics of Buthoidea (Scorpiones: Buthida). *Euscorpius* **23:** 1–40.

Folmer O, **Black M**, **Hoeh W**, **Lutz R**, **Vrijenhoek R. 1994.** DNA primers for amplification of mitochondrial Cytochrome *c* Oxidase Subunit I from diverse metazoan invertebrates. *Molecular Marine Biology and Biotechnology* **3:** 294–299.

Francke OF. 1985. Conspectus genericus scorpionorum 1758–1982 (Arachnida: Scorpiones). *Occasional Papers of the Museum, Texas Tech University* **98:** 1–32.

Ghassemi M, **Dalimi A**, **Navidpour SH. 2015.** Morphometric study on two different borrowing species of Buthidae scorpions from Khoozestan Province, Iran. *Journal of Animal and Veterinary Advances* **14:** 263–267.

Habibi T. 1971. Liste de scorpions de l'Iran. *Bulletin of the Faculty of Science, Teheran University* **2:** 24–31, 42–47 [in Farsi and French].

Hervé M. 2020. RVAideMemoire: Testing and Plotting Procedures for Biostatistics. R package version 0.9-74. Available at: https://CRAN.R-project.org/package=RVAideMemoire

Hijmans RJ, **Guarino L**, **Mathur P. 2004.** *DIVA-GIS, v.5.0. A geographic information system for the analysis of species distribution data*. Available at: http://www.diva-gis.org (accessed 21 August 2020).

Karataş A, **Moradi-Gharkheloo M**, **Ucak M. 2012.** Contribution to the distribution of the scorpions of Iran. *Zoology in the Middle East* **55:** 111–120.

Kassiri H, **Kasiri N**, **Dianat A. 2015.** Species composition, sex ratio, geographical distribution, seasonal and monthly activity of scorpions and epidemiological features of scorpionism in Zarrin-dasht County, Fars Province, southern Iran. *Asian Pacific Journal of Tropical Disease* **5:** S99–S103.

Kembel SW, **Cowan PD**, **Helmus MR**, **Cornwell WK**, **Morlon H**, **Ackerly DD**, **Blomberg SP**, **Webb CO. 2010.** Picante: R tools for integrating phylogenies and ecology. *Bioinformatics* **26:** 1463–1464.

Khalaf KI. 1963. Scorpions reported from Iraq. *Bulletin of Endemic Diseases (Baghdad)* **5:** 59–70.

Kinzelbach R. 1985. Vorderer Orient. Skorpione (Arachnida: Scorpiones). *Tübinger Atlas der Vorderer Orients (TAVO), Karte Nr. A* **VI:** 14.2.

Kovařík F. 1997. Results of the Czech Biological Expedition to Iran. Part 2. Arachnida: Scorpiones, with descriptions of *Iranobuthus krali* gen. n. et sp. n. and *Hottentotta zagrosensis* sp. n. (Buthidae). *Acta Societatis Zoologicae Bohemicae* **61:** 39–52.

Kovařík F. 1998. *Štíři*. Jihlava: Madagaskar, 175. [in Czech]

Kovařík F. 2002. A checklist of scorpions (Arachnida) in the collection of the Forschungsinstitut und Naturmuseum Senckenberg, Frankfurt am Main, Germany. *Serket* **8:** 1–23.

Kovařík F. 2009. *Illustrated Catalog of Scorpions. Part I. Introductory remarks; keys to families and genera; subfamily Scorpioninae with keys to* Heterometrus *and* Pandinus *species.* Prague: Clairon Production, 170.

Kraepelin K. 1891. Revision der Skorpione. I. Die Familie der Androctonidae. *Beiheft zum Jahrbuch der Hamburgischen Wissenschaftlichen Anstalten* **8:** 1–144.

Kraepelin K. 1899. Scorpiones und Pedipalpi. In: Dahl F, ed. *Das Tierreich, 8 (Arachnoidea)*. Berlin: Herausgegeben von der Deutschen Zoologischen Gesellschaft. R. Friedländer und Sohn Verlag, 1–265.

Kraepelin K. 1901. Catalogue des scorpions des collections du Muséum d'Histoire Naturelle de Paris. *Bulletin du Muséum National d'Histoire Naturelle, Paris* **7:** 265–273.

Kraepelin K. 1912. [1913] Neue Beiträge zur Systematik der Gliederspinnen. III. A. Bemerkungen zur Skorpionenfauna Indiens. B. Die Skorpione, Pedipalpen und Solifugen Deutsch-Ost-Afrikas. *Mitteilungen aus dem Naturhistorischen Museum (2. Beiheft zum Jahrbuch der Hamburgischen Wissenschaftlichen Anstalten)* **30:** 123–196.

Kumar S, **Stecher G**, **Tamura K. 2016.** MEGA7: molecular evolutionary genetics analysis v.7.0 for bigger datasets. *Molecular Biology and Evolution* **33:** 1870–1874.

Lamoral BH. 1979. The scorpions of Namibia. *Annals of the Natal Museum* **23:** 497–784.

Lourenço WR, **Duhem B. 2009.** Saharo-Sindian buthid scorpions; description of two new genera and species from occidental Sahara and Afghanistan. *ZooKeys* **14:** 37–54.

Lourenço WR, **Pézier A. 2002.** Taxonomic consideration of the genus *Odontobuthus* Vachon (Scorpiones, Buthidae), with description of a new species. *Revue Suisse de Zoologie* **109:** 115–125.

Lowe G. 2010. A new species of *Odontobuthus* (Scorpiones: Buthidae) from northern Oman. *Euscorpius* **96:** 1–22.

Lowe G, **Kutcher SR**, **Edwards D. 2003.** A powerful new light source for ultraviolet detection of scorpions in the field. *Euscorpius* **8:** 1–7.

Mir Z, **Mirshamsi O**, **Ghasemzadeh F. 2014.** Scorpionfauna study of the north of Sistan and Baluchistan province. *Proceedings of the 18th National and 6th International Congress of Biology in Iran*, 26–29 August 2014, Kharazmi University, 19.

Mirshamsi O, **Azghadi S**, **Navidpour S**, **Aliabadian M**, **Kovařík F. 2013.** *Odontobuthus tirgari* sp. nov. (Scorpiones, Buthidae) from the eastern region of the Iranian Plateau. *Zootaxa* **3731:** 153–170.

Moradi M, **Yağmur A**, **Moradi-Gharkheloo P. 2014.** Study of scorpion fauna (Arachnida: scorpions) on Zanjan Province. *Proceedings of the 18th National and 6th International Congress of Biology in Iran*, 26–29 August 2014, Kharazmi University, 8.

Moradi M, **Yagmur E**, **Pooyan-Moradi G**, **Ahmadi F. 2015.** Scorpion fauna of Zanjan Province, Iran (Arachnida: Scorpiones). *Journal of Applied Biological Sciences* **9:** 11–14.

Motevalli Haghi F, **Borna H**, **Dehghani R**, **Fazeli-Dinan M**, **Yazdani-Cherati J**, **Dehghan O**, **Sahraei-Rostami F**, **Nikookar SH. 2020.** [Faunistic study of scorpions (Arachnida: Scorpiones) in Qaenat County in Iran in 2017]. *Qom University of Medical Sciences Journal* **14:** 66–74 [in Farsi].

Mozaffari E, **Sedaghat MM**, **Dehkordi AS**, **Akbarzadeh K. 2013.** Biodiversity and species composition of scorpions (Arachnida, Scorpiones) in Ilam County, Iran. *Journal of Applied Scientific Research* **9:** 5412–5418.

Navarro N, **Zatarain X**, **Montuire S. 2004.** Effects of morphometric descriptor changes on statistical classification and morphospaces. *Biological Journal of the Linnean Society* **83:** 243–260.

Navidpour S, **Lowe G. 2009.** Revised diagnosis and redescription of *Apistobuthus susanae* (Scorpiones, Buthidae). *Journal of Arachnology* **37:** 45–59.

Navidpour S, **Mirshamsi O. 2014.** Two new species of the genus *Odontobuthus* (Scorpiones, Buthidae) from southern and eastern Iran. *Proceedings of the 28th European Congress of Arachnology*, Torino, Italy, 112.

Navidpour S, **Kovařík F**, **Soleglad ME**, **Fet V. 2008a.** Scorpions of Iran (Arachnida, Scorpiones). Part I. Khuzestan Province. *Euscorpius* **65:** 1–41.

Navidpour S, **Soleglad ME**, **Fet V**, **Kovařík F. 2008b.** Scorpions of Iran (Arachnida, Scorpiones). Part II. Bushehr Province. *Euscorpius* **67:** 1–33.

Navidpour S, **Fet V**, **Kovařík F**, **Soleglad ME. 2008c.** Scorpions of Iran (Arachnida, Scorpiones). Part III. Ilam Province. *Euscorpius* **69:** 1–29.

Navidpour S, **Kovařík F**, **Soleglad ME**, **Fet V. 2008d.** Scorpions of Iran (Arachnida, Scorpiones). Part IV. Kohgilouyeh and Boyer Ahmad Province. *Euscorpius* **74:** 1–24.

Navidpour S, **Ezatkhah M**, **Kovařík F**, **Soleglad ME**, **Fet V. 2011.** Scorpions of Iran (Arachnida: Scorpiones). Part VII. Kerman Province. *Euscorpius* **131:** 1–32.

Navidpour S, **Fet V**, **Kovařík F**, **Soleglad ME. 2012.** Scorpions of Iran (Arachnida, Scorpiones). Part VIII. Fars Province. *Euscorpius* **139:** 1–29.

Navidpour S, **Soleglad ME**, **Fet V**, **Kovařík F. 2013.** Scorpions of Iran (Arachnida, Scorpiones). Part IX. Hormozgan Province, with a description of *Odontobuthus tavighiae* sp. n. (Buthidae). *Euscorpius* **170:** 1–29.

Navidpour S, **Kovařík F**, **Soleglad ME**, **Fet V. 2019.** Scorpions of Iran (Arachnida, Scorpiones). Part X. Alborz, Markazi and Tehran provinces with a description of *Orthochirus carinatus* sp. n. (Buthidae). *Euscorpius* **276:** 1–20.

Nazari M, **Bahrami D**, **Davari B**, **Salehzadeh A. 2015.** Epidemiological survey of scorpion sting cases and identification of scorpion fauna in Hamadan City, Iran (2013). *Scientific Journal of Hamadan University of Medical Sciences* **22:** 255–262.

Nejati J, **Mozafari E**, **Saghafipour A**, **Kiyani M. 2014.** Scorpion fauna and epidemiological aspects of scorpionism

in southeastern Iran. *Asian Pacific Journal of Tropical Biomedicine* **4:** S217–S221.

Nejati J, **Saghafipour A**, **Rafinejad J**, **Mozaffari E**, **Keyhani A**, **Abolhasani A**, **Kareshk AT. 2018.** Scorpion composition and scorpionism in a high-risk area, the southwest of Iran. *Electronic Physician* **10:** 7138–7145.

Nenilin AB, **Fet V. 1992.** Zoogeographical analysis of the world scorpion fauna (Arachnida: Scorpiones). *Arthropoda Selecta* **1:** 3–31 [in Russian with extended English summary].

Newlands G. 1972. Ecological adaptations of Kruger National Park scorpionids (Arachnida: Scorpionides). *Koedoe* **15:** 37–48.

Paradis E, **Claude J**, **Strimmer K. 2004.** APE: analyses of phylogenetics and evolution in R language. *Bioinformatics* **20:** 289–290.

Pérez Minnocci S. 1974. Un inventario preliminar de los escorpiones de la region Paleartica y claves para la identificacion de los generos de la region Paleartica Occidental. *Universidad Complutense de Madrid, Facultad de Ciencias, Departamento de Zoologia, Catedra de Artropodos* **7:** 1–45.

Pirali-Kheirabadi K, **Navidpour S**, **Fet V**, **Kovařík F**, **Soleglad ME. 2009.** Scorpions of Iran (Arachnida, Scorpiones). Part V. Chahar Mahal and Bakhtiyari Province. *Euscorpius* **78:** 1–23.

Pirali-Kheirabadi K, **Khalaji-Pirbalouty V**, **Jazayeri A. 2013.** Geographical distribution of scorpions in Chaharmahal va Bakhteyari Province. *Veterinary Journal (Pajouhesh and Sazandegi)* **103:** 44–51.

Pocock RI. 1897. Descriptions of some new species of scorpions from India. *Journal of the Bombay Natural History Society* **11:** 102–117.

Pocock RI. 1900. Arachnida. In: Blandford WT, ed. *Fauna of British India including Ceylon and Burma*. London: Taylor and Francis, 279.

Pooladgar AR. 1999. Study on species frequency in Khuzestan province. *Pajouhesh and Sazandegi* **40:** 175–177.

Posada D. 2008. jModelTest: phylogenetic model averaging. *Molecular Biology and Evolution* **25:** 1253–1256.

Prendini L. 2001. Substratum specialization and speciation in southern African scorpions: the Effect Hypothesis revisited. In: Fet V, Selden PA, eds. *Scorpions 2001. In Memoriam Gary A. Polis.* Burnham Beeches: British Arachnological Society, 113–138.

Prendini L. 2004. Systematics of the genus *Pseudolychas* Kraepelin (Scorpiones: Buthidae). *Annals of the Entomological Society of America* **97:** 37–63.

Prendini L, **Wheeler WC. 2005.** Scorpion higher phylogeny and classification, taxonomic anarchy, and standards for peer review in online publishing. *Cladistics* **21:** 446–494.

Pringle G. 1960. Notes on the scorpions of Iraq. *Bulletin of Endemic Diseases* **3:** 73–87.

R Core Team. **2019.** *R: a language and environment for statistical computing.* Vienna: R Foundation for Statistical Computing. Available at: https://www.R-project.org. Accessed 15 September 2020.

Ramezani H, **Matlabi M**, **Rafinejad J**, **Amiri M. 2010.** The ecofaunistics of scorpions in Gonabad. *Ofogh-e-Danesh. GMUHS Journal* **16:** 54–62.

Roewer CF. 1943. Über eine neuerworbene Sammlung von Skorpionen des Natur-Museums Senckenberg. *Senckenbergiana* **26:** 205–244.

Ronquist F, **Huelsenbeck JP. 2003.** MrBayes 3: Bayesian phylogenetic inference under mixed models. *Bioinformatics* **19:** 1572–1574.

Rozas J, **Sanchez-DelBarrio JC**, **Messeguer X**, **Rozas R. 2003.** DnaSP, DNA polymorphism analyses by the coalescent and other methods. *Bioinformatics* **19:** 2496–2497.

Shahi M, **Aziz A**, **Ansarian N. 2008.** Scorpion fauna in areas with high scorpionism in Hormozgan Province 2006–2007. *Medical Journal of Hormozgan University* **12:** 207–214.

Sharifinia N, **Gowhari I**, **Hoseiny-Rad M**, **Aivazi AA. 2017.** Fauna and geographical distribution of scorpions in Ilam Province, south western Iran. *Journal of Arthropod-borne Diseases* **11:** 242–248.

Silvestro D, **Michalak I. 2012.** raxmlGUI: a graphical front-end for RAxML. *Organisms, Diversity and Evolution* **12:** 335–337.

Simon E. 1880. Scorpions du Mossoul (ancienne Ninive), sur le Tigre, en Mésopotamie. *Bulletin de la Société Entomologique de France* **10:** 29.

Simon C, **Frati F**, **Bechenbach A**, **Crespi B**, **Li H**, **Flook P. 1994.** Evolution, weighting, and phylogenetic utility of mitochondrial gene sequence and compilation of conserved polymerase chain reaction primers. *Annals of the Entomological Society of America* **87:** 651–701.

Sissom WD. 1990. Systematics, biogeography and paleontology. In: Polis GA, ed. *The biology of scorpions*. Stanford: Stanford University Press, 64–160.

Soleglad ME, **Fet V. 2003.** The scorpion sternum: structure and phylogeny (Scorpiones: Orthosterni). *Euscorpius* **5:** 1–34.

Stahnke HL. 1970. Scorpion nomenclature and mensuration. *Entomological News* **81:** 297–316.

Stahnke HL. 1972. Key to the genera of Buthidae (Scorpionida). *Entomological News* **83:** 121–133.

Takashima H. 1945. [Scorpions of eastern Asia]. *Acta Arachnologica* **9:** 68–106 [in Japanese].

Thorell T. 1876. Études scorpiologiques. *Atti della Società Italiana di Scienze Naturali Genova* **19:** 75–272.

Tikader BK, **Bastawade DB. 1983.** *The fauna of India, Vol. 3. Scorpions (Scorpionida: Arachnida)*. Calcutta: Zoological Survey of India, 671.

Vachon M. 1950. Études sur les scorpions. Chapitre III (suite). Description des scorpions du nord de l'Afrique. *Archives de l'Institut Pasteur d'Algérie* **28:** 152–216.

Vachon M. 1952. *Études sur les scorpions*. Algiers: Institut Pasteur d'Algerie, 482.

Vachon M. 1966. Liste des scorpions connus en Egypte, Arabie, Israël, Liban, Syrie, Jordanie, Turquie, Irak, Iran. *Toxicon* **4:** 209–218.

Vachon M. 1973. [1974]. Étude des caractères utilises pour classer les families et les genres de scorpions (Arachnides). 1. La trichobothriotaxie en arachnologie. Sigles trichobothriaux et types de trichobothriotaxie chez les scorpions. *Bulletin du Muséum National d'Histoire Naturelle, Paris* **140:** 857–958.

Vachon M, **Kinzelbach R. 1987.** On the taxonomy and distribution of the scorpions of the Middle East. In: Krupp F, Schneider W, Kinzelbach R, eds. *Proceedings of the Symposium on the Fauna and Zoogeography of the Middle East, Mainz, 1985. Beihefte zum Tübinger Atlas des Vorderen Orients, Reihe A (Naturwissenschaften)* **28**, 91–103.

Vatani H, **Khoobdel M. 2009.** The scorpions of the Taibad region and the scorpionism situation in military environments. *Military Medicine* **11:** 7–11.

Venables WN, **Ripley BD. 2002.** *Modern applied statistics with S, 4th edn.* New York: Springer.

Vignoli V, **Crucitti P. 2005.** Notes on the scorpion diversity (Arachnida, Scorpiones) of the Yazd Province, central Iran. *Acta Musei Moraviae, Scientiae Biologicae (Brno)* **90:** 1–11.

Volschenk E. 2005. A new technique for examining surface morphosculpture of scorpions. *Journal of Arachnology* **33:** 820–825.

Werner F. 1929. Beiträge zur Kenntnis der Fauna von Syrien und Persien. *Zoologischer Anzeiger* **81:** 238–245.

Werner F. 1936. Reptilien und Gliedertiere aus Persien. *Festschrift zum 60, Geburtstage von Professor Dr. Embrik Strand* **2:** 193–204.

Whittick RJ. 1955. Scorpions from Palestine, Syria, Irak and Iran. In: Field H, ed. *Contributions to the fauna and flora of southwestern Asia*. Coconut Grove: privately printed by Henry Field (*Miscellanea Asiatica Occidentalis* XII; Amer. Document. Inst. Microf. No. 4612, 76–81.)

Wickham H. 2016. *Ggplot2: elegant graphics for data analysis*. New York: Springer–Verlag.